



Search for pair-produced scalar and vector leptoquarks decaying into third-generation quarks and first- or second-generation leptons in pp collisions with the ATLAS detector

The ATLAS Collaboration

A search for pair-produced scalar and vector leptoquarks decaying into quarks and leptons of different generations is presented. It uses the full LHC Run 2 (2015–2018) data set of 139 fb^{-1} collected with the ATLAS detector in proton–proton collisions at a centre-of-mass energy of $\sqrt{s} = 13 \text{ TeV}$. Scalar leptoquarks with charge $-(1/3)e$ as well as scalar and vector leptoquarks with charge $+(2/3)e$ are considered. All possible decays of the pair-produced leptoquarks into quarks of the third generation (t, b) and charged or neutral leptons of the first or second generation (e, μ, ν) with exactly one electron or muon in the final state are investigated. No significant deviations from the Standard Model expectation are observed. Upper limits on the production cross-section are provided for eight models as a function of the leptoquark mass and the branching ratio of the leptoquark into the charged or neutral lepton. In addition, lower limits on the leptoquark masses are derived for all models across a range of branching ratios. Two of these models have the goal of providing an explanation for the recent B -anomalies. In both models, a vector leptoquark decays into charged and neutral leptons of the second generation with a similar branching fraction. Lower limits of 1980 GeV and 1710 GeV are set on the leptoquark mass for these two models.

Contents

1	Introduction	2
2	ATLAS detector	4
3	Data and simulated event samples	4
4	Event reconstruction	7
5	Event selection and categorisation	8
6	Neural network training	10
7	Systematic uncertainties	13
8	Statistical interpretation	14
9	Results	15
10	Conclusion	22

1 Introduction

Leptoquarks (LQs) have already been discussed for a few decades, as they provide a connection between the quark and lepton sectors, which exhibit similar structures. They are predicted by many extensions of the Standard Model (SM), e.g. in unified theories [1–3] and technicolor [4–6] or composite models [7–9]. Recent hints of a potential violation of lepton flavour universality in various measurements of B -meson decays (B -anomalies) [10–21] can also be attributed, if confirmed, to the exchange of leptoquarks [22–29]¹. In addition, some of these models [28, 29, 32] introducing LQs aim to simultaneously provide an explanation for the longstanding discrepancy between the measured and the predicted anomalous magnetic moment of the muon [33]. LQs are bosons carrying colour charge and fractional electrical charge. They possess non-zero baryon and lepton numbers and are assumed to decay into a quark–lepton pair. The branching ratio into a quark and a charged lepton is denoted by \mathcal{B} , and that into a quark and neutrino by $1 - \mathcal{B}$. Leptoquarks can be scalar or vector bosons and can be produced singly or in pairs in proton–proton collisions.

The assumption that LQs can only interact with leptons and quarks of the same generation [34], and are spin-0 particles, has been used in most of the searches for LQs. Recently, however, searches for LQs with couplings to quarks and leptons of different generations have aroused interest because these couplings are required in order to explain the B -anomalies mentioned above. The theoretical explanations usually require LQs with couplings to third-generation quarks and second-generation leptons. In particular, vector LQs with a charge of $2/3$, in units of the elementary charge e , have been identified recently as promising candidates [35, 36].

¹ After submission of the paper a new result from LHCb has been reported [30, 31] superseding Refs. [17, 20, 21] and indicating compatibility with the SM.

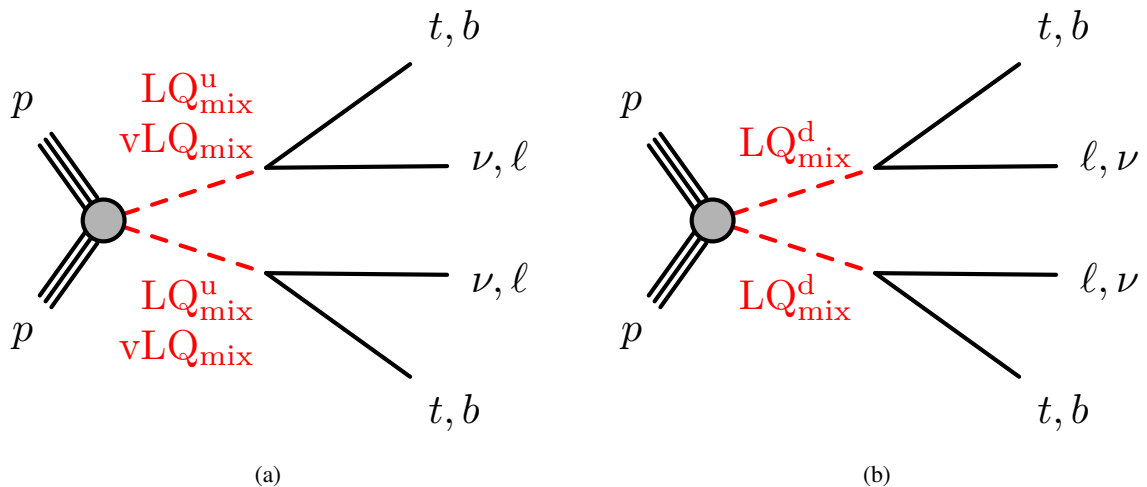


Figure 1: Pair production and decay of (a) up-type scalar (LQ_{mix}^u) and vector (vLQ_{mix}) LQs and (b) down-type scalar (LQ_{mix}^d) LQs with $\ell = e, \mu$. No distinction is made between particles and antiparticles.

First results of searches for LQs with couplings to quarks and leptons of different generations were published recently for pair-produced LQs decaying into charged leptons, i.e. in dilepton final states. Results from the full LHC Run 2 data set (2015–2018) of proton–proton collisions at $\sqrt{s} = 13$ TeV, corresponding to an integrated luminosity of 139 fb^{-1} , are available for pair-produced scalar LQs decaying into a top-quark and an electron or muon from the ATLAS [37] and the CMS Collaborations [38] and for the decay into a b -, c - or light-quark and an electron or muon [39] from ATLAS. In addition, using a partial (35.9 fb^{-1}) Run 2 data set, CMS has published a result for pair-produced vector LQs decaying into a top-quark and a muon, obtained by scaling the results for scalar LQs to the larger production cross-sections expected for vector LQs, assuming no kinematic differences [40].

Given the good coverage of large branching ratios \mathcal{B} by the dileptonic measurements described above, the results presented here use a single-lepton (electron or muon) final state optimised for medium to small \mathcal{B} . In this case, one of the LQs decays into a neutrino and the other decays into a charged lepton, or both decay into neutrinos and the charged lepton arises from a leptonically decaying top-quark (t_{lep}). The results are interpreted as searches for pair-produced LQs with charges of either $\pm(2/3)e$ (up-type) or $\pm(1/3)e$ (down-type). All possible decays of the pair-produced up-type and down-type LQs into a quark (t, b) of the third generation and a lepton (ℓ, ν) of the first or second generation are considered, as seen in Figure 1. With flavour off-diagonal couplings allowed, the model used for up-type (LQ_{mix}^u) and down-type (LQ_{mix}^d) scalar LQs is an extension of that [41] used in previous ATLAS searches [42], where all possible decays of the pair-produced up-type and down-type scalar LQs into a quark (t, b) and a lepton (τ, ν) of the third generation were considered. The present search for up-type LQs is also optimised for a vector LQ (vLQ) model [43] designed to provide an explanation for the various B -anomalies.

The analysis strategy is based on a final-state signature with one lepton, high missing transverse momentum and at least four jets due to a hadronically decaying top-quark (t_{had}) and a b -quark. Dedicated neural networks (NNs), trained in a common training region, are used for the separation of signal and background. This is done separately for scalar and vector LQ pair-production because they exhibit different kinematic behaviour for small values of \mathcal{B} , i.e. when the charged lepton arises mostly from the top-quark decay. For each of the models and for various branching ratios, a signal region (SR) based on the NN output

is defined. Control regions (CRs) are defined so as to be enriched in the various background processes. They are orthogonal to the SR, and orthogonal to each other. The statistical interpretation is based on a simultaneous fit to the CRs and the SR, in which the normalisations for top-quark pair ($t\bar{t}$), W +jets, and single top-quark production as well as a possible signal contribution are determined, while taking into account the experimental and theoretical systematic uncertainties. The results are presented as limits on the leptoquark mass as a function of the branching ratio.

2 ATLAS detector

The ATLAS experiment [44] at the LHC is a multipurpose particle detector with a forward–backward symmetric cylindrical geometry and a near 4π coverage in solid angle.² It consists of an inner tracking detector surrounded by a thin superconducting solenoid providing a 2 T axial magnetic field, electromagnetic and hadron calorimeters, and a muon spectrometer. The inner tracking detector (ID) covers the pseudorapidity range $|\eta| < 2.5$. It consists of silicon pixel, silicon microstrip, and transition radiation tracking detectors. Lead/liquid-argon (LAr) sampling calorimeters provide electromagnetic (EM) energy measurements with high granularity. A steel/scintillator-tile hadron calorimeter covers the central pseudorapidity range ($|\eta| < 1.7$). The endcap and forward regions are instrumented with LAr calorimeters for both the EM and hadronic energy measurements up to $|\eta| = 4.9$. The muon spectrometer (MS) surrounds the calorimeters and is based on three large superconducting air-core toroidal magnets with eight coils each. The field integral of the toroids ranges between 2.0 and 6.0 Tm across most of the detector. The muon spectrometer includes a system of precision tracking chambers and fast detectors for triggering. A two-level trigger system is used to select events. The first-level trigger is implemented in hardware and uses a subset of the detector information to accept events at a rate below 100 kHz. This is followed by a software-based trigger that reduces the accepted event rate to 1 kHz on average depending on the data-taking conditions. An extensive software suite [45] is used in the reconstruction and analysis of real and simulated data, in detector operations, and in the trigger and data acquisition systems of the experiment.

3 Data and simulated event samples

In this search, data from proton–proton collisions at $\sqrt{s} = 13$ TeV corresponding to an integrated luminosity of 139 fb^{-1} , collected in the years 2015 to 2018 with the ATLAS detector, are analysed. Data are required to have been collected during stable beam conditions and with all detector subsystems operational [46]. The average number of simultaneous pp interactions per bunch crossing, referred to as pile-up, is approximately 34, averaged over the whole data set.

Monte Carlo (MC) simulated event samples are used to model the signal and background processes. In all samples except those produced with SHERPA 2.2.1 or SHERPA 2.2.2 [47], decays of heavy-flavour hadrons were modelled with EVTGEN 1.2.0 or EVTGEN 1.6.0 [48], depending on the process. Pile-up was modelled by overlaying minimum-bias events generated with PYTHIA 8.186 [49] and the A3 [50] set of tuned

² ATLAS uses a right-handed coordinate system with its origin at the nominal interaction point (IP) in the centre of the detector and the z -axis along the beam pipe. The x -axis points from the IP to the centre of the LHC ring, and the y -axis points upwards. Cylindrical coordinates (r, ϕ) are used in the transverse plane, ϕ being the azimuthal angle around the z -axis. The pseudorapidity is defined in terms of the polar angle θ as $\eta = -\ln \tan(\theta/2)$. Angular distance is measured in units of $\Delta R \equiv \sqrt{(\Delta\eta)^2 + (\Delta\phi)^2}$.

parameters (referred to as the ‘tune’) onto the simulated hard-scatter events. A reweighting procedure was applied in order to match the pile-up profile of the recorded data. The ATLAS simulation infrastructure [51] was used to simulate the detector and its response. Nominal SM background samples were produced with a detailed GEANT4 [52] detector simulation, whereas a faster calorimeter simulation [51] was applied for the signal samples and systematic variations of the backgrounds. The same offline reconstruction methods used for data were applied to the simulated samples. Corrections were applied to the simulated events in order to match the selection efficiencies and energy and mass scales and resolutions of reconstructed simulated particles to those measured in data control samples.

Simulated events with pair-produced scalar LQs were generated at next-to-leading order (NLO) in quantum chromodynamics (QCD) with MADGRAPH5_AMC@NLO 2.6.0 [53] and the NNPDF3.0_{NLO} parton distribution function (PDF) [54] set with $\alpha_s = 0.118$. An extension of the LQ model of Ref. [41] was used, allowing flavour off-diagonal couplings. The model is based on previous fixed-order NLO QCD calculations [55, 56]. To retain information about spin correlations, the decays of LQs as well as top-quarks were handled with MADSPIN [57]. MADGRAPH5_AMC@NLO was interfaced with PYTHIA 8.230 [58] to model the parton shower (PS), hadronisation, and underlying event (UE). Here and in the following, PYTHIA was used with the A14 tune [59] and the NNPDF2.3_{LO} [60] set of PDFs. The coupling strength λ was set to 0.3, leading to a signal width of approximately 0.2%. The model parameter $\beta \in [0, 1]$ modifies the coupling of LQs to leptons, such that the coupling to charged leptons is given by $\sqrt{\beta}\lambda$ and to neutrinos by $\sqrt{1-\beta}\lambda$. It differs from the branching fraction \mathcal{B} into charged leptons because of phase-space corrections arising mainly from the large top-quark mass. The parameter β was set to 0.5 in the simulation. Different values for \mathcal{B} were achieved by reweighting the MC events according to their decay, as described in Ref. [42]. The LQ pair-production cross-sections were obtained from the calculation of direct top-squark pair production, as this process has the same production modes, computed at approximate next-to-next-to-leading order (NNLO) in QCD with resummation of next-to-next-to-leading logarithmic (NNLL) soft gluon terms [61–64]. The cross-sections do not include lepton t -channel contributions, which are neglected in Ref. [41] and may lead to corrections at the percent level [65]. For this analysis, signal samples were produced separately for electrons and muons and for both up- and down-type LQs with a mass spacing of 100 GeV from 300 GeV to 800 GeV and from 1600 GeV to 2500 GeV, and with a finer spacing of 50 GeV between 800 GeV and 1600 GeV to improve the resolution around the expected mass exclusion limit.

Simulated events with pair-produced up-type vector LQs were generated at leading order (LO) in QCD with MADGRAPH5_AMC@NLO 2.8.1 and the NNPDF3.0_{NLO} PDF set with $\alpha_s = 0.118$. Decays of the ν LQs and top-quarks were handled with MADSPIN, while the PS and hadronisation were simulated with PYTHIA 8.244. The U_1 ν LQ model in Ref. [43] is used for the muon channel, directly seeking an explanation for the various B -anomalies. Couplings to electrons are assumed to vanish in this model because of existing tight bounds from low-energy observables, mainly in the lepton-flavour-violating sector. Nevertheless, an extension of the model [66] was used in this analysis to also probe the electron channel. The samples were produced with a coupling strength of $g_U = 3.0$, leading to a signal width of approximately 11%. The large value of g_U is motivated by a suppression of the production cross-section for additional mediators in an ultraviolet-complete model, which might otherwise be in tension with existing LHC limits. The model accommodates both left- and right-handed couplings to fermions, where in the case of only left-handed couplings the coupling strengths to charged leptons and neutrinos are equal ($\beta = 0.5$). Although only left-handed couplings were used in producing the MC samples, the analysis uses the same reweighting of MC events as in the scalar LQ case to also probe different values of \mathcal{B} . The model allows use of either the minimal (ν LQ_{mix}^{min}) or the Yang–Mills (ν LQ_{mix}^{YM}) coupling scenario, where in the latter the ν LQ is a heavy gauge boson resulting in enhanced cross-sections. Kinematic differences between

the minimal and the Yang–Mills coupling scenario were found to be negligible, except for masses below about 500 GeV. Samples were produced separately for the two coupling scenarios and for both muons and electrons, with a mass spacing of 100 GeV from 300 GeV to 1400 GeV and from 2300 GeV to 2500 GeV, and with a finer spacing of 50 GeV between 1400 GeV and 2300 GeV. No higher-order cross-section computations are available for this model. Therefore, the cross-sections computed at leading order by MADGRAPH5_AMC@NLO are used in the analysis.

Dominant background processes in the search include $t\bar{t}$, W +jets and single top-quark production, the last being mainly associated production of a top-quark and W boson (tW). In addition, $t\bar{t}+V$ ($V = W, Z$), diboson, $t\bar{t}+H$, and Z +jets processes are also considered in the analysis. Contributions from multi-jet background with a jet misidentified as a lepton are negligible in the phase space of interest.

The production of $t\bar{t}$ events was modelled using the POWHEG BOX [67–70] v2 generator at NLO with the NNPDF3.0_{NLO} set of PDFs and the h_{damp} parameter³ set to $1.5 m_t$ [71]. The cross-section was corrected to the theory prediction at NNLO including resummation of NNLL soft-gluon terms calculated using TOP++ 2.0 [72]. The events were interfaced to PYTHIA 8.230 to model the PS, hadronisation, and UE.

The associated production of a top-quark and a W boson was modelled using the POWHEG BOX v2 generator at NLO in QCD using the five-flavour scheme and the NNPDF3.0_{NLO} set of PDFs. The diagram removal scheme [73] was used to avoid overlap with $t\bar{t}$ production because of interference. Single-top t -channel (s -channel) production was modelled using the POWHEG BOX v2 generator at NLO in QCD using the four-flavour (five-flavour) scheme and the corresponding NNPDF3.0_{NLO} PDF set. The events were interfaced with PYTHIA 8.230 in all cases, except for tW events with large missing transverse momenta, which were interfaced with PYTHIA 8.235.

The production of V +jets was simulated with the SHERPA 2.2.1 generator using NLO-accurate matrix elements for up to two jets, and LO-accurate matrix elements for up to four jets, calculated with the Comix [74] and OPENLOOPS [75, 76] libraries. They were matched with the SHERPA PS [77] using the MEPS@NLO prescription [78–81] using the set of tuned parameters developed by the SHERPA authors. The NNPDF3.0_{NNLO} set of PDFs was used and the samples were normalised to a NNLO prediction [82].

Samples of diboson final states (VV) were simulated with the SHERPA 2.2.1 or 2.2.2 generator, depending on the process, including off-shell effects and Higgs boson contributions, where appropriate. Fully leptonic final states and semileptonic final states, where one boson decays leptonically and the other hadronically, were generated using matrix elements at NLO accuracy in QCD for up to one additional parton and at LO accuracy for up to three additional parton emissions. The matrix element calculations were matched and merged with the SHERPA PS. The NNPDF3.0_{NNLO} set of PDFs was used, along with the internal SHERPA tune.

The production of $t\bar{t}+W$ and $t\bar{t}+Z$ events was modelled using the MADGRAPH5_AMC@NLO 2.3.3 generator at NLO with the NNPDF3.0_{NLO} PDF set. The events were interfaced to PYTHIA 8.210.

The production of $t\bar{t}+H$ events was modelled using the POWHEG BOX v2 generator at NLO with the NNPDF3.0_{NLO} PDF set, interfaced to PYTHIA 8.230.

An overview of the matrix element (ME) generator, PDF, shower generator and UE tune for signal and background samples is given in Table 1.

³ The h_{damp} parameter is a resummation damping factor and one of the parameters that controls the matching of POWHEG matrix elements to the PS and thus effectively regulates the high- p_T radiation against which the $t\bar{t}$ system recoils.

Table 1: List of ME generator and the order of the strong coupling constant in the perturbative calculation, PDF, shower generator and tune for the different signal and background processes.

Process	ME generator	ME order	PDF set	PS and hadronisation	UE tune
Scalar LQ	MADGRAPH5_AMC@NLO 2.6.0	NLO	NNPDF3.0NLO	PYTHIA 8.230	A14
Vector LQ	MADGRAPH5_AMC@NLO 2.8.1	LO	NNPDF3.0NLO	PYTHIA 8.244	A14
$t\bar{t}$ /single top	POWHEG BOX v2	NLO	NNPDF3.0NLO	PYTHIA 8.230/8.235	A14
V+jets	SHERPA 2.2.1	MEPS@NLO	NNPDF3.0NNLO	SHERPA	internal
Diboson	SHERPA 2.2.1/2.2.2	MEPS@NLO	NNPDF3.0NNLO	SHERPA	internal
$t\bar{t}+V$	MADGRAPH5_AMC@NLO 2.3.3	NLO	NNPDF3.0NLO	PYTHIA 8.210	A14
$t\bar{t}+H$	POWHEG BOX v2	NLO	NNPDF3.0NLO	PYTHIA 8.230	A14

4 Event reconstruction

Events studied in this analysis are required to have at least one reconstructed pp interaction vertex with at least two associated tracks with transverse momentum $p_T > 0.5$ GeV. The primary vertex is selected as the one with the largest sum of squared transverse momenta of tracks associated with the interaction vertex. In the analysis, a set of reconstructed objects is used, consisting of electrons, muons, and jets, as well as the missing transverse momentum. When identifying charged leptons, a staggered approach is used, where so-called baseline leptons fulfil less stringent requirements than signal leptons. Events are required to have exactly one signal lepton without any additional baseline leptons.

Electron candidates are reconstructed from energy deposits in the EM calorimeter matched to charged-particle tracks in the inner detector (ID). Requirements of $|d_0|/\sigma_{d_0} < 5$ on the transverse impact parameter d_0 (with uncertainty σ_{d_0}) and $|\Delta z_0 \sin \theta| < 0.5$ mm on the longitudinal track impact parameter z_0 ensure matching between track and vertex. Furthermore, electron candidates are required to lie within a pseudorapidity range of $|\eta| < 2.47$, excluding the EM calorimeter barrel–endcap transition region $1.37 < |\eta| < 1.52$. Baseline electrons must have $p_T > 10$ GeV and fulfil loose identification criteria, using a likelihood-based discriminant that combines information about tracks in the ID and energy deposits in the calorimeter system [83]. In addition, baseline electrons are required to have a hit in the innermost layer of the pixel detector. Isolation requirements in both the calorimeter and the ID are imposed [83]. Electron candidates are rejected if the scalar sum of transverse momenta of tracks within a cone of size $\Delta R = \min(10 \text{ GeV}/p_T, 0.2)$, excluding the electron itself, is larger than 15% of the electron p_T . Similarly, an electron is removed if, after subtracting contributions from pile-up and the electron itself, the transverse energy deposited in the calorimeter within a cone of size $\Delta R = 0.2$ exceeds 20% of the transverse energy of the electron. To suppress backgrounds due to hadrons misidentified as electrons, signal electrons must in addition pass the ‘tight’ identification working point, and have $p_T > 30$ GeV.

Muon candidates are reconstructed from charged-particle tracks in the ID and the MS and from energy deposits in the calorimeters. For the reconstruction of muon candidates, tracks in the ID combined with tracks in the MS are used in the range $|\eta| < 2.5$. In addition, muons in the range $|\eta| < 0.1$ are reconstructed from ID tracks matched to an energy deposit in the calorimeter compatible with a minimally ionising particle. These muon candidates are called calorimeter-tagged (CT). Track-to-vertex matching is ensured by requiring $|d_0|/\sigma_{d_0} < 3$ for the transverse impact parameter and $|\Delta z_0 \sin \theta| < 0.5$ mm for the longitudinal track impact parameter. Baseline muons are required to have $p_T > 10$ GeV and to have compatible individual measurements in the ID and the MS. Signal muons are required to have $p_T > 30$ GeV and CT muons are not accepted [84]. Additionally, signal muons are rejected if the scalar sum of transverse momenta of tracks within a cone of size $\Delta R = \min(10 \text{ GeV}/p_T, 0.3)$ around the muon exceeds 6% of its

transverse momentum. In accordance with other searches for pair-produced LQs within ATLAS [37, 39], signal muons above a p_T threshold of 800 GeV must fulfil stricter requirements on the number of hits in the MS to ensure good momentum resolution.

Small-radius (small- R) jet candidates are built from particle-flow objects [85, 86], using the anti- k_t algorithm [87, 88] with a radius parameter of $R = 0.4$. The particle-flow algorithm combines information about ID tracks and energy deposits in the calorimeters to form the input for jet reconstruction. Jets with $p_T < 25$ GeV or $|\eta| > 2.5$ are rejected. To reduce contributions from pile-up, jet candidates with $|\eta| < 2.4$ and $p_T < 60$ GeV are required to satisfy the ‘tight’ jet vertex tagger criterion [89]. Small- R jets are categorised as b -tagged if they satisfy a requirement on the output of a multivariate algorithm, operating at a tagging efficiency of 77% as determined with simulated $t\bar{t}$ events [90, 91]. The $R = 0.4$ jets are then reclustered with the anti- k_t algorithm with $R = 1.0$ to obtain large- R jets. Additionally, $R = 0.4$ jets are reclustered iteratively with the recursive method described in Ref. [92] to reconstruct hadronically decaying top-quark candidates (t_{had}). For this, the small- R jets are reclustered with an initial radius parameter of $R = 3.0$, which is iteratively reduced to $R(p_T) = 2m_{\text{top}}/p_T$ to match the jet radius to the top candidate’s transverse momentum. Top candidates losing large fractions of their p_T in the shrinking process are discarded. Finally, only the leading- p_T candidate with a mass larger than 150 GeV is kept.

The missing transverse momentum (with magnitude E_T^{miss}) in an event is defined as the negative vectorial sum of the transverse momenta of all calibrated objects [93]. It also includes an additional track-based soft term taking into account energy depositions not associated with any calibrated object.

An overlap removal procedure is applied to avoid ambiguities when reconstructing the objects described above, using the baseline lepton definitions. Electron–muon overlap is handled by removing any calorimeter-tagged muons sharing a track in the ID with an electron, and then removing any electrons sharing an ID track with a remaining muon. Subsequently, overlap between jets and leptons is removed by rejecting any jets within $\Delta R = 0.2$ of an electron and afterwards rejecting any electrons within $\Delta R = 0.4$ of a jet. Similarly, jets are discarded if they have fewer than three associated tracks and are within $\Delta R = 0.2$ of a muon candidate. Otherwise, the muon is rejected if it lies within $\Delta R = \min(0.4, 0.04 + 10 \text{ GeV}/p_T(\mu))$ of a jet.

5 Event selection and categorisation

Any event considered in this analysis must pass an E_T^{miss} trigger [94], as single-lepton triggers are found to be less efficient in particular in the muon channel. The E_T^{miss} trigger thresholds varied between 70 GeV and 110 GeV across the different data-taking periods. A requirement of $E_T^{\text{miss}} > 250$ GeV is imposed in the offline event selection to ensure full efficiency. Events are required to contain exactly one signal lepton. Additionally, a veto is applied on further baseline leptons. Since the final states of interest contain one hadronically decaying top-quark and one additional jet, only events with at least four small- R jets are selected. Only one of those jets needs to be b -tagged to preserve high efficiency for the signal. To suppress contributions from fake E_T^{miss} caused by mismeasurements of jets or leptons, events with $m_T(\ell, E_T^{\text{miss}}) = \sqrt{2p_T(\ell)E_T^{\text{miss}}(1 - \cos \Delta\phi(p_T(\ell), E_T^{\text{miss}}))} < 30$ GeV or $\Delta\phi(E_T^{\text{miss}}, j_{1,2}) < 0.4$, where $j_{1,2}$ indicates the highest- p_T and the second-highest- p_T small- R jet, respectively, are rejected.

The $t\bar{t}$ background is known not to be modelled accurately at high transverse momenta [95, 96]. Reweighting factors are derived in bins of the jet multiplicity as a function of m_{eff} , which is defined as the scalar sum of the transverse momenta of all reconstructed objects and the E_T^{miss} and corresponds approximately to the

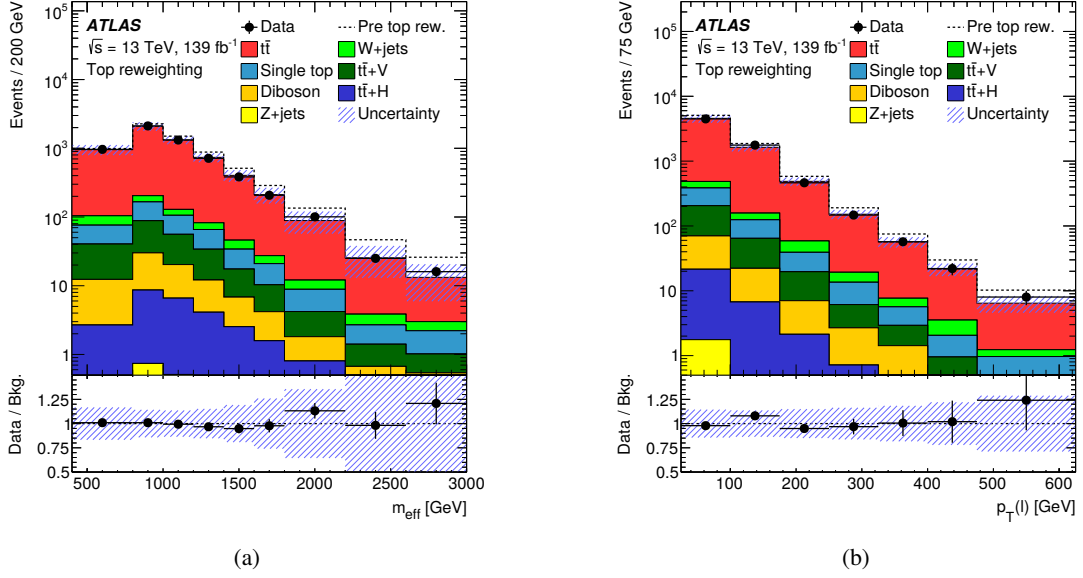


Figure 2: Distributions of (a) m_{eff} and (b) $p_T(\ell)$ in the top reweighting region after applying the top reweighting. The hatched bands include statistical and systematic uncertainties. The total background expectation before applying the top reweighting is shown as a dashed line. The ratios of the observed and expected numbers of background events are shown in the bottom panels. The last bin contains the overflow.

mass of the LQ pair. This procedure is referred to as ‘top reweighting’ in the following. The reweighting factors are determined for the sum of the $t\bar{t}$ and single-top backgrounds and are parameterised with a linear function, separately in each of the four jet multiplicity bins (4, 5, 6, ≥ 7). For this, a dedicated top reweighting region is defined with $am_{T2} < 200$ GeV, where the asymmetric transverse mass, am_{T2} , is a variant of m_{T2} [97] and allows the reconstruction of dileptonic $t\bar{t}$ events in which only one lepton is reconstructed [98, 99]. The reweighting factor is then applied to single-top and $t\bar{t}$ events in each of the training and control regions defined in the following. Figure 2 shows the m_{eff} and lepton- p_T distributions in the top reweighting region after applying the reweighting procedure, in addition to the total background expectation before reweighting. The modelling of kinematic variables is improved by the correction. A potential signal contribution is negligible in this region as it amounts to, e.g., 0.5% in the last four bins in Figure 2(a) for a scalar LQ with a mass of 1 TeV and $\mathcal{B} = 0.5$.

Control regions (CRs) enriched in the various backgrounds and with negligible signal contamination are defined. They are orthogonal to the top reweighting region by requiring $am_{T2} > 200$ GeV and are orthogonal to each other. The W +jets CR uses events in a window around the Jacobian peak, i.e. $50 \text{ GeV} \leq m_T(\ell, E_T^{\text{miss}}) < 120 \text{ GeV}$, with a b -jet multiplicity of $n_b = 1$ and no hadronically decaying top-quark candidate. To increase the purity of selected W +jets events, only events with a positively charged lepton are considered, because the cross-section for W^+ production is larger than that for W^- production in pp collisions. For the single-top CR a requirement of $m_T(\ell, E_T^{\text{miss}}) < 120 \text{ GeV}$ is imposed. In order to reduce contributions from W +jets production, events must have exactly two b -tagged jets, with an angular separation $\Delta R(b_1, b_2) > 1.2$. Events containing a large- R jet are vetoed. The purity of W +jets and single-top events in their respective CRs is 58% and 38%. Distributions of m_{eff} in these CRs are shown in Figure 3.

For the training of the NNs, a training region is defined so as to be orthogonal to the top reweighting region

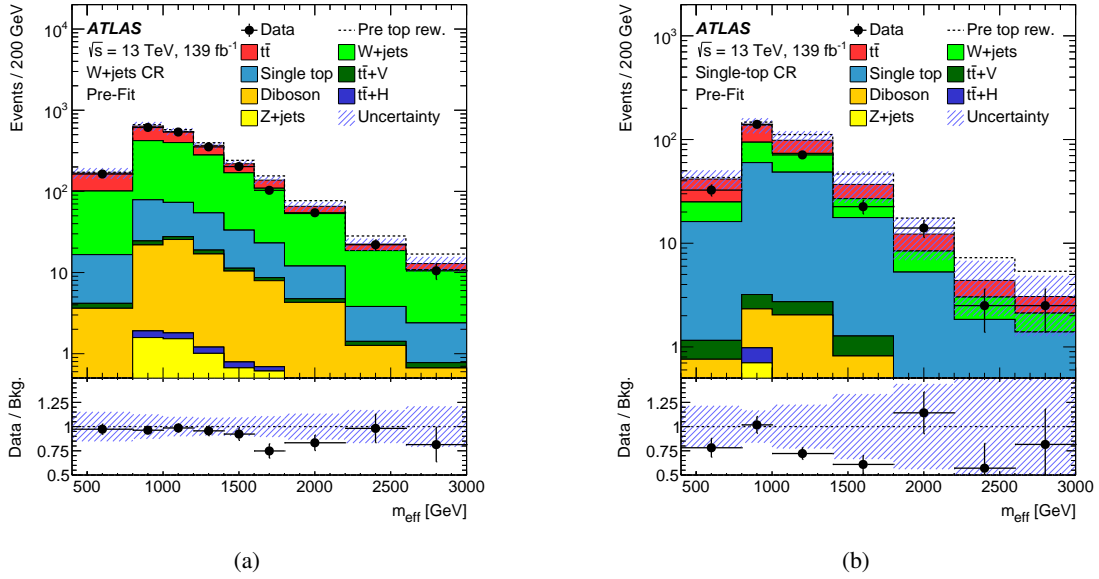


Figure 3: Distributions of m_{eff} in (a) the W +jets CR and (b) the single-top CR after applying the top reweighting, before the fit to data in CRs and SR. The hatched bands include statistical and systematic uncertainties. The total background expectation before applying the top reweighting is shown as a dashed line. The ratios of the observed and expected numbers of background events are shown in the bottom panels. The last bin contains the overflow.

and both control regions by requiring $am_{T2} > 200$ GeV and $m_T(\ell, E_T^{\text{miss}}) \geq 120$ GeV. An overview of the different selection requirements for the training and control regions is given in Table 2. The product of signal acceptance and efficiency in the training region is similar for signal hypotheses with couplings to electrons or muons. For $\mathcal{B} = 0.5$, it amounts to around 17% for up-type scalar LQs and to around 14% for down-type scalar LQs at $m_{\text{LQ}} = 1.4$ TeV. For vector LQs, it reaches 20% at the same mass for both the Yang–Mills coupling and the minimal coupling scenario.

6 Neural network training

Simulated signal and background events in the training region are used to train several NNs for the various signal hypotheses. The NNs are implemented using the NeuroBayes package [100, 101] which combines a three-layer feed-forward NN with a complex and robust preprocessing of the input variables prior to their presentation to the NN. The purpose of the preprocessing is to facilitate optimal network training by ordering the input variables according to their ability to discriminate between signal and background, taking correlations into account, and removing all but the most powerful ones.

NeuroBayes uses Bayesian regularisation techniques for the training process to improve the generalisation performance and to avoid overtraining. In general, the network infrastructure consists of one input node for each input variable plus one bias node, an arbitrary, user-defined number of hidden nodes, and one output node which gives a continuous NN output score (NN_{out}) in the interval $(0, +1)$, where large values indicate signal-like events and small values background-like events. For the NNs of this analysis, 15 nodes are used in the hidden layer and the ratio of signal to background events in the training is 1:1. The different background processes are weighted according to their expected number of events. Only $t\bar{t}$, W +jets,

Table 2: Overview of event selections applied in the different regions of the analysis.

Preselection			
E_T^{miss} triggers exactly one signal lepton veto on additional baseline leptons $E_T^{\text{miss}} > 250$ GeV ≥ 4 small- R jets $m_T(\ell, E_T^{\text{miss}}) > 30$ GeV $\Delta\phi(E_T^{\text{miss}}, j_{1,2}) > 0.4$			
Top reweighting region	W +jets CR	Single-top CR	Training region Low- NN_{out} CR/SR
$n_b \geq 1$	$n_b = 1$	$n_b = 2$	$n_b \geq 1$
$m_T(\ell, E_T^{\text{miss}}) \geq 120$ GeV	$50 \text{ GeV} \leq m_T(\ell, E_T^{\text{miss}}) < 120$ GeV	$m_T(\ell, E_T^{\text{miss}}) < 120$ GeV	$m_T(\ell, E_T^{\text{miss}}) \geq 120$ GeV
$am_{T2} < 200$ GeV	$am_{T2} > 200$ GeV	$am_{T2} > 200$ GeV	$am_{T2} > 200$ GeV
-	t_{had} candidate veto	large- R jet veto	-
-	lepton charge = $+1e$	-	-
-	-	$\Delta R(b_1, b_2) > 1.2$	-
-	-	-	$NN_{\text{out}} < 0.5 / \geq 0.5$

single-top-quark, and $t\bar{t}+V$ events are used as background processes in the training. As a check for potential overtraining, only 80% of the simulated events serve as input to the training, while the remaining 20% are used as a test sample. No signs of overtraining are observed. After the training step, samples of simulated signal and background events, as well as the observed events, are processed by the NNs in order to get an NN_{out} value for each event. For each NN, the training region is divided into a low- NN_{out} control region with $NN_{\text{out}} < 0.5$, enriched mainly in $t\bar{t}$ events, and the signal region above 0.5.

The input variables are chosen because of their ability to discriminate between signal and background. In total, 15 input variables are provided for the training, including the lepton flavour in order to distinguish between electrons and muons. This is because a final state with one lepton flavour has some sensitivity to a LQ model with the other flavour if the lepton stems from a top-quark decay, i.e. mainly in the low \mathcal{B} region. Table 3 lists the input variables in order of decreasing ability to discriminate between signal and background. The order is not absolute, as there is some dependence on the signal model and \mathcal{B} , e.g. the lepton flavour cannot discriminate at all in the region of low \mathcal{B} , but is important otherwise. The modelling of the input variables in the training region is good in general, as can be seen for the most important ones in Figure 4. Among the least well modelled of all input variables is $m_{\text{inv}}(b_1, \ell)$ shown in Figure 4(c). This is due to the interference between single-top and $t\bar{t}$ production, which is difficult to describe in MC simulations [102].

Figure 4 also displays three up-type signal hypotheses at a mass of 1.3 TeV. It can be seen that the signal shape depends not only on the value of \mathcal{B} but also on the spin of the LQ. The signal shape differences due to spin correlations are sizeable for low values of \mathcal{B} at small values of lepton p_T , where the lepton usually originates from a top-quark decay. Here, the lepton- p_T distribution in the vector LQ model is found to be similar in shape to the background in contrast to the scalar case as can be seen Figure 4(b). Therefore, separate NNs are trained for scalar and vector LQs as well as for various values of \mathcal{B} . A total of four NNs per lepton flavour at $\mathcal{B} = 0.0, 0.25, 0.5$, and 0.9 are used for up-type scalar and vector LQs. Since kinematic differences between the Yang–Mills coupling and the minimal coupling are negligible except for very low masses, the NNs for vector LQs are only trained on samples with the former coupling

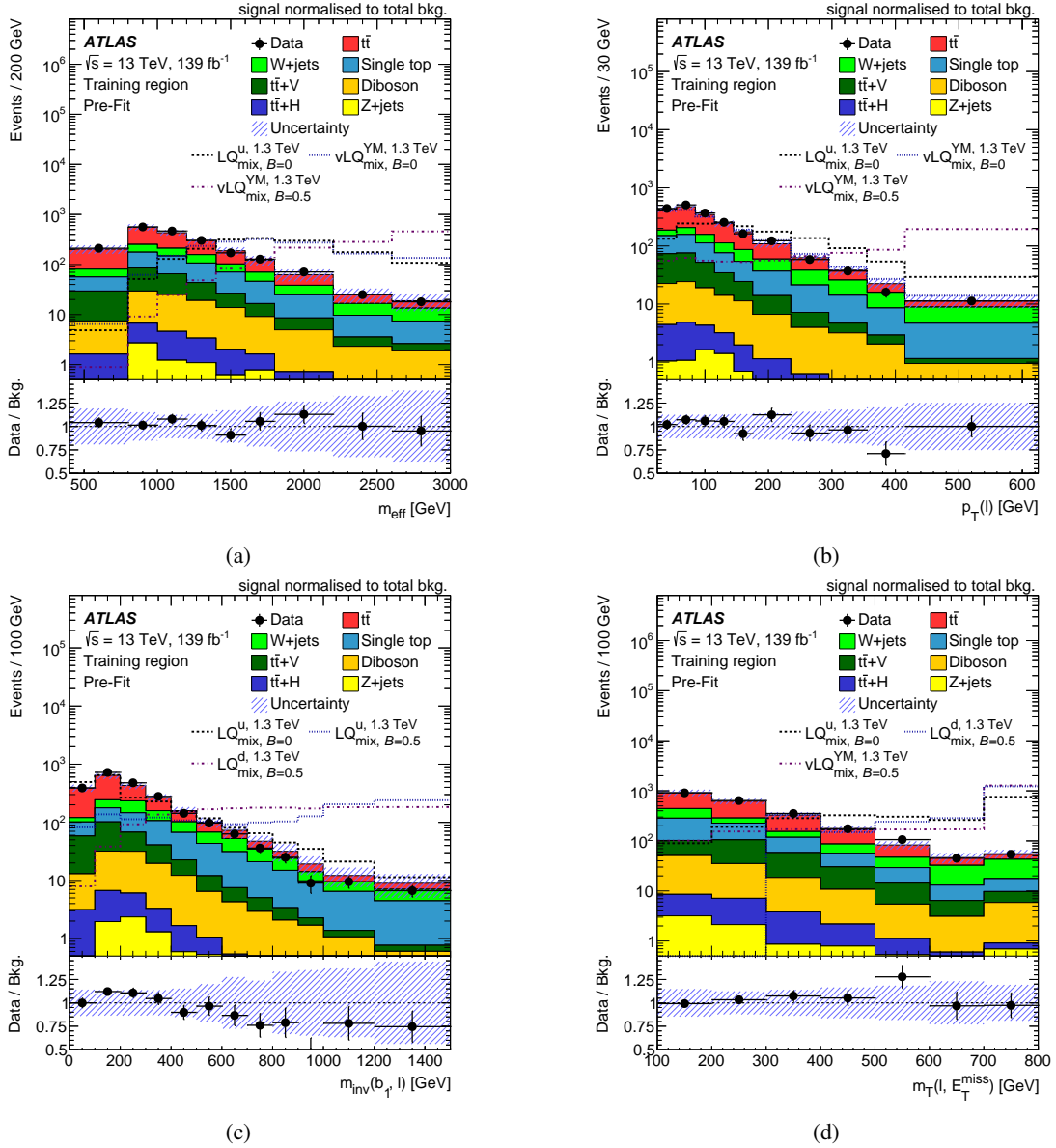


Figure 4: Distributions of (a) m_{eff} , (b) $p_T(\ell)$, (c) $m_{\text{inv}}(b_1, \ell)$, and (d) $m_T(\ell, E_T^{\text{miss}})$ in the training region after applying the top reweighting, before the fit to data in CRs and SR. The hatched bands include statistical and systematic uncertainties. Signal distributions normalised to the total background expectation are overlaid for up-type scalar LQs with $\mathcal{B} = 0.0$ and vector LQs with $\mathcal{B} = 0.0$ and 0.5 , each with $m_{\text{LQ}} = 1.3$ TeV. The ratios of the observed and expected numbers of background events are shown in the bottom panels. The last bin contains the overflow.

Table 3: Input variables for the NN training, approximately sorted in descending ability to discriminate between signal and background. The order is not absolute as there is some dependence on the signal model and \mathcal{B} . Some variables might not be defined in every event.

Variable	Description
$m_T(\ell, E_T^{\text{miss}})$	transverse mass of lepton and E_T^{miss}
m_{eff}	scalar sum of the transverse momenta of leptons, jets, and E_T^{miss}
Lepton flavour	flavour of the signal lepton
$p_T(\ell)$	transverse momentum of the lepton
$m_{\text{inv}}(b_1, \ell)$	invariant mass of the leading- p_T b -jet and the lepton
n_{large}	reclustered large- R jet multiplicity
am_{T2}	asymmetric transverse mass
E_T^{miss} significance	measure for assessing the compatibility of the observed E_T^{miss} with zero, taking resolutions into account
$m_T(b_1, E_T^{\text{miss}})$	transverse mass of leading- p_T b -jet and E_T^{miss}
$p_T(t_{\text{had}})$	transverse momentum of t_{had}
$\Delta\phi(E_T^{\text{miss}}, b_2)$	azimuthal angle separation between E_T^{miss} and subleading- p_T b -jet
$m_{\text{inv}}(b_2, \ell)$	invariant mass of subleading- p_T b -jet and lepton
$\Delta\phi(E_T^{\text{miss}}, b_1)$	azimuthal angle separation between E_T^{miss} and leading- p_T b -jet
$\Delta\phi(t_{\text{had}}, \ell)$	azimuthal angle separation between t_{had} and lepton
$p_T(b_1)$	transverse momentum of leading- p_T b -jet

and then applied to the latter as well. In the case of down-type scalar LQs, only one NN is trained for LQs decaying into muons and another is trained for LQs decaying into electrons. For both trainings, a branching ratio of 0.5 is assumed, since only events with one LQ decaying into a charged lepton and the other decaying into a neutrino contribute significantly to the phase space under consideration. For scalar LQs, signal samples produced with $m_{\text{LQ}} = 500$ GeV, 900 GeV, and 1300 GeV are combined in each training, as separate trainings for each signal mass did not yield a significant improvement for masses above about 600 GeV. For vector LQs, additional signal samples with $m_{\text{LQ}} = 1700$ GeV are used to take advantage of their higher production cross-sections and therefore higher expected mass limits when compared to scalar LQs.

7 Systematic uncertainties

The largest systematic uncertainties considered in the analysis are related to the modelling of the background processes. For $t\bar{t}$ production, the uncertainty due to the method used to match the matrix element to the parton shower is assessed by comparing a sample produced by MADGRAPH5_AMC@NLO with the nominal sample from POWHEG BOX, using the same parton shower. Conversely, an estimate of the uncertainties related to the underlying event, parton shower, and hadronisation is obtained by comparing a sample showered by HERWIG 7 [103] with the nominal sample showered by PYTHIA, using the same ME generator for both. The effects of uncertainties in the renormalisation and factorisation scales are estimated by independently varying the scales by a factor of two. The impact of initial-state radiation (ISR) is estimated by varying α_s in the A14 tune. Similarly, the uncertainty related to final-state radiation (FSR) is assessed by varying the renormalisation scale for final-state parton-shower emissions by a factor of two. Additionally,

an uncertainty related to the choice of value for the POWHEG BOX-specific h_{damp} parameter is evaluated by using a varied value of $h_{\text{damp}} = 3.0 m_t$. PDF uncertainties are obtained from the PDF4LHC15 PDF set [104].

For single top-quark production, uncertainties in ME-to-PS matching, the choice of parton shower, renormalisation and factorisation scales, ISR, FSR, and PDF are evaluated using the same procedures as for $t\bar{t}$ production. Large uncertainties arise due to interference effects between $t\bar{t}$ and tW production. They are estimated by comparing the nominal sample based on the diagram removal scheme with a sample using the diagram subtraction scheme [73, 105].

In the top reweighting procedure, the parameters of the linear fit are varied within their 2σ uncertainty to account for potential non-linearities in addition to the statistical uncertainty, treating the normalisation and the shape component in each of the four jet multiplicity bins independently. Compared to the 1σ variation, this choice has a negligible impact on the results.

For W +jets, Z +jets, diboson, $t\bar{t}+V$, and $t\bar{t}+H$ processes, renormalisation and factorisation scale variations are considered, following the same procedures as for $t\bar{t}$. In addition, an uncertainty of 50% is assigned to the heavy-flavour component of the W +jets background to cover differences in flavour composition between control and signal regions seen in MC studies.

Theoretical systematic uncertainties also include cross-section uncertainties for those background processes for which the normalisation is not determined in the fit. For diboson and Z +jets production, this uncertainty is taken to be 6% [106] and 5% [107], respectively. For $t\bar{t}+H$ production, it amounts to 11% [108] and for $t\bar{t}+Z$ production to 15% [108]. For $t\bar{t}+W$ production, the cross-section uncertainty is taken to be 50% to account for potential differences between predicted and measured values as reported in Ref. [109].

Systematic uncertainties in the signal prediction arise from acceptance effects due to renormalisation and factorisation scale, ISR/FSR, and PDF and α_s variations. They were found to not exceed 5% in total across the whole mass range, and this is therefore taken as a conservative estimate.

Additionally, detector-related uncertainties are considered, the dominant ones being the small- R jet energy scale and resolution uncertainties [86]. Furthermore, systematic uncertainties related to the jet mass scale and resolution, the lepton identification, isolation, and reconstruction efficiencies as well as the lepton energy scale and resolution [83, 84], the b -tagging efficiencies [90], and the $E_{\text{T}}^{\text{miss}}$ reconstruction [110] are taken into account. Minor contributions to the total systematic uncertainty also come from the uncertainty of 1.7% in the integrated luminosity [111], obtained using the LUCID-2 detector [112] for the primary luminosity measurements, and from an uncertainty related to pile-up reweighting.

All sources of systematic uncertainty affect the total event yield, and all, except the ones where the size of the uncertainty is explicitly stated above, also affect the shape of the distributions used in the fit.

8 Statistical interpretation

The binned distributions of the NN output are used to test for the presence of a signal. Simultaneous binned profile-likelihood fits are performed for hypothesis testing, following a modified frequentist method implemented in RooStats [113] and using the NN_{out} distribution in the signal region and the overall number of events in the low- NN_{out} , W +jets, and single-top control regions. Systematic uncertainties affecting signal and background expectations are accounted for by including them in the fit in the form of nuisance parameters. For uncertainties in the modelling of background processes for which the normalisation is

determined in the likelihood fit, only shape effects and acceptance differences between the CRs and the SR are considered, in order to avoid double-counting of normalisation uncertainties. This procedure is also used for pre-fit uncertainty bands in order to have an equivalent treatment of systematic uncertainties. A smoothing algorithm is applied to certain systematic variations in the signal region in order to reduce statistical fluctuations between bins. To simplify the fitting procedure, for each region and each process a nuisance parameter is only considered if the overall effect on the normalisation of the process is larger than 1%. In the case of the signal region, which has multiple bins, nuisance parameters are also considered if their effect in any bin within the signal region is above 1%.

The binned likelihood function $\mathcal{L}(\mu, \theta)$ is constructed as the product of Poisson probability terms over all bins considered in the analysis. It depends on the signal strength parameter μ , a multiplicative factor applied to the theoretical signal production cross-section, and θ , a set of nuisance parameters, implemented in the likelihood function as Gaussian priors for shape effects and as log-normal priors for normalisation effects. The expected number of events in a bin depends on μ and θ . The nuisance parameters θ adjust the expectations for signal and background according to the corresponding systematic uncertainties, and their fitted values correspond to the amounts that best fit the data.

The test statistic q_μ is defined as the profile likelihood ratio

$$q_\mu = -2 \ln \frac{\mathcal{L}(\mu, \hat{\theta})}{\mathcal{L}(\hat{\mu}, \hat{\theta})},$$

where $\hat{\mu}$ and $\hat{\theta}$ are the values of the parameters that maximise the likelihood function (with the constraints $0 \leq \hat{\mu} \leq \mu$), and $\hat{\theta}$ are the values of the nuisance parameters (NPs) that maximise the likelihood function for a given value of μ . This test statistic is used to determine whether the observed data are compatible with the background-only hypothesis, i.e. with $\mu = 0$. Furthermore, by using the CL_s method [114], upper limits on the signal production cross-section are derived for each of the signal scenarios considered in this analysis. For a given signal scenario, values of the production cross-section (parameterised by μ) yielding $\text{CL}_s < 0.05$, where CL_s is computed using the asymptotic approximation [115], are excluded at $\geq 95\%$ confidence level (CL).

9 Results

For each NN training, a separate fit to the NN_{out} distribution in the signal region and the overall number of events in the low- NN_{out} , W +jets, and single-top control regions is performed, with free normalisation parameters for the $t\bar{t}$, single-top, and W +jets background processes. The normalisation parameters obtained from fits to data using the background-only hypothesis are consistent across all trainings. They are always applied in the following and vary between 1.09 ± 0.22 and 1.29 ± 0.23 for $t\bar{t}$, between 0.84 ± 0.12 and 0.93 ± 0.12 for W +jets, and between 0.46 ± 0.27 and 0.54 ± 0.26 for single top. The normalisation parameter for the single-top process reduces the event yield by approximately a factor of two; however, the expected yield from the alternative scheme to model the interference between the $t\bar{t}$ and tW processes leads to an even smaller yield. Observed and expected event yields after the background-only fit are listed in Table 4 for one NN training.

The NN_{out} distributions after the background-only fit are validated with data–MC comparisons in the control regions, as shown in Figure 5 for one particular NN training. In general, good agreement is found for all trainings in all control regions, although the single-top CR is typically more problematic due to the

Table 4: Observed and expected event yields in the control and signal regions for a training for $\nu\text{LQ}_{\text{mix}}^{\text{YM}} \rightarrow b\mu/t\nu$ and $\mathcal{B} = 0.5$ after the background-only fit. The uncertainties in the background predictions include both the statistical and systematic components. For comparison, expected event yields are shown for a $\nu\text{LQ}_{\text{mix}}^{\text{YM}}$ signal at a mass point of 1700 GeV and $\mathcal{B} = 0.5$ including its pre-fit uncertainties.

	W+jets CR	Single-top CR	Low- NN_{out} CR	SR
$t\bar{t}$	860 ± 140	186 ± 35	1370 ± 150	53 ± 10
Single top	103 ± 87	131 ± 47	200 ± 110	36 ± 14
W+jets	1240 ± 130	101 ± 28	265 ± 55	32.4 ± 6.9
$t\bar{t}+V$	11.0 ± 1.8	4.47 ± 0.79	180 ± 28	16.7 ± 2.6
Diboson	94.3 ± 9.8	7.6 ± 1.9	94 ± 11	11.1 ± 1.2
$t\bar{t}+H$	1.27 ± 0.16	1.00 ± 0.12	14.4 ± 1.7	1.34 ± 0.18
Z+jets	6.46 ± 0.32	2.18 ± 0.11	7.20 ± 0.36	1.31 ± 0.07
Total background	2308 ± 48	433 ± 21	2126 ± 46	152 ± 13
Observed events	2310	430	2124	157
$\nu\text{LQ}_{\text{mix}}^{\text{YM}}$ (1.7 TeV, $\mathcal{B} = 0.5$)	0.109 ± 0.022	0.097 ± 0.016	1.57 ± 0.10	38.9 ± 2.6

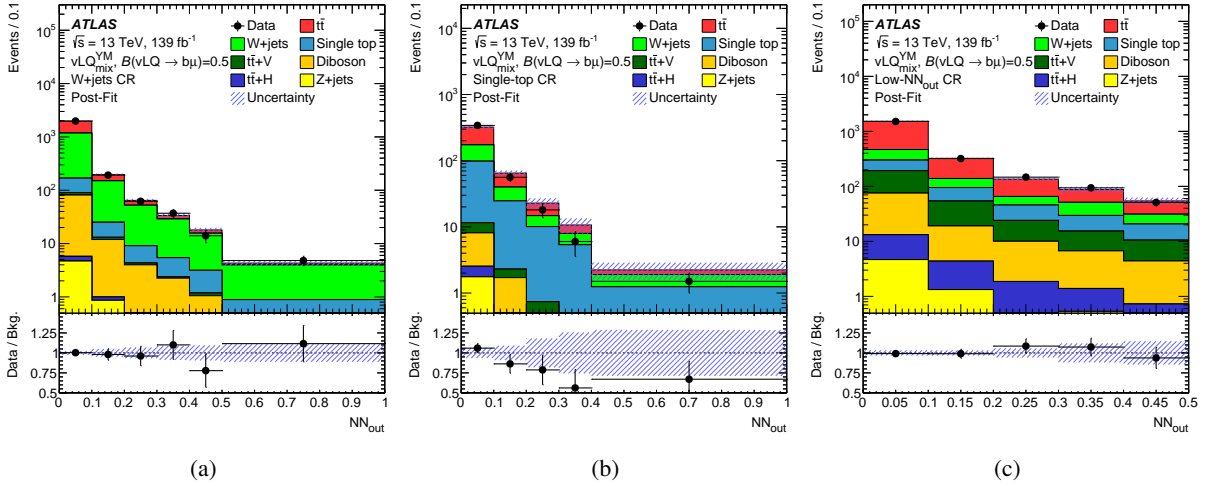


Figure 5: Data and background expectation in (a) the W+jets CR, (b) the single-top CR, and (c) the low- NN_{out} CR after the simultaneous background-only fit for a training with $\nu\text{LQ}_{\text{mix}}^{\text{YM}} \rightarrow b\mu/t\nu$ and $\mathcal{B} = 0.5$. The hatched band indicates the total post-fit uncertainty. The ratios of data to background expectation are shown in the bottom panels.

interference effects mentioned above [102]. NPs corresponding to the systematic uncertainties covering the observed differences between data and MC simulation are not constrained significantly because only the overall number of events in each CR enters the fit. The systematic uncertainties are therefore fully propagated to the SR.

A comparison between data and background expectation in the signal region is shown in Figure 6 after the background-only fit for three different NN trainings. Good agreement is found for all trainings. The largest discrepancies at high values of NN_{out} are observed for the $\text{LQ}_{\text{mix}}^{\text{u}}$ model with $\mathcal{B} = 0.0$, i.e. for the decay into top-quarks and neutrinos as shown in Figure 6(c).

No significant deviations of the data from the expected SM background are observed. Upper 95% CL limits

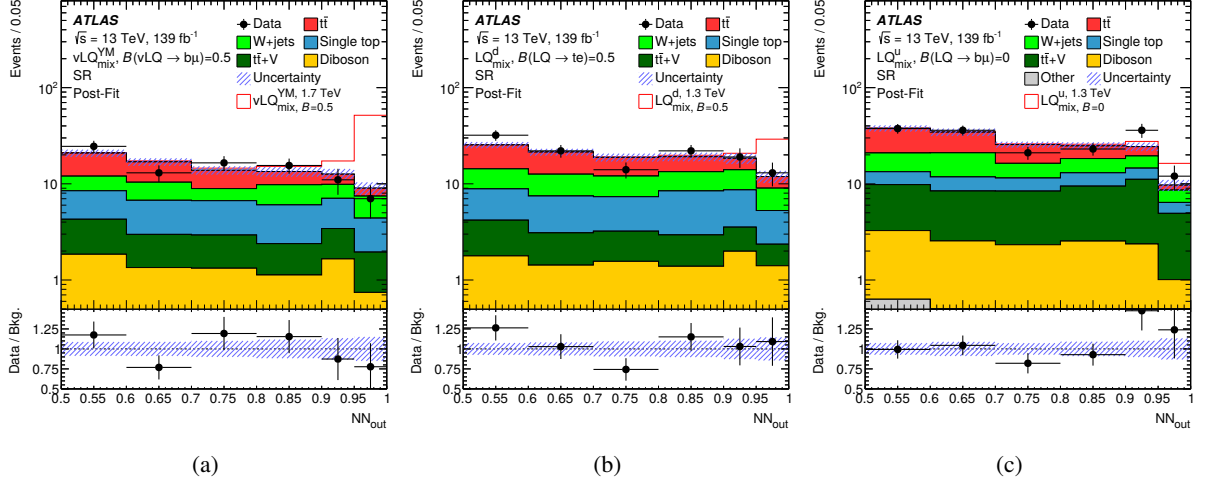


Figure 6: Data and background expectation in the signal region after the simultaneous background-only fit to data for (a) a training with $vLQ_{\text{mix}}^Y \rightarrow b\mu/t\nu$ and $\mathcal{B} = 0.5$, (b) a training with $LQ_{\text{mix}}^d \rightarrow te/b\nu$ with $\mathcal{B} = 0.5$, and (c) a training with $LQ_{\text{mix}}^u \rightarrow t\nu$, i.e. $\mathcal{B} = 0.0$. Minor background contributions from $t\bar{t}+H$ and Z +jets are combined into ‘other’. Expected pre-fit signal distributions with \mathcal{B} corresponding to the respective training are added on top of the background expectation, using a mass of 1700 GeV for vector LQs and 1300 GeV for scalar LQs. The hatched band indicates the total post-fit uncertainty. The ratios of data to background expectation are shown in the bottom panels.

on the cross-sections of pair-produced LQs can be calculated in simultaneous signal-plus-background fits to the CRs and the SR, in which the background normalisations and possible signal contributions are determined. The largest uncertainty in each of the resulting signal strengths is statistical in nature. For the three signal hypotheses shown in Figure 6, the statistical uncertainty exceeds 85% of the total uncertainty for the two scalar LQ models at $m_{LQ} = 1.3$ TeV and rises to nearly 100% for the vector LQ case at $m_{LQ} = 1.7$ TeV. The resulting limits on the cross-section for the four scalar LQ models are shown in Figure 7 as a function of the LQ mass for a fixed $\mathcal{B} = 0.5$. Corresponding limits for the four vector LQ models are shown in Figure 8.

These cross-section limits are compared with the theoretical cross-section predictions, shown in blue, resulting in lower limits on the signal mass for $\mathcal{B} = 0.5$. The uncertainty band around the theory prediction includes PDF, α_s , and renormalisation and factorisation scale uncertainties. The expected and observed limits for $\mathcal{B} = 0.5$ are summarised in Table 5 for the eight LQ models considered in this analysis. The total impact of systematic uncertainties on the cross-section limits reaches 15% for LQ masses above 1 TeV, corresponding to 20 GeV in the expected mass limit.

Limits on LQ pair-production are also evaluated across a wide range of values for the branching ratio of LQs into charged leptons. For that, the statistical interpretation is performed in steps of 0.05 in \mathcal{B} between 0.0 and 0.95 for up-type scalar and vector LQs and between 0.05 and 0.95 for down-type scalar LQs. For up-type LQs, for which NNs have been trained at four different values of \mathcal{B} , the NN resulting in the best expected cross-section limit is chosen at each step. The analysis is not sensitive to final states with zero or two leptons; therefore, $\mathcal{B} = 1.0$ is omitted for all LQs and so is $\mathcal{B} = 0.0$ for down-type LQs. The cross-section upper limits and the mass exclusion curves across the \mathcal{B} plane are shown in Figure 9 for scalar LQs and in Figure 10 for vector LQs.

Expected and observed limits on the leptoquark mass as a function of \mathcal{B} agree well everywhere, except for a small deviation for the LQ_{mix}^u model at $\mathcal{B} = 0.0$, as already discussed above in the context of Figure 6.

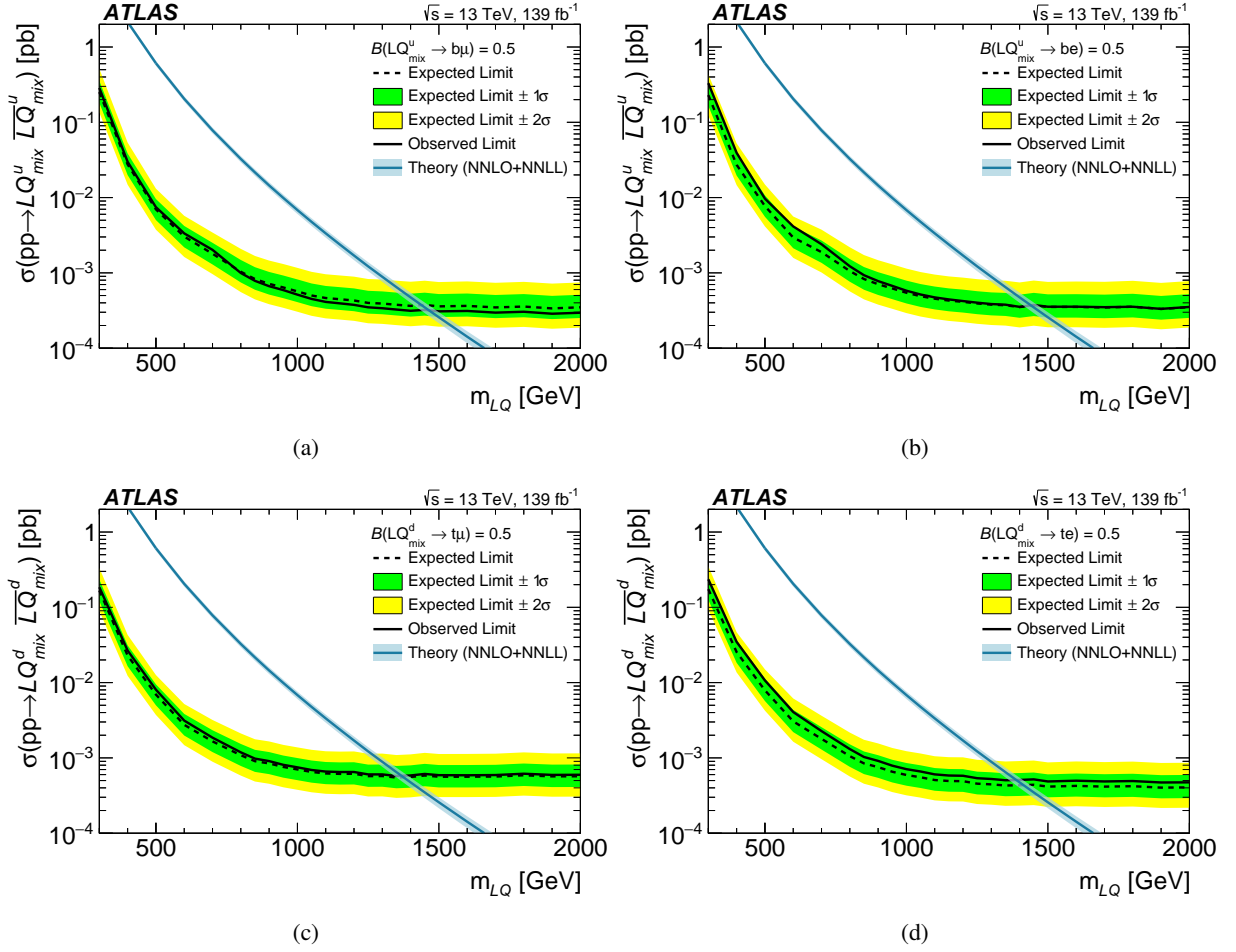


Figure 7: Expected (dashed black) and observed (solid black) 95% CL upper limits on the cross-section of pair-produced scalar LQs, assuming $\mathcal{B} = 0.5$. The green (yellow) band shows the $\pm 1\sigma$ ($\pm 2\sigma$) uncertainty region around the expected limit. The theoretical prediction and its $\pm 1\sigma$ uncertainty band are shown in blue. Limits are presented for (a) up-type scalar LQs decaying into muons, (b) up-type scalar LQs decaying into electrons, (c) down-type scalar LQs decaying into muons, and (d) down-type scalar LQs decaying into electrons.

Table 5: Expected and observed 95% CL lower limits on the LQ mass at $\mathcal{B} = 0.5$ for the eight signal hypotheses considered in this analysis.

	Exp. limit [GeV]	Obs. limit [GeV]
$LQ_{\text{mix}}^u \rightarrow tv/b\mu$	1440^{+60}_{-60}	1460
$LQ_{\text{mix}}^u \rightarrow tv/be$	1440^{+60}_{-60}	1440
$LQ_{\text{mix}}^d \rightarrow t\mu/b\nu$	1380^{+50}_{-60}	1370
$LQ_{\text{mix}}^d \rightarrow te/b\nu$	1410^{+60}_{-60}	1390
$\nu LQ_{\text{mix}}^{\text{YM}} \rightarrow tv/b\mu$	1930^{+50}_{-60}	1980
$\nu LQ_{\text{mix}}^{\text{YM}} \rightarrow tv/be$	1930^{+50}_{-70}	1900
$\nu LQ_{\text{mix}}^{\text{min}} \rightarrow tv/b\mu$	1660^{+50}_{-50}	1710
$\nu LQ_{\text{mix}}^{\text{min}} \rightarrow tv/be$	1650^{+50}_{-60}	1620

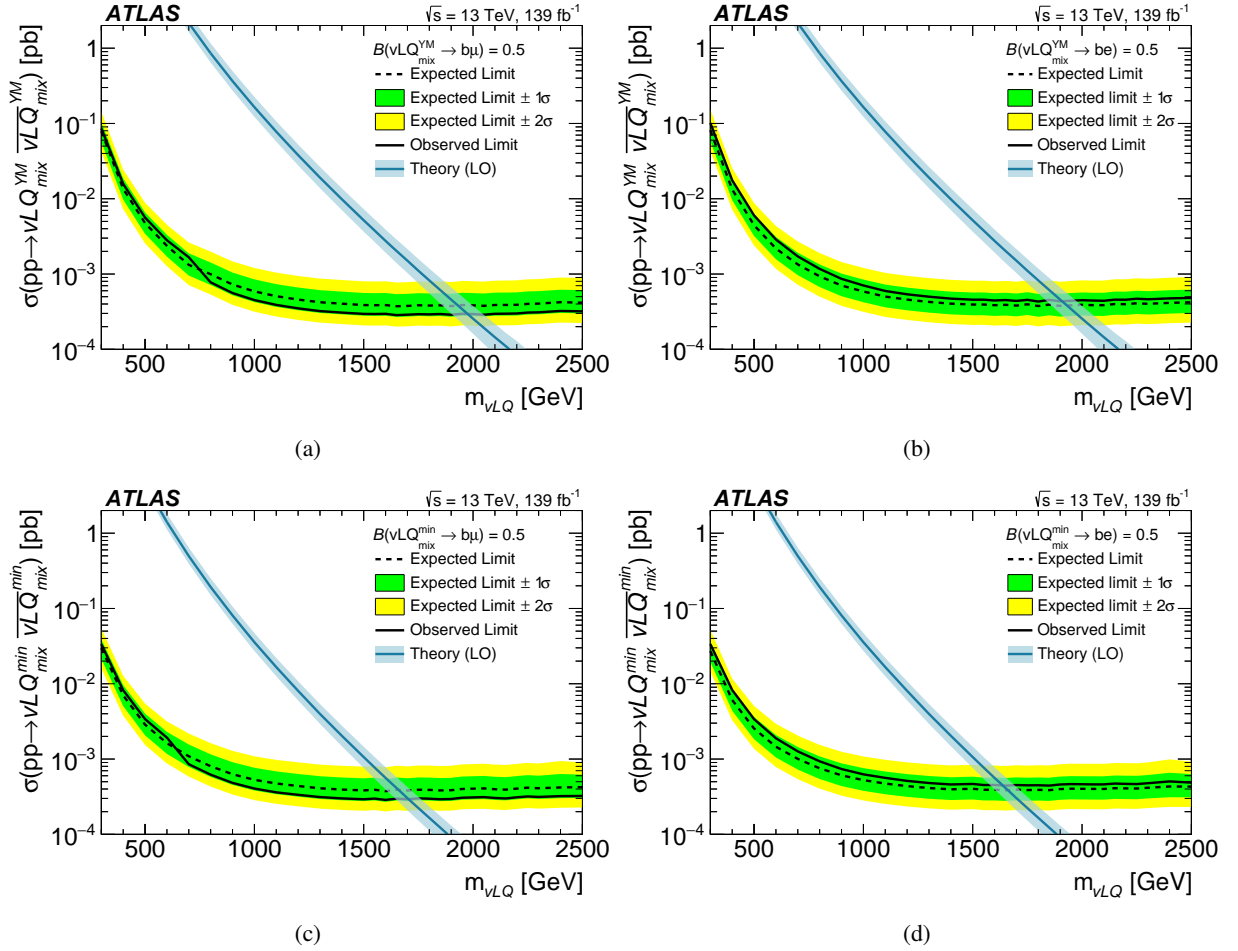


Figure 8: Expected (dashed black) and observed (solid black) 95% CL upper limits on the cross-section of pair-produced vector LQs, assuming $\mathcal{B} = 0.5$. The green (yellow) band shows the $\pm 1\sigma$ ($\pm 2\sigma$) uncertainty region around the expected limit. The theoretical prediction and its $\pm 1\sigma$ uncertainty band are shown in blue. Limits are presented for (a) vector LQs in the Yang–Mills coupling scenario decaying into muons, (b) vector LQs in the Yang–Mills coupling scenario decaying into electrons, (c) vector LQs in the minimal coupling scenario decaying into muons, and (d) vector LQs in the minimal coupling scenario decaying into electrons.

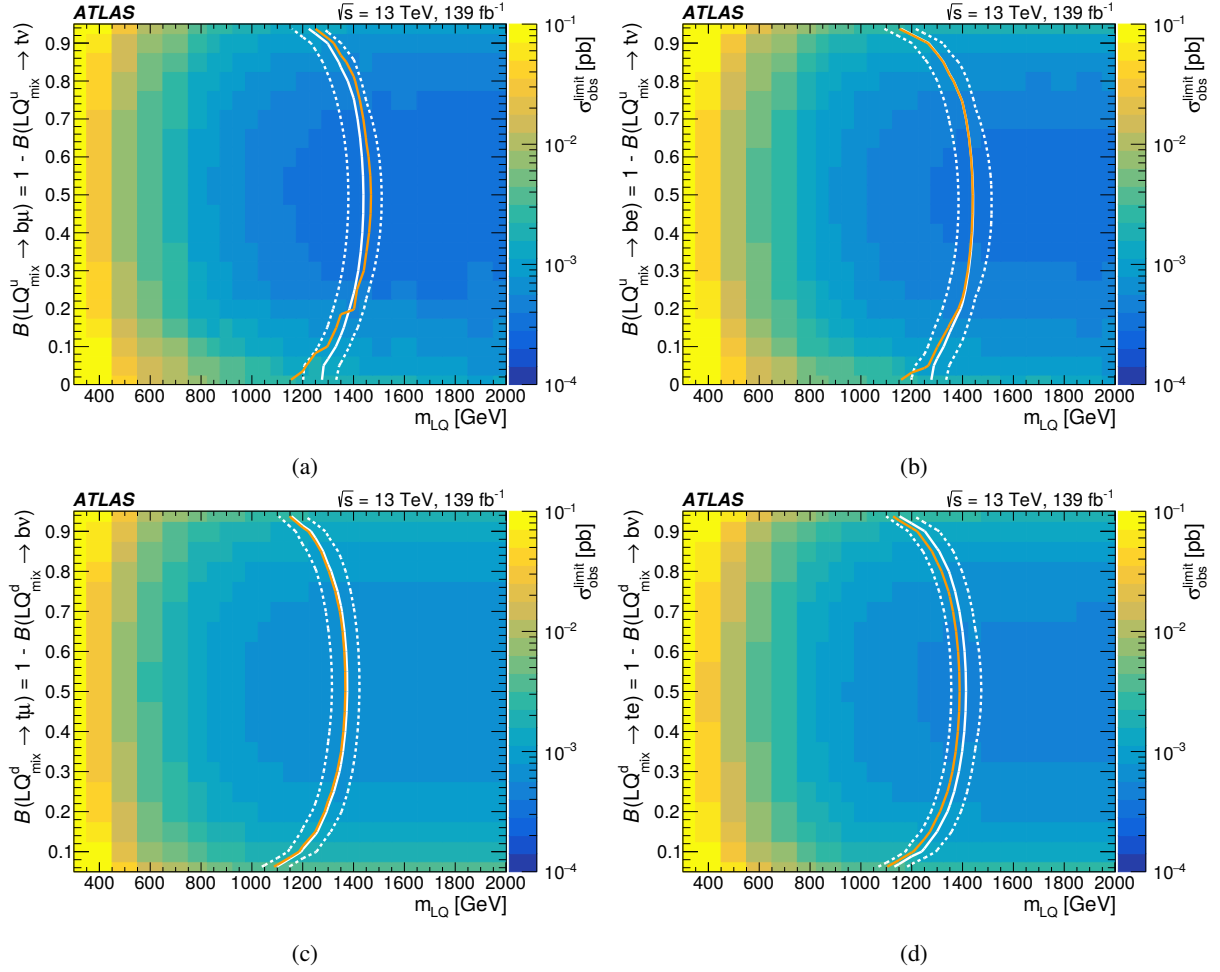


Figure 9: Expected (solid white, $\pm 1\sigma$ ranges dashed) and observed (solid orange) exclusion limits on the leptoquark mass as a function of the branching ratio into charged leptons at 95% CL. The observed upper limit on the signal cross-section in each bin is shown on the z-axis. Limits are presented for (a) up-type scalar LQs decaying into muons, (b) up-type scalar LQs decaying into electrons, (c) down-type scalar LQs decaying into muons, and (d) down-type scalar LQs decaying into electrons. For up-type LQs the range in \mathcal{B} is 0–0.95, for down-type it is 0.05–0.95.

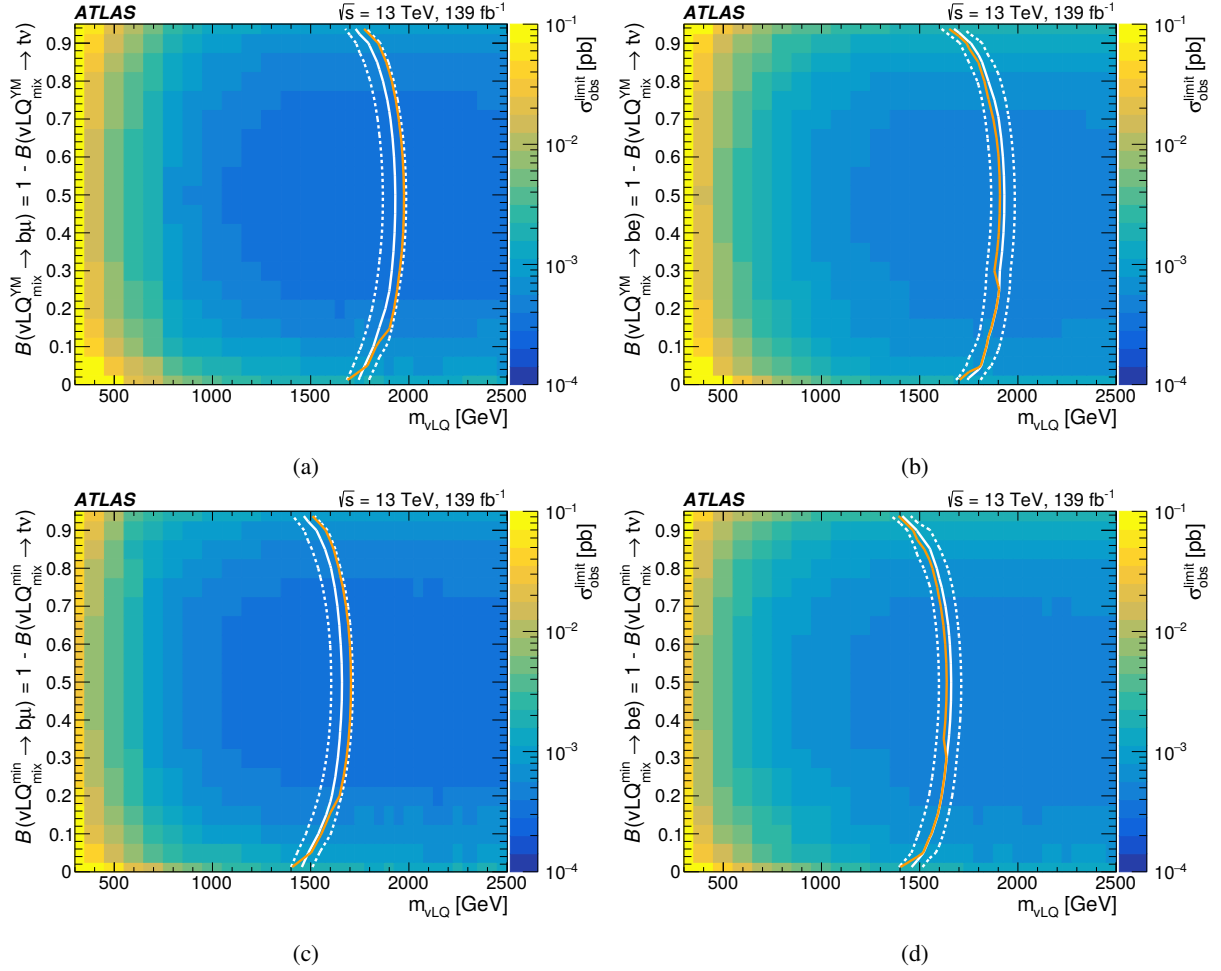


Figure 10: Expected (solid white, $\pm 1\sigma$ ranges dashed) and observed (solid orange) exclusion limits on the leptoquark mass as a function of the branching ratio into charged leptons at 95% CL. The observed upper limit on the signal cross-section in each bin is shown on the z-axis. Limits are presented for (a) vector LQs in the Yang–Mills coupling scenario decaying into muons, (b) vector LQs in the Yang–Mills coupling scenario decaying into electrons, (c) vector LQs in the minimal coupling scenario decaying into muons, and (d) vector LQs in the minimal coupling scenario decaying into electrons.

Differences between up- and down-type LQs can be observed especially for low values of \mathcal{B} , where events with $LQLQ \rightarrow t_{\text{lep}}\nu t_{\text{had}}\nu$ increase the sensitivity. The shapes of the exclusion limits for vector LQs with the Yang–Mills and the minimal coupling are very similar, since no significant kinematic differences exist at these higher masses. When comparing the limits for up-type scalar LQs with those for vector LQs, the kinematic differences due to spin correlations in $LQLQ \rightarrow t_{\text{lep}}\nu t_{\text{had}}\nu$ become relevant, i.e. when approaching $\mathcal{B} = 0.0$, the expected lower limit on the mass decreases faster for the vector LQ, as expected from Figure 4(b).

10 Conclusion

Results of a search for pair-produced scalar and vector leptoquarks decaying into quarks of the third generation and charged or neutral leptons of the first or second generation are presented, targeting the single-lepton final state. The analysis is based on data collected by the ATLAS experiment in $\sqrt{s} = 13$ TeV proton–proton collisions, corresponding to an integrated luminosity of 139 fb^{-1} . Several neural networks are trained for various signal hypotheses, covering a wide range of parameters. No significant deviations from the Standard Model expectation are observed and upper limits on the production cross-section are derived for eight models as a function of leptoquark mass and branching ratio into the charged lepton.

In addition, lower limits on the leptoquark mass are set across a range of branching ratios for all models. At a branching ratio of 0.5 they reach values of 1460 GeV (1440 GeV) for up-type scalar leptoquarks decaying into muons (electrons) and 1370 GeV (1390 GeV) for down-type scalar leptoquarks decaying into muons (electrons). For the first time, dedicated neural networks are used to search for U_1 vector leptoquarks. At a branching ratio of 0.5 the resulting lower limits on the mass for the decay into muons are 1980 GeV and 1710 GeV for the Yang–Mills and the minimal coupling scenario, respectively. The decay into electrons is also probed and limits of 1900 GeV (1620 GeV) for the Yang–Mills (minimal) coupling scenario are derived.

Acknowledgements

We thank CERN for the very successful operation of the LHC, as well as the support staff from our institutions without whom ATLAS could not be operated efficiently.

We acknowledge the support of ANPCyT, Argentina; YerPhI, Armenia; ARC, Australia; BMWFW and FWF, Austria; ANAS, Azerbaijan; SSTC, Belarus; CNPq and FAPESP, Brazil; NSERC, NRC and CFI, Canada; CERN; ANID, Chile; CAS, MOST and NSFC, China; Minciencias, Colombia; MEYS CR, Czech Republic; DNRf and DNSRC, Denmark; IN2P3-CNRS and CEA-DRF/IRFU, France; SRNSFG, Georgia; BMBF, HGF and MPG, Germany; GSRI, Greece; RGC and Hong Kong SAR, China; ISF and Benozio Center, Israel; INFN, Italy; MEXT and JSPS, Japan; CNRST, Morocco; NWO, Netherlands; RCN, Norway; MEiN, Poland; FCT, Portugal; MNE/IFA, Romania; JINR; MES of Russia and NRC KI, Russian Federation; MESTD, Serbia; MSSR, Slovakia; ARRS and MIZŠ, Slovenia; DSI/NRF, South Africa; MICINN, Spain; SRC and Wallenberg Foundation, Sweden; SERI, SNSF and Cantons of Bern and Geneva, Switzerland; MOST, Taiwan; TENMAK, Türkiye; STFC, United Kingdom; DOE and NSF, United States of America. In addition, individual groups and members have received support from BCKDF, CANARIE, Compute Canada and CRC, Canada; COST, ERC, ERDF, Horizon 2020 and Marie Skłodowska-Curie Actions, European Union; Investissements d’Avenir Labex, Investissements d’Avenir Idex and ANR, France; DFG

and AvH Foundation, Germany; Herakleitos, Thales and Aristeia programmes co-financed by EU-ESF and the Greek NSRF, Greece; BSF-NSF and GIF, Israel; Norwegian Financial Mechanism 2014-2021, Norway; NCN and NAWA, Poland; La Caixa Banking Foundation, CERCA Programme Generalitat de Catalunya and PROMETEO and GenT Programmes Generalitat Valenciana, Spain; Göran Gustafssons Stiftelse, Sweden; The Royal Society and Leverhulme Trust, United Kingdom.

The crucial computing support from all WLCG partners is acknowledged gratefully, in particular from CERN, the ATLAS Tier-1 facilities at TRIUMF (Canada), NDGF (Denmark, Norway, Sweden), CC-IN2P3 (France), KIT/GridKA (Germany), INFN-CNAF (Italy), NL-T1 (Netherlands), PIC (Spain), ASGC (Taiwan), RAL (UK) and BNL (USA), the Tier-2 facilities worldwide and large non-WLCG resource providers. Major contributors of computing resources are listed in Ref. [116].

References

- [1] H. Georgi and S. Glashow, *Unity of All Elementary Particle Forces*, [Phys. Rev. Lett. **32** \(1974\) 438](#).
- [2] J. C. Pati and A. Salam, *Lepton number as the fourth “color”*, [Phys. Rev. D **10** \(1974\) 275](#).
- [3] W. Buchmüller and D. Wyler, *Constraints on SU(5)-type leptoquarks*, [Phys. Lett. B **177** \(1986\) 377](#).
- [4] S. Dimopoulos and L. Susskind, *Mass without scalars*, [Nucl. Phys. B **155** \(1979\) 237](#).
- [5] S. Dimopoulos, *Technicoloured signatures*, [Nucl. Phys. B **168** \(1980\) 69](#).
- [6] E. Eichten and K. Lane, *Dynamical breaking of weak interaction symmetries*, [Phys. Lett. B **90** \(1980\) 125](#).
- [7] L. F. Abbott and E. Farhi, *Are the weak interactions strong?*, [Phys. Lett. B **101** \(1981\) 69](#).
- [8] L. F. Abbott and E. Farhi, *A confining model of the weak interactions*, [Nucl. Phys. B **189** \(1981\) 547](#).
- [9] B. Schrempp and F. Schrempp, *Light leptoquarks*, [Phys. Lett. B **153** \(1985\) 101](#).
- [10] BaBar Collaboration, *Measurement of an excess of $\bar{B} \rightarrow D^{(*)} \tau^- \bar{\nu}_\tau$ decays and implications for charged Higgs bosons*, [Phys. Rev. D **88** \(2013\) 072012](#), arXiv: [1303.0571](#).
- [11] Belle Collaboration, *Measurement of the branching ratio of $\bar{B} \rightarrow D^{(*)} \tau^- \bar{\nu}_\tau$ relative to $\bar{B} \rightarrow D^{(*)} \ell^- \bar{\nu}_\ell$ decays with hadronic tagging at Belle*, [Phys. Rev. D **92** \(2015\) 072014](#), arXiv: [1507.03233](#).
- [12] LHCb Collaboration, *Measurement of the Ratio of Branching Fractions $\mathcal{B}(\bar{B}^0 \rightarrow D^{*+} \tau^- \bar{\nu}_\tau) / \mathcal{B}(\bar{B}^0 \rightarrow D^{*+} \mu^- \bar{\nu}_\mu)$* , [Phys. Rev. Lett. **115** \(2015\) 111803](#), arXiv: [1506.08614](#),
Erratum: [Phys. Rev. Lett. **115** \(2015\) 159901](#).
- [13] LHCb Collaboration, *Angular analysis of the $B^0 \rightarrow K^{*0} \mu^+ \mu^-$ decay using 3 fb^{-1} of integrated luminosity*, [JHEP **02** \(2016\) 104](#), arXiv: [1512.04442 \[hep-ex\]](#).
- [14] Belle Collaboration, *Measurement of the τ Lepton Polarization and $R(D^*)$ in the Decay $\bar{B} \rightarrow D^* \tau^- \bar{\nu}_\tau$* , [Phys. Rev. Lett. **118** \(2017\) 211801](#), arXiv: [1612.00529 \[hep-ex\]](#).
- [15] Belle Collaboration, *Measurement of the branching ratio of $\bar{B}^0 \rightarrow D^{*+} \tau^- \bar{\nu}_\tau$ relative to $\bar{B}^0 \rightarrow D^{*+} \ell^- \bar{\nu}_\ell$ decays with a semileptonic tagging method*, [Phys. Rev. D **94** \(2016\) 072007](#), arXiv: [1607.07923 \[hep-ex\]](#).
- [16] Belle Collaboration, *Lepton-Flavor-Dependent Angular Analysis of $B \rightarrow K^* \ell^+ \ell^-$* , [Phys. Rev. Lett. **118** \(2017\) 111801](#), arXiv: [1612.05014 \[hep-ex\]](#).
- [17] LHCb Collaboration, *Test of lepton universality with $B^0 \rightarrow K^{*0} \ell^+ \ell^-$ decays*, [JHEP **08** \(2017\) 055](#), arXiv: [1705.05802](#).
- [18] LHCb Collaboration, *Measurement of the ratio of the $B^0 \rightarrow D^{*-} \tau^+ \nu_\tau$ and $B^0 \rightarrow D^{*-} \mu^+ \nu_\mu$ branching fractions using three-prong τ -lepton decays*, [Phys. Rev. Lett. **120** \(2018\) 171802](#), arXiv: [1708.08856 \[hep-ex\]](#).

- [19] LHCb Collaboration, *Measurement of the Ratio of Branching Fractions $\mathcal{B}(B_c^+ \rightarrow J/\psi\tau^+\nu_\tau) / \mathcal{B}(B_c^+ \rightarrow J/\psi\mu^+\nu_\mu)$* , *Phys. Rev. Lett.* **120** (2018) 121801, arXiv: [1711.05623 \[hep-ex\]](#).
- [20] LHCb Collaboration, *Search for lepton-universality violation in $B^+ \rightarrow K^+\ell^+\ell^-$ decays*, *Phys. Rev. Lett.* **122** (2019) 191801, arXiv: [1903.09252 \[hep-ex\]](#).
- [21] LHCb Collaboration, *Test of lepton universality in beauty-quark decays*, *Nature Phys.* **18** (2022) 277, arXiv: [2103.11769 \[hep-ex\]](#).
- [22] G. Hiller and M. Schmaltz, *R_K and future $b \rightarrow s\ell\ell$ physics beyond the standard model opportunities*, *Phys. Rev. D* **90** (2014) 054014, arXiv: [1408.1627 \[hep-ph\]](#).
- [23] B. Gripaios, M. Nardecchia and S. A. Renner, *Composite leptoquarks and anomalies in B -meson decays*, *JHEP* **05** (2015) 006, arXiv: [1412.1791 \[hep-ph\]](#).
- [24] M. Freytsis, Z. Ligeti and J. T. Ruderman, *Flavor models for $\bar{B} \rightarrow D^{(*)}\tau\bar{\nu}$* , *Phys. Rev. D* **92** (2015) 054018, arXiv: [1506.08896 \[hep-ph\]](#).
- [25] L. Di Luzio and M. Nardecchia, *What is the scale of new physics behind the B -flavour anomalies?*, *Eur. Phys. J. C* **77** (2017) 536, arXiv: [1706.01868 \[hep-ph\]](#).
- [26] D. Buttazzo, A. Greljo, G. Isidori and D. Marzocca, *B -physics anomalies: a guide to combined explanations*, *JHEP* **11** (2017) 044, arXiv: [1706.07808 \[hep-ph\]](#).
- [27] J. M. Cline, *B decay anomalies and dark matter from vectorlike confinement*, *Phys. Rev. D* **97** (2018) 015013, arXiv: [1710.02140 \[hep-ph\]](#).
- [28] M. Bauer and M. Neubert, *Minimal Leptoquark Explanation for the $R_{D^{(*)}}$, R_K , and $(g-2)_g$ Anomalies*, *Phys. Rev. Lett.* **116** (2016) 141802, arXiv: [1511.01900 \[hep-ph\]](#).
- [29] E. C. Leskow, G. D'Ambrosio, A. Crivellin and D. Müller, *$(g-2)_\mu$, lepton flavor violation, and Z decays with leptoquarks: Correlations and future prospects*, *Phys. Rev. D* **95** (2017) 055018, arXiv: [1612.06858 \[hep-ph\]](#).
- [30] LHCb Collaboration, *Test of lepton universality in $b \rightarrow s\ell^+\ell^-$ decays*, (2022), arXiv: [2212.09152 \[hep-ex\]](#).
- [31] LHCb Collaboration, *Measurement of lepton universality parameters in $B^+ \rightarrow K^+\ell^+\ell^-$ and $B^0 \rightarrow K^{*0}\ell^+\ell^-$ decays*, (2022), arXiv: [2212.09153 \[hep-ex\]](#).
- [32] D. Chakraverty, D. Choudhury and A. Datta, *A nonsupersymmetric resolution of the anomalous muon magnetic moment*, *Phys. Lett. B* **506** (2001) 103, arXiv: [hep-ph/0102180](#).
- [33] Muon $g-2$ Collaboration, *Measurement of the Positive Muon Anomalous Magnetic Moment to 0.46 ppm*, *Phys. Rev. Lett.* **126** (2021) 141801, arXiv: [2104.03281 \[hep-ex\]](#).
- [34] W. Buchmüller, R. Rückl and D. Wyler, *Leptoquarks in lepton - quark collisions*, *Phys. Lett. B* **191** (1987) 442, Erratum: *Phys. Lett. B* **448** (1999) 320.

- [35] R. Alonso, B. Grinstein and J. Martin Camalich, *Lepton universality violation and lepton flavor conservation in B-meson decays*, [JHEP **10** \(2015\) 184](#), arXiv: [1505.05164 \[hep-ph\]](#).
- [36] R. Barbieri, G. Isidori, A. Pattori and F. Senia, *Anomalies in B-decays and U(2) flavor symmetry*, [Eur. Phys. J. C **76** \(2016\) 67](#), arXiv: [1512.01560 \[hep-ph\]](#).
- [37] ATLAS Collaboration, *Search for pair production of scalar leptoquarks decaying into first- or second-generation leptons and top quarks in proton–proton collisions at $\sqrt{s} = 13$ TeV with the ATLAS detector*, [Eur. Phys. J. C **81** \(2021\) 313](#), arXiv: [2010.02098 \[hep-ex\]](#).
- [38] CMS Collaboration, *Inclusive nonresonant multilepton probes of new phenomena at $\sqrt{s} = 13$ TeV*, [Phys. Rev. D **105** \(2022\) 112007](#), arXiv: [2202.08676 \[hep-ex\]](#).
- [39] ATLAS Collaboration, *Search for pairs of scalar leptoquarks decaying into quarks and electrons or muons in $\sqrt{s} = 13$ TeV pp collisions with the ATLAS detector*, [JHEP **10** \(2020\) 112](#), arXiv: [2006.05872 \[hep-ex\]](#).
- [40] CMS Collaboration, *Search for Leptoquarks Coupled to Third-Generation Quarks in Proton–Proton Collisions at $\sqrt{s} = 13$ TeV*, [Phys. Rev. Lett. **121** \(2018\) 241802](#), arXiv: [1809.05558 \[hep-ex\]](#).
- [41] T. Mandal, S. Mitra and S. Seth, *Pair production of scalar leptoquarks at the LHC to NLO parton shower accuracy*, [Phys. Rev. D **93** \(2016\) 035018](#), arXiv: [1506.07369 \[hep-ph\]](#).
- [42] ATLAS Collaboration, *Searches for third-generation scalar leptoquarks in $\sqrt{s} = 13$ TeV pp collisions with the ATLAS detector*, [JHEP **06** \(2019\) 144](#), arXiv: [1902.08103 \[hep-ex\]](#).
- [43] M. J. Baker, J. Fuentes-Martín, G. Isidori and M. König, *High- p_T signatures in vector–leptoquark models*, [Eur. Phys. J. C **79** \(2019\) 334](#), arXiv: [1901.10480 \[hep-ph\]](#).
- [44] ATLAS Collaboration, *The ATLAS Experiment at the CERN Large Hadron Collider*, [JINST **3** \(2008\) S08003](#).
- [45] ATLAS Collaboration, *The ATLAS Collaboration Software and Firmware*, ATL-SOFT-PUB-2021-001, 2021, URL: <https://cds.cern.ch/record/2767187>.
- [46] ATLAS Collaboration, *ATLAS data quality operations and performance for 2015–2018 data-taking*, [JINST **15** \(2020\) P04003](#), arXiv: [1911.04632 \[physics.ins-det\]](#).
- [47] E. Bothmann et al., *Event generation with Sherpa 2.2*, [SciPost Phys. **7** \(2019\) 034](#), arXiv: [1905.09127 \[hep-ph\]](#).
- [48] D. J. Lange, *The EvtGen particle decay simulation package*, [Nucl. Instrum. Meth. A **462** \(2001\) 152](#).
- [49] T. Sjöstrand, S. Mrenna and P. Skands, *A brief introduction to PYTHIA 8.1*, [Comput. Phys. Commun. **178** \(2008\) 852](#), arXiv: [0710.3820 \[hep-ph\]](#).
- [50] ATLAS Collaboration, *The Pythia 8 A3 tune description of ATLAS minimum bias and inelastic measurements incorporating the Donnachie–Landshoff diffractive model*, ATL-PHYS-PUB-2016-017, 2016, URL: <https://cds.cern.ch/record/2206965>.

- [51] ATLAS Collaboration, *The ATLAS Simulation Infrastructure*, *Eur. Phys. J. C* **70** (2010) 823, arXiv: [1005.4568 \[physics.ins-det\]](#).
- [52] GEANT4 Collaboration, S. Agostinelli et al., *GEANT4 – a simulation toolkit*, *Nucl. Instrum. Meth. A* **506** (2003) 250.
- [53] J. Alwall et al., *The automated computation of tree-level and next-to-leading order differential cross sections, and their matching to parton shower simulations*, *JHEP* **07** (2014) 079, arXiv: [1405.0301 \[hep-ph\]](#).
- [54] R. D. Ball et al., *Parton distributions for the LHC run II*, *JHEP* **04** (2015) 040, arXiv: [1410.8849 \[hep-ph\]](#).
- [55] M. Krämer, T. Plehn, M. Spira and P. M. Zerwas, *Pair production of scalar leptoquarks at the CERN LHC*, *Phys. Rev. D* **71** (2005) 057503, arXiv: [hep-ph/0411038](#).
- [56] M. Krämer, T. Plehn, M. Spira and P. M. Zerwas, *Pair Production of Scalar Leptoquarks at the Fermilab Tevatron*, *Phys. Rev. Lett.* **79** (1997) 341, arXiv: [hep-ph/9704322](#).
- [57] P. Artoisenet, R. Frederix, O. Mattelaer and R. Rietkerk, *Automatic spin-entangled decays of heavy resonances in Monte Carlo simulations*, *JHEP* **03** (2013) 015, arXiv: [1212.3460 \[hep-ph\]](#).
- [58] T. Sjöstrand et al., *An introduction to PYTHIA 8.2*, *Comput. Phys. Commun.* **191** (2015) 159, arXiv: [1410.3012 \[hep-ph\]](#).
- [59] ATLAS Collaboration, *ATLAS Pythia 8 tunes to 7 TeV data*, ATL-PHYS-PUB-2014-021, 2014, URL: <https://cds.cern.ch/record/1966419>.
- [60] R. D. Ball et al., *Parton distributions with LHC data*, *Nucl. Phys. B* **867** (2013) 244, arXiv: [1207.1303 \[hep-ph\]](#).
- [61] W. Beenakker, C. Borschensky, M. Krämer, A. Kulesza and E. Laenen, *NNLL-fast: predictions for coloured supersymmetric particle production at the LHC with threshold and Coulomb resummation*, *JHEP* **12** (2016) 133, arXiv: [1607.07741 \[hep-ph\]](#).
- [62] W. Beenakker, M. Krämer, T. Plehn, M. Spira and P. M. Zerwas, *Stop production at hadron colliders*, *Nucl. Phys. B* **515** (1998) 3, arXiv: [hep-ph/9710451](#).
- [63] W. Beenakker et al., *Supersymmetric top and bottom squark production at hadron colliders*, *JHEP* **08** (2010) 098, arXiv: [1006.4771 \[hep-ph\]](#).
- [64] W. Beenakker et al., *NNLL resummation for stop pair-production at the LHC*, *JHEP* **05** (2016) 153, arXiv: [1601.02954 \[hep-ph\]](#).
- [65] C. Borschensky, B. Fuks, A. Kulesza and D. Schwartländer, *Scalar leptoquark pair production at hadron colliders*, *Phys. Rev. D* **101** (2020) 115017, arXiv: [2002.08971 \[hep-ph\]](#).
- [66] URL: <https://feynrules.irmp.ucl.ac.be/wiki/LeptoQuark>.
- [67] S. Frixione, G. Ridolfi and P. Nason, *A positive-weight next-to-leading-order Monte Carlo for heavy flavour hadroproduction*, *JHEP* **09** (2007) 126, arXiv: [0707.3088 \[hep-ph\]](#).
- [68] P. Nason, *A new method for combining NLO QCD with shower Monte Carlo algorithms*, *JHEP* **11** (2004) 040, arXiv: [hep-ph/0409146](#).

- [69] S. Frixione, P. Nason and C. Oleari, *Matching NLO QCD computations with parton shower simulations: the POWHEG method*, [JHEP **11** \(2007\) 070](#), arXiv: [0709.2092 \[hep-ph\]](#).
- [70] S. Alioli, P. Nason, C. Oleari and E. Re, *A general framework for implementing NLO calculations in shower Monte Carlo programs: the POWHEG BOX*, [JHEP **06** \(2010\) 043](#), arXiv: [1002.2581 \[hep-ph\]](#).
- [71] ATLAS Collaboration, *Studies on top-quark Monte Carlo modelling for Top2016*, ATL-PHYS-PUB-2016-020, 2016, URL: <https://cds.cern.ch/record/2216168>.
- [72] M. Czakon and A. Mitov, *Top++: A program for the calculation of the top-pair cross-section at hadron colliders*, [Comput. Phys. Commun. **185** \(2014\) 2930](#), arXiv: [1112.5675 \[hep-ph\]](#).
- [73] S. Frixione, E. Laenen, P. Motylinski, C. White and B. R. Webber, *Single-top hadroproduction in association with a W boson*, [JHEP **07** \(2008\) 029](#), arXiv: [0805.3067 \[hep-ph\]](#).
- [74] T. Gleisberg and S. Höche, *Comix, a new matrix element generator*, [JHEP **12** \(2008\) 039](#), arXiv: [0808.3674 \[hep-ph\]](#).
- [75] F. Cascioli, P. Maierhöfer and S. Pozzorini, *Scattering Amplitudes with Open Loops*, [Phys. Rev. Lett. **108** \(2012\) 111601](#), arXiv: [1111.5206 \[hep-ph\]](#).
- [76] A. Denner, S. Dittmaier and L. Hofer, *COLLIER: A fortran-based complex one-loop library in extended regularizations*, [Comput. Phys. Commun. **212** \(2017\) 220](#), arXiv: [1604.06792 \[hep-ph\]](#).
- [77] S. Schumann and F. Krauss, *A parton shower algorithm based on Catani–Seymour dipole factorisation*, [JHEP **03** \(2008\) 038](#), arXiv: [0709.1027 \[hep-ph\]](#).
- [78] S. Höche, F. Krauss, M. Schönherr and F. Siegert, *A critical appraisal of NLO+PS matching methods*, [JHEP **09** \(2012\) 049](#), arXiv: [1111.1220 \[hep-ph\]](#).
- [79] S. Höche, F. Krauss, M. Schönherr and F. Siegert, *QCD matrix elements + parton showers. The NLO case*, [JHEP **04** \(2013\) 027](#), arXiv: [1207.5030 \[hep-ph\]](#).
- [80] S. Catani, F. Krauss, B. R. Webber and R. Kuhn, *QCD Matrix Elements + Parton Showers*, [JHEP **11** \(2001\) 063](#), arXiv: [hep-ph/0109231](#).
- [81] S. Höche, F. Krauss, S. Schumann and F. Siegert, *QCD matrix elements and truncated showers*, [JHEP **05** \(2009\) 053](#), arXiv: [0903.1219 \[hep-ph\]](#).
- [82] C. Anastasiou, L. Dixon, K. Melnikov and F. Petriello, *High-precision QCD at hadron colliders: Electroweak gauge boson rapidity distributions at next-to-next-to leading order*, [Phys. Rev. D **69** \(2004\) 094008](#), arXiv: [hep-ph/0312266](#).
- [83] ATLAS Collaboration, *Electron and photon performance measurements with the ATLAS detector using the 2015–2017 LHC proton–proton collision data*, [JINST **14** \(2019\) P12006](#), arXiv: [1908.00005 \[hep-ex\]](#).
- [84] ATLAS Collaboration, *Muon reconstruction and identification efficiency in ATLAS using the full Run 2 pp collision data set at $\sqrt{s} = 13$ TeV*, [Eur. Phys. J. C **81** \(2021\) 578](#), arXiv: [2012.00578 \[hep-ex\]](#).

- [85] ATLAS Collaboration, *Jet reconstruction and performance using particle flow with the ATLAS Detector*, *Eur. Phys. J. C* **77** (2017) 466, arXiv: [1703.10485 \[hep-ex\]](#).
- [86] ATLAS Collaboration, *Jet energy scale and resolution measured in proton–proton collisions at $\sqrt{s} = 13$ TeV with the ATLAS detector*, *Eur. Phys. J. C* **81** (2020) 689, arXiv: [2007.02645 \[hep-ex\]](#).
- [87] M. Cacciari, G. P. Salam and G. Soyez, *The anti- k_t jet clustering algorithm*, *JHEP* **04** (2008) 063, arXiv: [0802.1189 \[hep-ph\]](#).
- [88] M. Cacciari, G. P. Salam and G. Soyez, *FastJet user manual*, *Eur. Phys. J. C* **72** (2012) 1896, arXiv: [1111.6097 \[hep-ph\]](#).
- [89] ATLAS Collaboration, *Tagging and suppression of pileup jets with the ATLAS detector*, ATLAS-CONF-2014-018, 2014, URL: <https://cds.cern.ch/record/1700870>.
- [90] ATLAS Collaboration, *ATLAS b -jet identification performance and efficiency measurement with $t\bar{t}$ events in pp collisions at $\sqrt{s} = 13$ TeV*, *Eur. Phys. J. C* **79** (2019) 970, arXiv: [1907.05120 \[hep-ex\]](#).
- [91] ATLAS Collaboration, *Optimisation and performance studies of the ATLAS b -tagging algorithms for the 2017-18 LHC run*, ATL-PHYS-PUB-2017-013, 2017, URL: <https://cds.cern.ch/record/2273281>.
- [92] ATLAS Collaboration, *Search for top-squark pair production in final states with one lepton, jets, and missing transverse momentum using 36fb^{-1} of $\sqrt{s} = 13$ TeV pp collision data with the ATLAS detector*, *JHEP* **06** (2018) 108, arXiv: [1711.11520 \[hep-ex\]](#).
- [93] ATLAS Collaboration, *Performance of missing transverse momentum reconstruction with the ATLAS detector using proton–proton collisions at $\sqrt{s} = 13$ TeV*, *Eur. Phys. J. C* **78** (2018) 903, arXiv: [1802.08168 \[hep-ex\]](#).
- [94] ATLAS Collaboration, *Performance of the missing transverse momentum triggers for the ATLAS detector during Run-2 data taking*, *JHEP* **08** (2020) 080, arXiv: [2005.09554 \[hep-ex\]](#).
- [95] ATLAS Collaboration, *Measurement of the $t\bar{t}$ production cross-section and lepton differential distributions in $e\mu$ dilepton events from pp collisions at $\sqrt{s} = 13$ TeV with the ATLAS detector*, *Eur. Phys. J. C* **80** (2020) 528, arXiv: [1910.08819 \[hep-ex\]](#).
- [96] ATLAS Collaboration, *Measurements of top-quark pair differential and double-differential cross-sections in the ℓ +jets channel with pp collisions at $\sqrt{s} = 13$ TeV using the ATLAS detector*, *Eur. Phys. J. C* **79** (2019) 1028, arXiv: [1908.07305 \[hep-ex\]](#), Erratum: *Eur. Phys. J. C* **80** (2020) 1092.
- [97] C. Lester and D. Summers, *Measuring masses of semi-invisibly decaying particle pairs produced at hadron colliders*, *Phys. Lett. B* **463** (1999) 99, arXiv: [hep-ph/9906349](#).
- [98] A. J. Barr, B. Gripaios and C. G. Lester, *Transverse masses and kinematic constraints: from the boundary to the crease*, *JHEP* **11** (2009) 096, arXiv: [0908.3779 \[hep-ph\]](#).
- [99] Y. Bai, H.-C. Cheng, J. Gallicchio and J. Gu, *Stop the top background of the stop search*, *JHEP* **07** (2012) 110, arXiv: [1203.4813 \[hep-ph\]](#).

- [100] M. Feindt, *A Neural Bayesian Estimator for Conditional Probability Densities*, 2004, arXiv: [physics/0402093](https://arxiv.org/abs/physics/0402093) [[physics.data-an](#)].
- [101] M. Feindt and U. Kerzel, *The NeuroBayes Neural Network Package*, *Nucl. Instrum. Meth. A* **559** (2006) 190.
- [102] ATLAS Collaboration, *Studies of $t\bar{t}/tW$ interference effects in $b\bar{b}\ell^+\ell'^-\nu\bar{\nu}'$ final states with POWHEG and MADGRAPH5_AMC@NLO setups*, ATL-PHYS-PUB-2021-042, 2021, URL: <https://cds.cern.ch/record/2792254>.
- [103] J. Bellm et al., *Herwig 7.1 Release Note*, (2017), arXiv: [1705.06919](https://arxiv.org/abs/1705.06919) [[hep-ph](#)].
- [104] J. Butterworth et al., *PDF4LHC recommendations for LHC Run II*, *J. Phys. G* **43** (2016) 023001, arXiv: [1510.03865](https://arxiv.org/abs/1510.03865) [[hep-ph](#)].
- [105] E. Re, *Single-top Wt -channel production matched with parton showers using the POWHEG method*, *Eur. Phys. J. C* **71** (2011) 1547, arXiv: [1009.2450](https://arxiv.org/abs/1009.2450) [[hep-ph](#)].
- [106] ATLAS Collaboration, *Multi-boson simulation for 13 TeV ATLAS analyses*, ATL-PHYS-PUB-2016-002, 2016, URL: <https://cds.cern.ch/record/2119986>.
- [107] ATLAS Collaboration, *Measurement of W^\pm and Z-boson production cross sections in pp collisions at $\sqrt{s} = 13$ TeV with the ATLAS detector*, *Phys. Lett. B* **759** (2016) 601, arXiv: [1603.09222](https://arxiv.org/abs/1603.09222) [[hep-ex](#)].
- [108] D. de Florian et al., *Handbook of LHC Higgs Cross Sections: 4. Deciphering the Nature of the Higgs Sector*, (2016), arXiv: [1610.07922](https://arxiv.org/abs/1610.07922) [[hep-ph](#)].
- [109] ATLAS Collaboration, *Measurement of the $t\bar{t}Z$ and $t\bar{t}W$ cross sections in proton–proton collisions at $\sqrt{s} = 13$ TeV with the ATLAS detector*, *Phys. Rev. D* **99** (2019) 072009, arXiv: [1901.03584](https://arxiv.org/abs/1901.03584) [[hep-ex](#)].
- [110] ATLAS Collaboration, *E_T^{miss} performance in the ATLAS detector using 2015–2016 LHC pp collisions*, ATLAS-CONF-2018-023, 2018, URL: <https://cds.cern.ch/record/2625233>.
- [111] ATLAS Collaboration, *Luminosity determination in pp collisions at $\sqrt{s} = 13$ TeV using the ATLAS detector at the LHC*, ATLAS-CONF-2019-021, 2019, URL: <https://cds.cern.ch/record/2677054>.
- [112] G. Avoni et al., *The new LUCID-2 detector for luminosity measurement and monitoring in ATLAS*, *JINST* **13** (2018) P07017.
- [113] W. Verkerke and D. Kirkby, *The RooFit toolkit for data modeling*, 2003, arXiv: [physics/0306116](https://arxiv.org/abs/physics/0306116) [[physics.data-an](#)].
- [114] A. L. Read, *Presentation of search results: the CL_S technique*, *J. Phys. G* **28** (2002) 2693.
- [115] G. Cowan, K. Cranmer, E. Gross and O. Vitells, *Asymptotic formulae for likelihood-based tests of new physics*, *Eur. Phys. J. C* **71** (2011) 1554, arXiv: [1007.1727](https://arxiv.org/abs/1007.1727) [[physics.data-an](#)], Erratum: *Eur. Phys. J. C* **73** (2013) 2501.
- [116] ATLAS Collaboration, *ATLAS Computing Acknowledgements*, ATL-SOFT-PUB-2021-003, URL: <https://cds.cern.ch/record/2776662>.

The ATLAS Collaboration

G. Aad¹⁰¹, B. Abbott¹¹⁹, D.C. Abbott¹⁰², K. Abeling⁵⁵, S.H. Abidi²⁹, A. Abouhorma^{35e},
H. Abramowicz¹⁵⁰, H. Abreu¹⁴⁹, Y. Abulaiti¹¹⁶, A.C. Abusleme Hoffman^{136a}, B.S. Acharya^{68a,68b,o},
B. Achkar⁵⁵, L. Adam⁹⁹, C. Adam Bourdarios⁴, L. Adamczyk^{84a}, L. Adamek¹⁵⁴, S.V. Addepalli²⁶,
J. Adelman¹¹⁴, A. Adiguzel^{21c}, S. Adorni⁵⁶, T. Adye¹³³, A.A. Affolder¹³⁵, Y. Afik³⁶, M.N. Agaras¹³,
J. Agarwala^{72a,72b}, A. Aggarwal⁹⁹, C. Agheorghiesei^{27c}, J.A. Aguilar-Saavedra^{129f}, A. Ahmad³⁶,
F. Ahmadov^{38,w}, W.S. Ahmed¹⁰³, X. Ai⁴⁸, G. Aielli^{75a,75b}, I. Aizenberg¹⁶⁷, M. Akbiyik⁹⁹,
T.P.A. Åkesson⁹⁷, A.V. Akimov³⁷, K. Al Khoury⁴¹, G.L. Alberghi^{23b}, J. Albert¹⁶³, P. Albicocco⁵³,
M.J. Alconada Verzini⁸⁹, S. Alderweireldt⁵², M. Aleksa³⁶, I.N. Aleksandrov³⁸, C. Alexa^{27b},
T. Alexopoulos¹⁰, A. Alfonsi¹¹³, F. Alfonsi^{23b}, M. Alhroob¹¹⁹, B. Ali¹³¹, S. Ali¹⁴⁷, M. Aliev³⁷,
G. Alimonti^{70a}, C. Allaire³⁶, B.M.M. Allbrooke¹⁴⁵, P.P. Allport²⁰, A. Aloisio^{71a,71b}, F. Alonso⁸⁹,
C. Alpigiani¹³⁷, E. Alunno Camelia^{75a,75b}, M. Alvarez Estevez⁹⁸, M.G. Alvigi^{71a,71b},
Y. Amaral Coutinho^{81b}, A. Ambler¹⁰³, C. Amelung³⁶, C.G. Ames¹⁰⁸, D. Amidei¹⁰⁵,
S.P. Amor Dos Santos^{129a}, S. Amoroso⁴⁸, K.R. Amos¹⁶¹, C.S. Amrouche⁵⁶, V. Ananiev¹²⁴,
C. Anastopoulos¹³⁸, N. Andari¹³⁴, T. Andeen¹¹, J.K. Anders¹⁹, S.Y. Andrean^{47a,47b}, A. Andreazza^{70a,70b},
S. Angelidakis⁹, A. Angerami^{41,y}, A.V. Anisenkov³⁷, A. Annovi^{73a}, C. Antel⁵⁶, M.T. Anthony¹³⁸,
E. Antipov¹²⁰, M. Antonelli⁵³, D.J.A. Antrim^{17a}, F. Anulli^{74a}, M. Aoki⁸², J.A. Aparisi Pozo¹⁶¹,
M.A. Aparo¹⁴⁵, L. Aperio Bella⁴⁸, C. Appelt¹⁸, N. Aranzabal³⁶, V. Araujo Ferraz^{81a}, C. Arcangeletti⁵³,
A.T.H. Arce⁵¹, E. Arena⁹¹, J-F. Arguin¹⁰⁷, S. Argyropoulos⁵⁴, J.-H. Arling⁴⁸, A.J. Armbruster³⁶,
O. Arnaez¹⁵⁴, H. Arnold¹¹³, Z.P. Arrubarrena Tame¹⁰⁸, G. Artoni^{74a,74b}, H. Asada¹¹⁰, K. Asai¹¹⁷,
S. Asai¹⁵², N.A. Asbah⁶¹, E.M. Asimakopoulou¹⁵⁹, J. Assahsah^{35d}, K. Assamagan²⁹, R. Astalos^{28a},
R.J. Atkin^{33a}, M. Atkinson¹⁶⁰, N.B. Atlay¹⁸, H. Atmani^{62b}, P.A. Atmasiddha¹⁰⁵, K. Augsten¹³¹,
S. Auricchio^{71a,71b}, A.D. Aurio²⁰, V.A. Austrup¹⁶⁹, G. Avner¹⁴⁹, G. Avolio³⁶, K. Axiotis⁵⁶,
M.K. Ayoub^{14c}, G. Azuelos^{107,ac}, D. Babal^{28a}, H. Bachacou¹³⁴, K. Bachas^{151,q}, A. Bachi³⁴,
F. Backman^{47a,47b}, A. Badea⁶¹, P. Bagnaia^{74a,74b}, M. Bahmani¹⁸, A.J. Bailey¹⁶¹, V.R. Bailey¹⁶⁰,
J.T. Baines¹³³, C. Bakalis¹⁰, O.K. Baker¹⁷⁰, P.J. Bakker¹¹³, E. Bakos¹⁵, D. Bakshi Gupta⁸, S. Balaji¹⁴⁶,
R. Balasubramanian¹¹³, E.M. Baldin³⁷, P. Balek¹³², E. Ballabene^{70a,70b}, F. Balli¹³⁴, L.M. Baltés^{63a},
W.K. Balunas³², J. Balz⁹⁹, E. Banas⁸⁵, M. Bandieramonte¹²⁸, A. Bandyopadhyay²⁴, S. Bansal²⁴,
L. Barak¹⁵⁰, E.L. Barberio¹⁰⁴, D. Barberis^{57b,57a}, M. Barbero¹⁰¹, G. Barbour⁹⁵, K.N. Barends^{33a},
T. Barillari¹⁰⁹, M-S. Barisits³⁶, J. Barkeloo¹²², T. Barklow¹⁴², R.M. Barnett^{17a}, P. Baron¹²¹,
D.A. Baron Moreno¹⁰⁰, A. Baroncelli^{62a}, G. Barone²⁹, A.J. Barr¹²⁵, L. Barranco Navarro^{47a,47b},
F. Barreiro⁹⁸, J. Barreiro Guimarães da Costa^{14a}, U. Barron¹⁵⁰, M.G. Barros Teixeira^{129a}, S. Barsov³⁷,
F. Bartels^{63a}, R. Bartoldus¹⁴², A.E. Barton⁹⁰, P. Bartos^{28a}, A. Basalae⁴⁸, A. Basan⁹⁹, M. Baselga⁴⁹,
I. Bashta^{76a,76b}, A. Bassalat^{66,z}, M.J. Basso¹⁵⁴, C.R. Basson¹⁰⁰, R.L. Bates⁵⁹, S. Batlamous^{35e},
J.R. Batley³², B. Batool¹⁴⁰, M. Battaglia¹³⁵, M. Bause^{74a,74b}, P. Bauer²⁴, A. Bayirli^{21a}, J.B. Beacham⁵¹,
T. Beau¹²⁶, P.H. Beauchemin¹⁵⁷, F. Becherer⁵⁴, P. Bechtel²⁴, H.P. Beck^{19,p}, K. Becker¹⁶⁵, C. Becot⁴⁸,
A.J. Beddall^{21d}, V.A. Bednyakov³⁸, C.P. Bee¹⁴⁴, L.J. Beemster¹⁵, T.A. Beermann³⁶, M. Begalli^{81b,81d},
M. Begel²⁹, A. Behara¹⁴⁴, J.K. Behr⁴⁸, C. Beirao Da Cruz E Silva³⁶, J.F. Beirer^{55,36}, F. Beisiegel²⁴,
M. Belfkir^{115b}, G. Bella¹⁵⁰, L. Bellagamba^{23b}, A. Bellerive³⁴, P. Bellos²⁰, K. Beloborodov³⁷,
K. Belotskiy³⁷, N.L. Belyaev³⁷, D. Bencheekroun^{35a}, F. Bendebba^{35a}, Y. Benhammou¹⁵⁰, D.P. Benjamin²⁹,
M. Benoit²⁹, J.R. Bensinger²⁶, S. Bentvelsen¹¹³, L. Beresford³⁶, M. Beretta⁵³, D. Berge¹⁸,
E. Bergeas Kuutmann¹⁵⁹, N. Berger⁴, B. Bergmann¹³¹, J. Beringer^{17a}, S. Berlendis⁷, G. Bernardi⁵,
C. Bernius¹⁴², F.U. Bernlochner²⁴, T. Berry⁹⁴, P. Berta¹³², A. Berthold⁵⁰, I.A. Bertram⁹⁰,
O. Bessidskaia Bylund¹⁶⁹, S. Bethke¹⁰⁹, A. Betti⁴⁴, A.J. Bevan⁹³, M. Bhamjee^{33c}, S. Bhatta¹⁴⁴,
D.S. Bhattacharya¹⁶⁴, P. Bhattarai²⁶, V.S. Bhopatkar⁶, R. Bi¹²⁸, R. Bi^{29,af}, R.M. Bianchi¹²⁸, O. Biebel¹⁰⁸,

R. Bielski¹²², N.V. Biesuz^{73a,73b}, M. Biglietti^{76a}, T.R.V. Billoud¹³¹, M. Bindi⁵⁵, A. Bingul^{21b}, C. Bini^{74a,74b}, S. Biondi^{23b,23a}, A. Biondini⁹¹, C.J. Birch-sykes¹⁰⁰, G.A. Bird^{20,133}, M. Birman¹⁶⁷, T. Bisanz³⁶, D. Biswas^{168,k}, A. Bitadze¹⁰⁰, K. Bjørke¹²⁴, I. Bloch⁴⁸, C. Blocker²⁶, A. Blue⁵⁹, U. Blumenschein⁹³, J. Blumenthal⁹⁹, G.J. Bobbink¹¹³, V.S. Bobrovnikov³⁷, M. Boehler⁵⁴, D. Bogavac³⁶, A.G. Bogdanchikov³⁷, C. Bohm^{47a}, V. Boisvert⁹⁴, P. Bokan⁴⁸, T. Bold^{84a}, M. Bomben⁵, M. Bona⁹³, M. Boonekamp¹³⁴, C.D. Booth⁹⁴, A.G. Borbély⁵⁹, H.M. Borecka-Bielska¹⁰⁷, L.S. Borgna⁹⁵, G. Borisso⁹⁰, D. Bortoletto¹²⁵, D. Boscherini^{23b}, M. Bosman¹³, J.D. Bossio Sola³⁶, K. Bouaouda^{35a}, J. Boudreau¹²⁸, E.V. Bouhova-Thacker⁹⁰, D. Boumediene⁴⁰, R. Bouquet⁵, A. Boveia¹¹⁸, J. Boyd³⁶, D. Boye²⁹, I.R. Boyko³⁸, J. Bracinik²⁰, N. Brahimi^{62d,62c}, G. Brandt¹⁶⁹, O. Brandt³², F. Braren⁴⁸, B. Brau¹⁰², J.E. Brau¹²², W.D. Breaden Madden⁵⁹, K. Brendlinger⁴⁸, R. Brenner¹⁶⁷, L. Brenner³⁶, R. Brenner¹⁵⁹, S. Bressler¹⁶⁷, B. Brickwedde⁹⁹, D. Britton⁵⁹, D. Britzger¹⁰⁹, I. Brock²⁴, G. Brooijmans⁴¹, W.K. Brooks^{136f}, E. Brost²⁹, P.A. Bruckman de Renstrom⁸⁵, B. Brüers⁴⁸, D. Bruncko^{28b,*}, A. Bruni^{23b}, G. Bruni^{23b}, M. Bruschi^{23b}, N. Brusino^{74a,74b}, L. Bryngemark¹⁴², T. Buanes¹⁶, Q. Buat¹³⁷, P. Buchholz¹⁴⁰, A.G. Buckley⁵⁹, I.A. Budagov^{38,*}, M.K. Bugge¹²⁴, O. Bulekov³⁷, B.A. Bullard⁶¹, S. Burdin⁹¹, C.D. Burgard⁴⁸, A.M. Burger⁴⁰, B. Burghgrave⁸, J.T.P. Burr³², C.D. Burton¹¹, J.C. Burzynski¹⁴¹, E.L. Busch⁴¹, V. Büscher⁹⁹, P.J. Bussey⁵⁹, J.M. Butler²⁵, C.M. Buttar⁵⁹, J.M. Butterworth⁹⁵, W. Buttinger¹³³, C.J. Buxo Vazquez¹⁰⁶, A.R. Buzykaev³⁷, G. Cabras^{23b}, S. Cabrera Urbán¹⁶¹, D. Caforio⁵⁸, H. Cai¹²⁸, Y. Cai^{14a,14d}, V.M.M. Cairo³⁶, O. Cakir^{3a}, N. Calace³⁶, P. Calafiura^{17a}, G. Calderini¹²⁶, P. Calfayan⁶⁷, G. Callea⁵⁹, L.P. Caloba^{81b}, D. Calvet⁴⁰, S. Calvet⁴⁰, T.P. Calvet¹⁰¹, M. Calvetti^{73a,73b}, R. Camacho Toro¹²⁶, S. Camarda³⁶, D. Camarero Munoz⁹⁸, P. Camarri^{75a,75b}, M.T. Camerlingo^{76a,76b}, D. Cameron¹²⁴, C. Camincher¹⁶³, M. Campanelli⁹⁵, A. Camplani⁴², V. Canale^{71a,71b}, A. Canesse¹⁰³, M. Cano Bret⁷⁹, J. Cantero¹⁶¹, Y. Cao¹⁶⁰, F. Capocasa²⁶, M. Capua^{43b,43a}, A. Carbone^{70a,70b}, R. Cardarelli^{75a}, J.C.J. Cardenas⁸, F. Cardillo¹⁶¹, T. Carli³⁶, G. Carlino^{71a}, B.T. Carlson^{128,r}, E.M. Carlson^{163,155a}, L. Carminati^{70a,70b}, M. Carnesale^{74a,74b}, S. Caron¹¹², E. Carquin^{136f}, S. Carrá^{70a,70b}, G. Carratta^{23b,23a}, F. Carrio Argos^{33g}, J.W.S. Carter¹⁵⁴, T.M. Carter⁵², M.P. Casado^{13,h}, A.F. Casha¹⁵⁴, E.G. Castiglia¹⁷⁰, F.L. Castillo^{63a}, L. Castillo Garcia¹³, V. Castillo Gimenez¹⁶¹, N.F. Castro^{129a,129e}, A. Catinaccio³⁶, J.R. Catmore¹²⁴, V. Cavaliere²⁹, N. Cavalli^{23b,23a}, V. Cavasinni^{73a,73b}, E. Celebi^{21a}, F. Celli¹²⁵, M.S. Centonze^{69a,69b}, K. Cerny¹²¹, A.S. Cerqueira^{81a}, A. Cerri¹⁴⁵, L. Cerrito^{75a,75b}, F. Cerutti^{17a}, A. Cervelli^{23b}, S.A. Cetin^{21d}, Z. Chadi^{35a}, D. Chakraborty¹¹⁴, M. Chala^{129f}, J. Chan¹⁶⁸, W.S. Chan¹¹³, W.Y. Chan¹⁵², J.D. Chapman³², B. Chargeishvili^{148b}, D.G. Charlton²⁰, T.P. Charman⁹³, M. Chatterjee¹⁹, S. Chekanov⁶, S.V. Chekulaev^{155a}, G.A. Chelkov^{38,a}, A. Chen¹⁰⁵, B. Chen¹⁵⁰, B. Chen¹⁶³, C. Chen^{62a}, H. Chen^{14c}, H. Chen²⁹, J. Chen^{62c}, J. Chen²⁶, S. Chen¹⁵², S.J. Chen^{14c}, X. Chen^{62c}, X. Chen^{14b,ab}, Y. Chen^{62a}, C.L. Cheng¹⁶⁸, H.C. Cheng^{64a}, A. Cheplakov³⁸, E. Cheremushkina⁴⁸, E. Cherepanova¹¹³, R. Cherkaoui El Moursli^{35e}, E. Cheu⁷, K. Cheung⁶⁵, L. Chevalier¹³⁴, V. Chiarella⁵³, G. Chiarelli^{73a}, G. Chiodini^{69a}, A.S. Chisholm²⁰, A. Chitan^{27b}, Y.H. Chiu¹⁶³, M.V. Chizhov³⁸, K. Choi¹¹, A.R. Chomont^{74a,74b}, Y. Chou¹⁰², E.Y.S. Chow¹¹³, T. Chowdhury^{33g}, L.D. Christopher^{33g}, K.L. Chu^{64a}, M.C. Chu^{64a}, X. Chu^{14a,14d}, J. Chudoba¹³⁰, J.J. Chwastowski⁸⁵, D. Cieri¹⁰⁹, K.M. Ciesla^{84a}, V. Cindro⁹², A. Ciocio^{17a}, F. Ciotto^{71a,71b}, Z.H. Citron^{167,1}, M. Citterio^{70a}, D.A. Ciubotaru^{27b}, B.M. Ciungu¹⁵⁴, A. Clark⁵⁶, P.J. Clark⁵², J.M. Clavijo Columbie⁴⁸, S.E. Clawson¹⁰⁰, C. Clement^{47a,47b}, J. Clercx⁴⁸, L. Clissa^{23b,23a}, Y. Coadou¹⁰¹, M. Cobal^{168a,68c}, A. Coccaro^{57b}, R.F. Coelho Barrue^{129a}, R. Coelho Lopes De Sa¹⁰², S. Coelli^{70a}, H. Cohen¹⁵⁰, A.E.C. Coimbra^{70a,70b}, B. Cole⁴¹, J. Collot⁶⁰, P. Conde Muiño^{129a,129g}, S.H. Connell^{33c}, I.A. Connelly⁵⁹, E.I. Conroy¹²⁵, F. Conventi^{71a,ad}, H.G. Cooke²⁰, A.M. Cooper-Sarkar¹²⁵, F. Cormier¹⁶², L.D. Corpe³⁶, M. Corradi^{74a,74b}, E.E. Corrigan⁹⁷, F. Corriveau^{103,v}, A. Cortes-Gonzalez¹⁸, M.J. Costa¹⁶¹, F. Costanza⁴, D. Costanzo¹³⁸, B.M. Cote¹¹⁸, G. Cowan⁹⁴, J.W. Cowley³², K. Cranmer¹¹⁶, S. Crépe-Renaudin⁶⁰, F. Crescioli¹²⁶, M. Cristinziani¹⁴⁰, M. Cristoforetti^{77a,77b,c}, V. Croft¹⁵⁷, G. Crosetti^{43b,43a}, A. Cueto³⁶, T. Cuhadar Donszelmann¹⁵⁸, H. Cui^{14a,14d}, Z. Cui⁷, A.R. Cukierman¹⁴², W.R. Cunningham⁵⁹, F. Curcio^{43b,43a}, P. Czodrowski³⁶,

M.M. Czurylo^{63b}, M.J. Da Cunha Sargedas De Sousa^{62a}, J.V. Da Fonseca Pinto^{81b}, C. Da Via¹⁰⁰, W. Dabrowski^{84a}, T. Dado⁴⁹, S. Dahbi^{33g}, T. Dai¹⁰⁵, C. Dallapiccola¹⁰², M. Dam⁴², G. D'amen²⁹, V. D'Amico^{76a,76b}, J. Damp⁹⁹, J.R. Dandoy¹²⁷, M.F. Daneri³⁰, M. Danninger¹⁴¹, V. Dao³⁶, G. Darbo^{57b}, S. Darmora⁶, S.J. Das²⁹, A. Dattagupta¹²², S. D'Auria^{70a,70b}, C. David^{155b}, T. Davidek¹³², D.R. Davis⁵¹, B. Davis-Purcell³⁴, I. Dawson⁹³, K. De⁸, R. De Asmundis^{71a}, M. De Beurs¹¹³, S. De Castro^{23b,23a}, N. De Groot¹¹², P. de Jong¹¹³, H. De la Torre¹⁰⁶, A. De Maria^{14c}, A. De Salvo^{74a}, U. De Sanctis^{75a,75b}, M. De Santis^{75a,75b}, A. De Santo¹⁴⁵, J.B. De Vivie De Regie⁶⁰, D.V. Dedovich³⁸, J. Degens¹¹³, A.M. Deiana⁴⁴, F. Del Corso^{23b,23a}, J. Del Peso⁹⁸, F. Del Rio^{63a}, F. Deliot¹³⁴, C.M. Delitzsch⁴⁹, M. Della Pietra^{71a,71b}, D. Della Volpe⁵⁶, A. Dell'Acqua³⁶, L. Dell'Asta^{70a,70b}, M. Delmastro⁴, P.A. Delsart⁶⁰, S. Demers¹⁷⁰, M. Demichev³⁸, S.P. Denisov³⁷, L. D'Eramo¹¹⁴, D. Derendarz⁸⁵, F. Derue¹²⁶, P. Dervan⁹¹, K. Desch²⁴, K. Dette¹⁵⁴, C. Deutsch²⁴, P.O. Deviveiros³⁶, F.A. Di Bello^{74a,74b}, A. Di Ciaccio^{75a,75b}, L. Di Ciaccio⁴, A. Di Domenico^{74a,74b}, C. Di Donato^{71a,71b}, A. Di Girolamo³⁶, G. Di Gregorio^{73a,73b}, A. Di Luca^{77a,77b}, B. Di Micco^{76a,76b}, R. Di Nardo^{76a,76b}, C. Diaconu¹⁰¹, F.A. Dias¹¹³, T. Dias Do Vale¹⁴¹, M.A. Diaz^{136a,136b}, F.G. Diaz Capriles²⁴, M. Didenko¹⁶¹, E.B. Diehl¹⁰⁵, L. Diehl⁵⁴, S. Díez Cornell⁴⁸, C. Díez Pardos¹⁴⁰, C. Dimitriadi^{24,159}, A. Dimitrievska^{17a}, W. Ding^{14b}, J. Dingfelder²⁴, I.M. Dinu^{27b}, S.J. Dittmeier^{63b}, F. Dittus³⁶, F. Djama¹⁰¹, T. Djobava^{148b}, J.I. Djuvsland¹⁶, D. Dodsworth²⁶, C. Doglioni^{100,97}, J. Dolejsi¹³², Z. Dolezal¹³², M. Donadelli^{81c}, B. Dong^{62c}, J. Donini⁴⁰, A. D'Onofrio^{14c}, M. D'Onofrio⁹¹, J. Dopke¹³³, A. Doria^{71a}, M.T. Dova⁸⁹, A.T. Doyle⁵⁹, M.A. Draguet¹²⁵, E. Drechsler¹⁴¹, E. Dreyer¹⁶⁷, I. Drivas-koulouris¹⁰, A.S. Drobac¹⁵⁷, D. Du^{62a}, T.A. du Pree¹¹³, F. Dubinin³⁷, M. Dubovsky^{28a}, E. Duchovni¹⁶⁷, G. Duckeck¹⁰⁸, O.A. Ducu³⁶, D. Duda¹⁰⁹, A. Dudarev³⁶, M. D'uffizi¹⁰⁰, L. Duflot⁶⁶, M. Dührssen³⁶, C. Dülsen¹⁶⁹, A.E. Dumitriu^{27b}, M. Dunford^{63a}, S. Dungs⁴⁹, K. Dunne^{47a,47b}, A. Duperrin¹⁰¹, H. Duran Yildiz^{3a}, M. Düren⁵⁸, A. Durglishvili^{148b}, B.L. Dwyer¹¹⁴, G.I. Dyckes^{17a}, M. Dyndal^{84a}, S. Dysch¹⁰⁰, B.S. Dziedzic⁸⁵, Z.O. Earnshaw¹⁴⁵, B. Eckerova^{28a}, M.G. Eggleston⁵¹, E. Egidio Purcino De Souza^{81b}, L.F. Ehrke⁵⁶, G. Eigen¹⁶, K. Einsweiler^{17a}, T. Ekelof¹⁵⁹, P.A. Ekman⁹⁷, Y. El Ghazali^{35b}, H. El Jarrari^{35e,147}, A. El Moussaouy^{35a}, V. Ellajosyula¹⁵⁹, M. Ellert¹⁵⁹, F. Ellinghaus¹⁶⁹, A.A. Elliot⁹³, N. Ellis³⁶, J. Elmsheuser²⁹, M. Elsing³⁶, D. Emel'yanov¹³³, A. Emerman⁴¹, Y. Enari¹⁵², I. Ene^{17a}, S. Epari¹³, J. Erdmann⁴⁹, A. Ereditato¹⁹, P.A. Erland⁸⁵, M. Errenst¹⁶⁹, M. Escalier⁶⁶, C. Escobar¹⁶¹, E. Etzion¹⁵⁰, G. Evans^{129a}, H. Evans⁶⁷, M.O. Evans¹⁴⁵, A. Ezhilov³⁷, S. Ezzarqtouni^{35a}, F. Fabbri⁵⁹, L. Fabbri^{23b,23a}, G. Facini⁹⁵, V. Fadeyev¹³⁵, R.M. Fakhruddinov³⁷, S. Falciano^{74a}, P.J. Falke²⁴, S. Falke³⁶, J. Faltova¹³², Y. Fan^{14a}, Y. Fang^{14a,14d}, G. Fanourakis⁴⁶, M. Fanti^{70a,70b}, M. Faraj^{68a,68b}, A. Farbin⁸, A. Farilla^{76a}, T. Farooque¹⁰⁶, S.M. Farrington⁵², F. Fassi^{35e}, D. Fassouliotis⁹, M. Faucci Giannelli^{75a,75b}, W.J. Fawcett³², L. Fayard⁶⁶, O.L. Fedin^{37,a}, G. Fedotov³⁷, M. Feickert¹⁶⁰, L. Feligioni¹⁰¹, A. Fell¹³⁸, D.E. Fellers¹²², C. Feng^{62b}, M. Feng^{14b}, M.J. Fenton¹⁵⁸, A.B. Fenyuk³⁷, L. Ferencz⁴⁸, S.W. Ferguson⁴⁵, J.A. Fernandez Pretel⁵⁴, J. Ferrando⁴⁸, A. Ferrari¹⁵⁹, P. Ferrari¹¹³, R. Ferrari^{72a}, D. Ferrere⁵⁶, C. Ferretti¹⁰⁵, F. Fiedler⁹⁹, A. Filipčič⁹², E.K. Filmer¹, F. Filthaut¹¹², M.C.N. Fiolhais^{129a,129c,b}, L. Fiorini¹⁶¹, F. Fischer¹⁴⁰, W.C. Fisher¹⁰⁶, T. Fitschen^{20,66}, I. Fleck¹⁴⁰, P. Fleischmann¹⁰⁵, T. Flick¹⁶⁹, L. Flores¹²⁷, M. Flores^{33d}, L.R. Flores Castillo^{64a}, F.M. Follega^{77a,77b}, N. Fomin¹⁶, J.H. Foo¹⁵⁴, B.C. Forland⁶⁷, A. Formica¹³⁴, A.C. Forti¹⁰⁰, E. Fortin¹⁰¹, A.W. Fortman⁶¹, M.G. Foti^{17a}, L. Fountas⁹, D. Fournier⁶⁶, H. Fox⁹⁰, P. Francavilla^{73a,73b}, S. Francescato⁶¹, M. Franchini^{23b,23a}, S. Franchino^{63a}, D. Francis³⁶, L. Franco¹¹², L. Franconi¹⁹, M. Franklin⁶¹, G. Frattari²⁶, A.C. Freegard⁹³, P.M. Freeman²⁰, W.S. Freund^{81b}, N. Fritzsche⁵⁰, A. Froch⁵⁴, D. Froidevaux³⁶, J.A. Frost¹²⁵, Y. Fu^{62a}, M. Fujimoto¹¹⁷, E. Fullana Torregrosa^{161,*}, J. Fuster¹⁶¹, A. Gabrielli^{23b,23a}, A. Gabrielli³⁶, P. Gadow⁴⁸, G. Gagliardi^{57b,57a}, L.G. Gagnon^{17a}, G.E. Gallardo¹²⁵, E.J. Gallas¹²⁵, B.J. Gallop¹³³, R. Gamboa Goni⁹³, K.K. Gan¹¹⁸, S. Ganguly¹⁵², J. Gao^{62a}, Y. Gao⁵², F.M. Garay Walls^{136a,136b}, B. Garcia^{29,af}, C. García¹⁶¹, J.E. García Navarro¹⁶¹, J.A. García Pascual^{14a}, M. Garcia-Sciveres^{17a}, R.W. Gardner³⁹, D. Garg⁷⁹, R.B. Garg¹⁴², S. Gargiulo⁵⁴, C.A. Garner¹⁵⁴, V. Garonne²⁹, S.J. Gasiorowski¹³⁷, P. Gaspar^{81b}, G. Gaudio^{72a}, V. Gautam¹³, P. Gauzzi^{74a,74b},

I.L. Gavrilenko³⁷, A. Gavrilyuk³⁷, C. Gay¹⁶², G. Gaycken⁴⁸, E.N. Gazis¹⁰, A.A. Geanta^{27b}, C.M. Gee¹³⁵, J. Geisen⁹⁷, M. Geisen⁹⁹, C. Gemme^{57b}, M.H. Genest⁶⁰, S. Gentile^{74a,74b}, S. George⁹⁴, W.F. George²⁰, T. Geralis⁴⁶, L.O. Gerlach⁵⁵, P. Gessinger-Befurt³⁶, M. Ghasemi Bostanabad¹⁶³, M. Ghneimat¹⁴⁰, A. Ghosal¹⁴⁰, A. Ghosh¹⁵⁸, A. Ghosh⁷, B. Giacobbe^{23b}, S. Giagu^{74a,74b}, N. Giangiacomi¹⁵⁴, P. Giannetti^{73a}, A. Giannini^{62a}, S.M. Gibson⁹⁴, M. Gignac¹³⁵, D.T. Gil^{84b}, A.K. Gilbert^{84a}, B.J. Gilbert⁴¹, D. Gillberg³⁴, G. Gilles¹¹³, N.E.K. Gillwald⁴⁸, L. Ginabat¹²⁶, D.M. Gingrich^{2,ac}, M.P. Giordani^{68a,68c}, P.F. Giraud¹³⁴, G. Giugliarelli^{68a,68c}, D. Giugni^{70a}, F. Giuli³⁶, I. Gkialas^{9,i}, L.K. Gladilin³⁷, C. Glasman⁹⁸, G.R. Gledhill¹²², M. Glisic¹²², I. Gnesi^{43b,e}, Y. Go^{29,af}, M. Goblirsch-Kolb²⁶, D. Godin¹⁰⁷, S. Goldfarb¹⁰⁴, T. Golling⁵⁶, M.G.D. Gololo^{33g}, D. Golubkov³⁷, J.P. Gombas¹⁰⁶, A. Gomes^{129a,129b}, G. Gomes Da Silva¹⁴⁰, A.J. Gomez Delegido¹⁶¹, R. Goncalves Gama⁵⁵, R. Gonçalo^{129a,129c}, G. Gonella¹²², L. Gonella²⁰, A. Gongadze³⁸, F. Gonnella²⁰, J.L. Gonski⁴¹, S. González de la Hoz¹⁶¹, S. Gonzalez Fernandez¹³, R. Gonzalez Lopez⁹¹, C. Gonzalez Renteria^{17a}, R. Gonzalez Suarez¹⁵⁹, S. Gonzalez-Sevilla⁵⁶, G.R. Gonzalvo Rodriguez¹⁶¹, R.Y. González Andana⁵², L. Goossens³⁶, N.A. Gorasia²⁰, P.A. Gorbounov³⁷, B. Gorini³⁶, E. Gorini^{69a,69b}, A. Gorišek⁹², A.T. Goshaw⁵¹, M.I. Gostkin³⁸, C.A. Gottardo¹¹², M. Gouighri^{35b}, V. Goumarre⁴⁸, A.G. Goussiou¹³⁷, N. Govender^{33c}, C. Goy⁴, I. Grabowska-Bold^{84a}, K. Graham³⁴, E. Gramstad¹²⁴, S. Grancagnolo¹⁸, M. Grandi¹⁴⁵, V. Gratchev^{37,*}, P.M. Gravila^{27f}, F.G. Gravili^{69a,69b}, H.M. Gray^{17a}, M. Greco^{69a,69b}, C. Grefe²⁴, I.M. Gregor⁴⁸, P. Grenier¹⁴², C. Grieco¹³, A.A. Grillo¹³⁵, K. Grimm^{31,m}, S. Grinstein^{13,t}, J.-F. Grivaz⁶⁶, E. Gross¹⁶⁷, J. Grosse-Knetter⁵⁵, C. Grud¹⁰⁵, A. Grummer¹¹¹, J.C. Grundy¹²⁵, L. Guan¹⁰⁵, W. Guan¹⁶⁸, C. Gubbels¹⁶², J.G.R. Guerrero Rojas¹⁶¹, G. Guerrieri^{68a,68c}, F. Guescini¹⁰⁹, R. Gugel⁹⁹, J.A.M. Guhit¹⁰⁵, A. Guida⁴⁸, T. Guillemin⁴, E. Guilloton^{165,133}, S. Guindon³⁶, F. Guo^{14a,14d}, J. Guo^{62c}, L. Guo⁶⁶, Y. Guo¹⁰⁵, R. Gupta⁴⁸, S. Gurbuz²⁴, S.S. Gurdasani⁵⁴, G. Gustavino³⁶, M. Guth⁵⁶, P. Gutierrez¹¹⁹, L.F. Gutierrez Zagazeta¹²⁷, C. Gutschow⁹⁵, C. Guyot¹³⁴, C. Gwenlan¹²⁵, C.B. Gwilliam⁹¹, E.S. Haaland¹²⁴, A. Haas¹¹⁶, M. Habedank⁴⁸, C. Haber^{17a}, H.K. Hadavand⁸, A. Hader⁹⁹, S. Hadzic¹⁰⁹, M. Haleem¹⁶⁴, J. Haley¹²⁰, J.J. Hall¹³⁸, G.D. Hallelwell¹⁰¹, L. Halser¹⁹, K. Hamano¹⁶³, H. Hamdaoui^{35e}, M. Hamer²⁴, G.N. Hamity⁵², J. Han^{62b}, K. Han^{62a}, L. Han^{14c}, L. Han^{62a}, S. Han^{17a}, Y.F. Han¹⁵⁴, K. Hanagaki⁸², M. Hance¹³⁵, D.A. Hangal^{41,y}, M.D. Hank³⁹, R. Hankache¹⁰⁰, J.B. Hansen⁴², J.D. Hansen⁴², P.H. Hansen⁴², K. Hara¹⁵⁶, D. Harada⁵⁶, T. Harenberg¹⁶⁹, S. Harkusha³⁷, Y.T. Harris¹²⁵, P.F. Harrison¹⁶⁵, N.M. Hartman¹⁴², N.M. Hartmann¹⁰⁸, Y. Hasegawa¹³⁹, A. Hasib⁵², S. Haug¹⁹, R. Hauser¹⁰⁶, M. Havranek¹³¹, C.M. Hawkes²⁰, R.J. Hawkins³⁶, S. Hayashida¹¹⁰, D. Hayden¹⁰⁶, C. Hayes¹⁰⁵, R.L. Hayes¹⁶², C.P. Hays¹²⁵, J.M. Hays⁹³, H.S. Hayward⁹¹, F. He^{62a}, Y. He¹⁵³, Y. He¹²⁶, M.P. Heath⁵², V. Hedberg⁹⁷, A.L. Heggelund¹²⁴, N.D. Hehir⁹³, C. Heidegger⁵⁴, K.K. Heidegger⁵⁴, W.D. Heidorn⁸⁰, J. Heilman³⁴, S. Heim⁴⁸, T. Heim^{17a}, J.G. Heinlein¹²⁷, J.J. Heinrich¹²², L. Heinrich³⁶, J. Hejbal¹³⁰, L. Helary⁴⁸, A. Held¹¹⁶, S. Hellesund¹²⁴, C.M. Helling¹⁶², S. Hellman^{47a,47b}, C. Helsens³⁶, R.C.W. Henderson⁹⁰, L. Henkelmann³², A.M. Henriques Correia³⁶, H. Herde¹⁴², Y. Hernández Jiménez¹⁴⁴, H. Herr⁹⁹, M.G. Herrmann¹⁰⁸, T. Herrmann⁵⁰, G. Herten⁵⁴, R. Hertenberger¹⁰⁸, L. Hervas³⁶, N.P. Hesse^{155a}, H. Hibi⁸³, E. Higón-Rodríguez¹⁶¹, S.J. Hillier²⁰, I. Hinchliffe^{17a}, F. Hinterkeuser²⁴, M. Hirose¹²³, S. Hirose¹⁵⁶, D. Hirschbuehl¹⁶⁹, T.G. Hitchings¹⁰⁰, B. Hiti⁹², J. Hobbs¹⁴⁴, R. Hobincu^{27e}, N. Hod¹⁶⁷, M.C. Hodgkinson¹³⁸, B.H. Hodgkinson³², A. Hoecker³⁶, J. Hofer⁴⁸, D. Hohn⁵⁴, T. Holm²⁴, M. Holzbock¹⁰⁹, L.B.A.H. Hommels³², B.P. Honan¹⁰⁰, J. Hong^{62c}, T.M. Hong¹²⁸, Y. Hong⁵⁵, J.C. Honig⁵⁴, A. Hönle¹⁰⁹, B.H. Hooberman¹⁶⁰, W.H. Hopkins⁶, Y. Horii¹¹⁰, S. Hou¹⁴⁷, A.S. Howard⁹², J. Howarth⁵⁹, J. Hoya⁸⁹, M. Hrabovsky¹²¹, A. Hrynevich³⁷, T. Hryn'ova⁴, P.J. Hsu⁶⁵, S.-C. Hsu¹³⁷, Q. Hu^{41,y}, Y.F. Hu^{14a,14d,ae}, D.P. Huang⁹⁵, S. Huang^{64b}, X. Huang^{14c}, Y. Huang^{62a}, Y. Huang^{14a}, Z. Huang¹⁰⁰, Z. Hubacek¹³¹, M. Huebner²⁴, F. Huegging²⁴, T.B. Huffman¹²⁵, M. Huhtinen³⁶, S.K. Huiberts¹⁶, R. Hulskén¹⁰³, N. Huseynov^{12,a}, J. Huston¹⁰⁶, J. Huth⁶¹, R. Hyneman¹⁴², S. Hyrych^{28a}, G. Iacobucci⁵⁶, G. Iakovidis²⁹, I. Ibragimov¹⁴⁰, L. Iconomidou-Fayard⁶⁶, P. Iengo^{71a,71b}, R. Iguchi¹⁵², T. Iizawa⁵⁶, Y. Ikegami⁸², A. Ilg¹⁹, N. Ilic¹⁵⁴, H. Imam^{35a}, T. Ingebretsen Carlson^{47a,47b}, G. Introzzi^{72a,72b}, M. Iodice^{76a}, V. Ippolito^{74a,74b}, M. Ishino¹⁵², W. Islam¹⁶⁸, C. Issever^{18,48}, S. Istin^{21a,ag},

H. Ito¹⁶⁶, J.M. Iturbe Ponce^{64a}, R. Iuppa^{77a,77b}, A. Ivina¹⁶⁷, J.M. Izen⁴⁵, V. Izzo^{71a}, P. Jacka^{130,131}, P. Jackson¹, R.M. Jacobs⁴⁸, B.P. Jaeger¹⁴¹, C.S. Jagfeld¹⁰⁸, G. Jäkel¹⁶⁹, K. Jakobs⁵⁴, T. Jakoubek¹⁶⁷, J. Jamieson⁵⁹, K.W. Janas^{84a}, G. Jarlskog⁹⁷, A.E. Jaspan⁹¹, T. Javůrek³⁶, M. Javurkova¹⁰², F. Jeanneau¹³⁴, L. Jeanty¹²², J. Jejelava^{148a,x}, P. Jenni^{54,f}, C.E. Jessiman³⁴, S. Jézéquel⁴, J. Jia¹⁴⁴, X. Jia⁶¹, X. Jia^{14a,14d}, Z. Jia^{14c}, Y. Jiang^{62a}, S. Jiggins⁵², J. Jimenez Pena¹⁰⁹, S. Jin^{14c}, A. Jinaru^{27b}, O. Jinnouchi¹⁵³, H. Jivan^{33g}, P. Johansson¹³⁸, K.A. Johns⁷, C.A. Johnson⁶⁷, D.M. Jones³², E. Jones¹⁶⁵, P. Jones³², R.W.L. Jones⁹⁰, T.J. Jones⁹¹, J. Jovicevic¹⁵, X. Ju^{17a}, J.J. Junggeburth³⁶, A. Juste Rozas^{13,t}, S. Kabana^{136e}, A. Kaczmarska⁸⁵, M. Kado^{74a,74b}, H. Kagan¹¹⁸, M. Kagan¹⁴², A. Kahn⁴¹, A. Kahn¹²⁷, C. Kahra⁹⁹, T. Kaji¹⁶⁶, E. Kajomovitz¹⁴⁹, N. Kakati¹⁶⁷, C.W. Kalderon²⁹, A. Kamenshchikov¹⁵⁴, N.J. Kang¹³⁵, Y. Kano¹¹⁰, D. Kar^{33g}, K. Karava¹²⁵, M.J. Kareem^{155b}, E. Karentzos⁵⁴, I. Karkanas¹⁵¹, S.N. Karpov³⁸, Z.M. Karpova³⁸, V. Kartvelishvili⁹⁰, A.N. Karyukhin³⁷, E. Kasimi¹⁵¹, C. Kato^{62d}, J. Katzy⁴⁸, S. Kaur³⁴, K. Kawade¹³⁹, K. Kawagoe⁸⁸, T. Kawaguchi¹¹⁰, T. Kawamoto¹³⁴, G. Kawamura⁵⁵, E.F. Kay¹⁶³, F.I. Kaya¹⁵⁷, S. Kazakos¹³, V.F. Kazanin³⁷, Y. Ke¹⁴⁴, J.M. Keaveney^{33a}, R. Keeler¹⁶³, G.V. Kehris⁶¹, J.S. Keller³⁴, A.S. Kelly⁹⁵, D. Kelsey¹⁴⁵, J.J. Kempster²⁰, J. Kendrick²⁰, K.E. Kennedy⁴¹, O. Kepka¹³⁰, B.P. Kerridge¹⁶⁵, S. Kersten¹⁶⁹, B.P. Kerševan⁹², L. Keszeghova^{28a}, S. Ketabchi Haghghat¹⁵⁴, M. Khandoga¹²⁶, A. Khanov¹²⁰, A.G. Kharlamov³⁷, T. Kharlamova³⁷, E.E. Khoda¹³⁷, T.J. Khoo¹⁸, G. Khorauli¹⁶⁴, J. Khubua^{148b}, Y.A.R. Khwaira⁶⁶, M. Kiehn³⁶, A. Kilgallon¹²², D.W. Kim^{47a,47b}, E. Kim¹⁵³, Y.K. Kim³⁹, N. Kimura⁹⁵, A. Kirchhoff⁵⁵, D. Kirchmeier⁵⁰, C. Kirfel²⁴, J. Kirk¹³³, A.E. Kiryunin¹⁰⁹, T. Kishimoto¹⁵², D.P. Kisliuk¹⁵⁴, C. Kitsaki¹⁰, O. Kivernyk²⁴, M. Klassen^{63a}, C. Klein³⁴, L. Klein¹⁶⁴, M.H. Klein¹⁰⁵, M. Klein⁹¹, U. Klein⁹¹, P. Klimek³⁶, A. Klimentov²⁹, F. Klimpel¹⁰⁹, T. Klingl²⁴, T. Klioutchnikova³⁶, F.F. Klitzner¹⁰⁸, P. Kluit¹¹³, S. Kluth¹⁰⁹, E. Kneringer⁷⁸, T.M. Knight¹⁵⁴, A. Knue⁵⁴, D. Kobayashi⁸⁸, R. Kobayashi⁸⁶, M. Kocian¹⁴², T. Kodama¹⁵², P. Kodyš¹³², D.M. Koeck¹⁴⁵, P.T. Koenig²⁴, T. Koffas³⁴, N.M. Köhler³⁶, M. Kolb¹³⁴, I. Koletsou⁴, T. Komarek¹²¹, K. Köneke⁵⁴, A.X.Y. Kong¹, T. Kono¹¹⁷, N. Konstantinidis⁹⁵, B. Konya⁹⁷, R. Kopeliainsky⁶⁷, S. Koperny^{84a}, K. Korcyl⁸⁵, K. Kordas¹⁵¹, G. Koren¹⁵⁰, A. Korn⁹⁵, S. Korn⁵⁵, I. Korolkov¹³, N. Korotkova³⁷, B. Kortman¹¹³, O. Kortner¹⁰⁹, S. Kortner¹⁰⁹, W.H. Kostecka¹¹⁴, V.V. Kostyukhin¹⁴⁰, A. Kotsokechagia⁶⁶, A. Kotwal⁵¹, A. Koulouris³⁶, A. Kourkouveli-Charalampidi^{72a,72b}, C. Kourkouvelis⁹, E. Kourlitis⁶, O. Kovanda¹⁴⁵, R. Kowalewski¹⁶³, W. Kozanecki¹³⁴, A.S. Kozhin³⁷, V.A. Kramarenko³⁷, G. Kramberger⁹², P. Kramer⁹⁹, M.W. Krasny¹²⁶, A. Krasznahorkay³⁶, J.A. Kremer⁹⁹, T. Kresse⁵⁰, J. Kretschmar⁹¹, K. Kreul¹⁸, P. Krieger¹⁵⁴, F. Krieter¹⁰⁸, S. Krishnamurthy¹⁰², A. Krishnan^{63b}, M. Krivos¹³², K. Krizka^{17a}, K. Kroeninger⁴⁹, H. Kroha¹⁰⁹, J. Kroll¹³⁰, J. Kroll¹²⁷, K.S. Krowpman¹⁰⁶, U. Kruchonak³⁸, H. Krüger²⁴, N. Krumnack⁸⁰, M.C. Kruse⁵¹, J.A. Krzysiak⁸⁵, A. Kubota¹⁵³, O. Kuchinskaia³⁷, S. Kuday^{3a}, D. Kuechler⁴⁸, J.T. Kuechler⁴⁸, S. Kuehn³⁶, T. Kuhl⁴⁸, V. Kukhtin³⁸, Y. Kulchitsky^{37,a}, S. Kuleshov^{136d,136b}, M. Kumar^{33g}, N. Kumari¹⁰¹, M. Kuna⁶⁰, A. Kupco¹³⁰, T. Kupfer⁴⁹, A. Kupich³⁷, O. Kuprash⁵⁴, H. Kurashige⁸³, L.L. Kurchaninov^{155a}, Y.A. Kurochkin³⁷, A. Kurova³⁷, E.S. Kuwertz³⁶, M. Kuze¹⁵³, A.K. Kvam¹⁰², J. Kvita¹²¹, T. Kwan¹⁰³, K.W. Kwok^{64a}, C. Lacasta¹⁶¹, F. Lacava^{74a,74b}, H. Lacker¹⁸, D. Lacour¹²⁶, N.N. Lad⁹⁵, E. Ladygin³⁸, B. Laforge¹²⁶, T. Lagouri^{136e}, S. Lai⁵⁵, I.K. Lakomic^{84a}, N. Lalloue⁶⁰, J.E. Lambert¹¹⁹, S. Lammers⁶⁷, W. Lampl⁷, C. Lampoudis¹⁵¹, A.N. Lancaster¹¹⁴, E. Lançon²⁹, U. Landgraf⁵⁴, M.P.J. Landon⁹³, V.S. Lang⁵⁴, R.J. Langenberg¹⁰², A.J. Lankford¹⁵⁸, F. Lanni²⁹, K. Lantzsch²⁴, A. Lanza^{72a}, A. Lapertosa^{57b,57a}, J.F. Laporte¹³⁴, T. Lari^{70a}, F. Lasagni Manghi^{23b}, M. Lassnig³⁶, V. Latonova¹³⁰, T.S. Lau^{64a}, A. Laudrain⁹⁹, A. Laurier³⁴, S.D. Lawlor⁹⁴, Z. Lawrence¹⁰⁰, M. Lazzaroni^{70a,70b}, B. Le¹⁰⁰, B. Leban⁹², A. Lebedev⁸⁰, M. LeBlanc³⁶, T. LeCompte⁶, F. Ledroit-Guillon⁶⁰, A.C.A. Lee⁹⁵, G.R. Lee¹⁶, L. Lee⁶¹, S.C. Lee¹⁴⁷, S. Lee^{47a,47b}, L.L. Leeuw^{33c}, H.P. Lefebvre⁹⁴, M. Lefebvre¹⁶³, C. Leggett^{17a}, K. Lehmann¹⁴¹, G. Lehmann Miotto³⁶, W.A. Leight¹⁰², A. Leisos^{151,s}, M.A.L. Leite^{81c}, C.E. Leitgeb⁴⁸, R. Leitner¹³², K.J.C. Leney⁴⁴, T. Lenz²⁴, S. Leone^{73a}, C. Leonidopoulos⁵², A. Leopold¹⁴³, C. Leroy¹⁰⁷, R. Les¹⁰⁶, C.G. Lester³², M. Levchenko³⁷, J. Levêque⁴, D. Levin¹⁰⁵, L.J. Levinson¹⁶⁷, D.J. Lewis²⁰, B. Li^{14b}, B. Li^{62b}, C. Li^{62a}, C-Q. Li^{62c,62d},

H. Li^{62a}, H. Li^{62b}, H. Li^{14c}, H. Li^{62b}, J. Li^{62c}, K. Li¹³⁷, L. Li^{62c}, M. Li^{14a,14d}, Q.Y. Li^{62a}, S. Li^{62d,62c,d},
 T. Li^{62b}, X. Li¹⁰³, Z. Li^{62b}, Z. Li¹²⁵, Z. Li¹⁰³, Z. Li⁹¹, Z. Liang^{14a}, M. Liberatore⁴⁸, B. Liberti^{75a}, K. Lie^{64c},
 J. Lieber Marin^{81b}, K. Lin¹⁰⁶, R.A. Linck⁶⁷, R.E. Lindley⁷, J.H. Lindon², A. Linss⁴⁸, E. Lipeles¹²⁷,
 A. Lipniacka¹⁶, T.M. Liss^{160,aa}, A. Lister¹⁶², J.D. Little⁴, B. Liu^{14a}, B.X. Liu¹⁴¹, D. Liu^{62d,62c}, J.B. Liu^{62a},
 J.K.K. Liu³², K. Liu^{62d,62c}, M. Liu^{62a}, M.Y. Liu^{62a}, P. Liu^{14a}, Q. Liu^{62d,137,62c}, X. Liu^{62a}, Y. Liu⁴⁸,
 Y. Liu^{14c,14d}, Y.L. Liu¹⁰⁵, Y.W. Liu^{62a}, M. Livan^{72a,72b}, J. Llorente Merino¹⁴¹, S.L. Lloyd⁹³,
 E.M. Lobodzinska⁴⁸, P. Loch⁷, S. Loffredo^{75a,75b}, T. Lohse¹⁸, K. Lohwasser¹³⁸, M. Lokajicek¹³⁰,
 J.D. Long¹⁶⁰, I. Longarini^{74a,74b}, L. Longo^{69a,69b}, R. Longo¹⁶⁰, I. Lopez Paz³⁶, A. Lopez Solis⁴⁸,
 J. Lorenz¹⁰⁸, N. Lorenzo Martinez⁴, A.M. Lory¹⁰⁸, A. Lösle⁵⁴, X. Lou^{47a,47b}, X. Lou^{14a,14d}, A. Lounis⁶⁶,
 J. Love⁶, P.A. Love⁹⁰, J.J. Lozano Bahilo¹⁶¹, G. Lu^{14a,14d}, M. Lu⁷⁹, S. Lu¹²⁷, Y.J. Lu⁶⁵, H.J. Lubatti¹³⁷,
 C. Luci^{74a,74b}, F.L. Lucio Alves^{14c}, A. Lucotte⁶⁰, F. Luehring⁶⁷, I. Luise¹⁴⁴, O. Lukianchuk⁶⁶,
 O. Lundberg¹⁴³, B. Lund-Jensen¹⁴³, N.A. Luongo¹²², M.S. Lutz¹⁵⁰, D. Lynn²⁹, H. Lyons⁹¹, R. Lysak¹³⁰,
 E. Lytken⁹⁷, F. Lyu^{14a}, V. Lyubushkin³⁸, T. Lyubushkina³⁸, H. Ma²⁹, L.L. Ma^{62b}, Y. Ma⁹⁵,
 D.M. Mac Donell¹⁶³, G. Maccarrone⁵³, J.C. MacDonald¹³⁸, R. Madar⁴⁰, W.F. Mader⁵⁰, J. Maeda⁸³,
 T. Maeno²⁹, M. Maerker⁵⁰, V. Magerl⁵⁴, J. Magro^{68a,68c}, H. Maguire¹³⁸, D.J. Mahon⁴¹, C. Maidantchik^{81b},
 A. Maio^{129a,129b,129d}, K. Maj^{84a}, O. Majersky^{28a}, S. Majewski¹²², N. Makovec⁶⁶, V. Maksimovic¹⁵,
 B. Malaescu¹²⁶, Pa. Malecki⁸⁵, V.P. Maleev³⁷, F. Malek⁶⁰, D. Malito^{43b,43a}, U. Mallik⁷⁹, C. Malone³²,
 S. Maltezos¹⁰, S. Malyukov³⁸, J. Mamuzic¹³, G. Mancini⁵³, G. Manco^{72a,72b}, J.P. Mandalia⁹³, I. Mandić⁹²,
 L. Manhaes de Andrade Filho^{81a}, I.M. Maniatis¹⁵¹, M. Manisha¹³⁴, J. Manjarres Ramos⁵⁰,
 D.C. Mankad¹⁶⁷, K.H. Mankinen⁹⁷, A. Mann¹⁰⁸, A. Manousos⁷⁸, B. Mansoulie¹³⁴, S. Manzoni³⁶,
 A. Marantis¹⁵¹, G. Marchiori⁵, M. Marcisovsky¹³⁰, L. Marcoccia^{75a,75b}, C. Marcon⁹⁷, M. Marinescu²⁰,
 M. Marjanovic¹¹⁹, Z. Marshall^{17a}, S. Marti-Garcia¹⁶¹, T.A. Martin¹⁶⁵, V.J. Martin⁵²,
 B. Martin dit Latour¹⁶, L. Martinelli^{74a,74b}, M. Martinez^{13,t}, P. Martinez Agullo¹⁶¹,
 V.I. Martinez Outschoorn¹⁰², P. Martinez Suarez¹³, S. Martin-Haugh¹³³, V.S. Martoiu^{27b},
 A.C. Martyniuk⁹⁵, A. Marzin³⁶, S.R. Maschek¹⁰⁹, L. Masetti⁹⁹, T. Mashimo¹⁵², J. Masik¹⁰⁰,
 A.L. Maslennikov³⁷, L. Massa^{23b}, P. Massarotti^{71a,71b}, P. Mastrandrea^{73a,73b}, A. Mastroberardino^{43b,43a},
 T. Masubuchi¹⁵², T. Mathisen¹⁵⁹, A. Matic¹⁰⁸, N. Matsuzawa¹⁵², J. Maurer^{27b}, B. Maček⁹²,
 D.A. Maximov³⁷, R. Mazini¹⁴⁷, I. Maznas¹⁵¹, M. Mazza¹⁰⁶, S.M. Mazza¹³⁵, C. Mc Ginn^{29,af},
 J.P. Mc Gowan¹⁰³, S.P. Mc Kee¹⁰⁵, T.G. McCarthy¹⁰⁹, W.P. McCormack^{17a}, E.F. McDonald¹⁰⁴,
 A.E. McDougall¹¹³, J.A. Mcfayden¹⁴⁵, G. Mchedlidze^{148b}, R.P. Mckenzie^{33g}, T.C. Mclachlan⁴⁸,
 D.J. McLaughlin⁹⁵, K.D. McLean¹⁶³, S.J. McMahon¹³³, P.C. McNamara¹⁰⁴, R.A. McPherson^{163,v},
 J.E. Mdhului^{33g}, S. Meehan³⁶, T. Megy⁴⁰, S. Mehlhase¹⁰⁸, A. Mehta⁹¹, B. Meirose⁴⁵, D. Melini¹⁴⁹,
 B.R. Mellado Garcia^{33g}, A.H. Melo⁵⁵, F. Meloni⁴⁸, E.D. Mendes Gouveia^{129a},
 A.M. Mendes Jacques Da Costa²⁰, H.Y. Meng¹⁵⁴, L. Meng⁹⁰, S. Menke¹⁰⁹, M. Mentink³⁶, E. Meoni^{43b,43a},
 C. Merlassino¹²⁵, L. Merola^{71a,71b}, C. Meroni^{70a}, G. Merz¹⁰⁵, O. Meshkov³⁷, J.K.R. Meshreki¹⁴⁰,
 J. Metcalfe⁶, A.S. Mete⁶, C. Meyer⁶⁷, J-P. Meyer¹³⁴, M. Michetti¹⁸, R.P. Middleton¹³³, L. Mijovic⁵²,
 G. Mikenberg¹⁶⁷, M. Mikesikova¹³⁰, M. Mikuž⁹², H. Mildner¹³⁸, A. Milic¹⁵⁴, C.D. Milke⁴⁴,
 D.W. Miller³⁹, L.S. Miller³⁴, A. Milov¹⁶⁷, D.A. Milstead^{47a,47b}, T. Min^{14c}, A.A. Minaenko³⁷,
 I.A. Minashvili^{148b}, L. Mince⁵⁹, A.I. Mincer¹¹⁶, B. Mindur^{84a}, M. Mineev³⁸, Y. Minegishi¹⁵², Y. Mino⁸⁶,
 L.M. Mir¹³, M. Miralles Lopez¹⁶¹, M. Mironova¹²⁵, T. Mitani¹⁶⁶, A. Mitra¹⁶⁵, V.A. Mitsou¹⁶¹, O. Miu¹⁵⁴,
 P.S. Miyagawa⁹³, Y. Miyazaki⁸⁸, A. Mizukami⁸², J.U. Mjörnmark⁹⁷, T. Mkrtchyan^{63a}, M. Mlynarikova¹¹⁴,
 T. Moa^{47a,47b}, S. Mobius⁵⁵, K. Mochizuki¹⁰⁷, P. Moder⁴⁸, P. Mogg¹⁰⁸, A.F. Mohammed^{14a,14d},
 S. Mohapatra⁴¹, G. Mokgatitswane^{33g}, B. Mondal¹⁴⁰, S. Mondal¹³¹, K. Mönig⁴⁸, E. Monnier¹⁰¹,
 L. Monsonis Romero¹⁶¹, J. Montejo Berlingen³⁶, M. Montella¹¹⁸, F. Monticelli⁸⁹, N. Morange⁶⁶,
 A.L. Moreira De Carvalho^{129a}, M. Moreno Llácer¹⁶¹, C. Moreno Martinez¹³, P. Morettini^{57b},
 S. Morgenstern¹⁶⁵, M. Morii⁶¹, M. Morinaga¹⁵², V. Morisbak¹²⁴, A.K. Morley³⁶, F. Morodei^{74a,74b},
 L. Morvaj³⁶, P. Moschovakos³⁶, B. Moser³⁶, M. Mosidze^{148b}, T. Moskalets⁵⁴, P. Moskvitina¹¹²,

J. Moss^{31,n}, E.J.W. Moyse¹⁰², S. Muanza¹⁰¹, J. Mueller¹²⁸, D. Muenstermann⁹⁰, R. Müller¹⁹, G.A. Mullier⁹⁷, J.J. Mullin¹²⁷, D.P. Mungo^{70a,70b}, J.L. Munoz Martinez¹³, D. Munoz Perez¹⁶¹, F.J. Munoz Sanchez¹⁰⁰, M. Murin¹⁰⁰, W.J. Murray^{165,133}, A. Murrone^{70a,70b}, J.M. Muse¹¹⁹, M. Muškinja^{17a}, C. Mwewa²⁹, A.G. Myagkov^{37,a}, A.J. Myers⁸, A.A. Myers¹²⁸, G. Myers⁶⁷, M. Myska¹³¹, B.P. Nachman^{17a}, O. Nackenhorst⁴⁹, A.Nag Nag⁵⁰, K. Nagai¹²⁵, K. Nagano⁸², J.L. Nagle^{29,af}, E. Nagy¹⁰¹, A.M. Nairz³⁶, Y. Nakahama⁸², K. Nakamura⁸², H. Nanjo¹²³, R. Narayan⁴⁴, E.A. Narayanan¹¹¹, I. Naryshkin³⁷, M. Naseri³⁴, C. Nass²⁴, G. Navarro^{22a}, J. Navarro-Gonzalez¹⁶¹, R. Nayak¹⁵⁰, P.Y. Nechaeva³⁷, F. Nechansky⁴⁸, T.J. Neep²⁰, A. Negri^{72a,72b}, M. Negrini^{23b}, C. Nellist¹¹², C. Nelson¹⁰³, K. Nelson¹⁰⁵, S. Nemecek¹³⁰, M. Nessi^{36,g}, M.S. Neubauer¹⁶⁰, F. Neuhaus⁹⁹, J. Neundorff⁴⁸, R. Newhouse¹⁶², P.R. Newman²⁰, C.W. Ng¹²⁸, Y.S. Ng¹⁸, Y.W.Y. Ng¹⁵⁸, B. Ngair^{35e}, H.D.N. Nguyen¹⁰⁷, R.B. Nickerson¹²⁵, R. Nicolaidou¹³⁴, J. Nielsen¹³⁵, M. Niemeyer⁵⁵, N. Nikiforou³⁶, V. Nikolaenko^{37,a}, I. Nikolic-Audit¹²⁶, K. Nikolopoulos²⁰, P. Nilsson²⁹, H.R. Nindhito⁵⁶, A. Nisati^{74a}, N. Nishu², R. Nisius¹⁰⁹, J-E. Nitschke⁵⁰, E.K. Nkadimeng^{33g}, S.J. Noacco Rosende⁸⁹, T. Nobe¹⁵², D.L. Noel³², Y. Noguchi⁸⁶, T. Nommensen¹⁴⁶, M.A. Nomura²⁹, M.B. Norfolk¹³⁸, R.R.B. Norisam⁹⁵, B.J. Norman³⁴, J. Novak⁹², T. Novak⁴⁸, O. Novgorodova⁵⁰, L. Novotny¹³¹, R. Novotny¹¹¹, L. Nozka¹²¹, K. Ntekas¹⁵⁸, E. Nurse⁹⁵, F.G. Oakham^{34,ac}, J. Ocariz¹²⁶, A. Ochi⁸³, I. Ochoa^{129a}, S. Oda⁸⁸, S. Oerdek¹⁵⁹, A. Ogrodnik^{84a}, A. Oh¹⁰⁰, C.C. Ohm¹⁴³, H. Oide¹⁵³, R. Oishi¹⁵², M.L. Ojeda⁴⁸, Y. Okazaki⁸⁶, M.W. O'Keefe⁹¹, Y. Okumura¹⁵², A. Olariu^{27b}, L.F. Oleiro Seabra^{129a}, S.A. Olivares Pino^{136e}, D. Oliveira Damazio²⁹, D. Oliveira Goncalves^{81a}, J.L. Oliver¹⁵⁸, M.J.R. Olsson¹⁵⁸, A. Olszewski⁸⁵, J. Olszowska^{85,*}, Ö.O. Öncel⁵⁴, D.C. O'Neil¹⁴¹, A.P. O'Neill¹⁹, A. Onofre^{129a,129e}, P.U.E. Onyisi¹¹, M.J. Oreglia³⁹, G.E. Orellana⁸⁹, D. Orestano^{76a,76b}, N. Orlando¹³, R.S. Orr¹⁵⁴, V. O'Shea⁵⁹, R. Ospanov^{62a}, G. Otero y Garzon³⁰, H. Otono⁸⁸, P.S. Ott^{63a}, G.J. Ottino^{17a}, M. Ouchrif^{35d}, J. Ouellette^{29,af}, F. Ould-Saada¹²⁴, M. Owen⁵⁹, R.E. Owen¹³³, K.Y. Oyulmaz^{21a}, V.E. Ozcan^{21a}, N. Ozturk⁸, S. Ozturk^{21d}, J. Pacalt¹²¹, H.A. Pacey³², K. Pachal⁵¹, A. Pacheco Pages¹³, C. Padilla Aranda¹³, G. Padovano^{74a,74b}, S. Pagan Griso^{17a}, G. Palacino⁶⁷, A. Palazzo^{69a,69b}, S. Palazzo⁵², S. Palestini³⁶, M. Palka^{84b}, J. Pan¹⁷⁰, T. Pan^{64a}, D.K. Panchal¹¹, C.E. Pandini¹¹³, J.G. Panduro Vazquez⁹⁴, P. Pani⁴⁸, G. Panizzo^{68a,68c}, L. Paolozzi⁵⁶, C. Papadatos¹⁰⁷, S. Parajuli⁴⁴, A. Paramonov⁶, C. Paraskevopoulos¹⁰, D. Paredes Hernandez^{64b}, T.H. Park¹⁵⁴, M.A. Parker³², F. Parodi^{57b,57a}, E.W. Parrish¹¹⁴, V.A. Parrish⁵², J.A. Parsons⁴¹, U. Parzefall⁵⁴, B. Pascual Dias¹⁰⁷, L. Pascual Dominguez¹⁵⁰, V.R. Pascuzzi^{17a}, F. Pasquali¹¹³, E. Pasqualucci^{74a}, S. Passaggio^{57b}, F. Pastore⁹⁴, P. Pasuwan^{47a,47b}, J.R. Pater¹⁰⁰, J. Patton⁹¹, T. Pauly³⁶, J. Pearkes¹⁴², M. Pedersen¹²⁴, R. Pedro^{129a}, S.V. Peleganchuk³⁷, O. Penc¹³⁰, C. Peng^{64b}, H. Peng^{62a}, M. Penzin³⁷, B.S. Peralva^{81a,81d}, A.P. Pereira Peixoto⁶⁰, L. Pereira Sanchez^{47a,47b}, D.V. Perepelitsa^{29,af}, E. Perez Codina^{155a}, M. Perganti¹⁰, L. Perini^{70a,70b,*}, H. Pernegger³⁶, S. Perrella³⁶, A. Perrevoort¹¹², O. Perrin⁴⁰, K. Peters⁴⁸, R.F.Y. Peters¹⁰⁰, B.A. Petersen³⁶, T.C. Petersen⁴², E. Petit¹⁰¹, V. Petousis¹³¹, C. Petridou¹⁵¹, A. Petrukhin¹⁴⁰, M. Pettee^{17a}, N.E. Pettersson³⁶, A. Petukhov³⁷, K. Petukhova¹³², A. Peyaud¹³⁴, R. Pezoa^{136f}, L. Pezzotti³⁶, G. Pezzullo¹⁷⁰, T. Pham¹⁰⁴, P.W. Phillips¹³³, M.W. Phipps¹⁶⁰, G. Piacquadio¹⁴⁴, E. Pianori^{17a}, F. Piazza^{70a,70b}, R. Piegai³⁰, D. Pietreanu^{27b}, A.D. Pilkington¹⁰⁰, M. Pinamonti^{68a,68c}, J.L. Pinfeld², B.C. Pinheiro Pereira^{129a}, C. Pitman Donaldson⁹⁵, D.A. Pizzi³⁴, L. Pizzimento^{75a,75b}, A. Pizzini¹¹³, M.-A. Pleier²⁹, V. Plesanovs⁵⁴, V. Pleskot¹³², E. Plotnikova³⁸, G. Poddar⁴, R. Poettgen⁹⁷, R. Poggi⁵⁶, L. Poggioli¹²⁶, I. Pogrebnyak¹⁰⁶, D. Pohl²⁴, I. Pokharel⁵⁵, S. Polacek¹³², G. Polesello^{72a}, A. Poley^{141,155a}, R. Polifka¹³¹, A. Polini^{23b}, C.S. Pollard¹²⁵, Z.B. Pollock¹¹⁸, V. Polychronakos²⁹, D. Ponomarenko³⁷, L. Pontecorvo³⁶, S. Popa^{27a}, G.A. Popeneciu^{27d}, D.M. Portillo Quintero^{155a}, S. Pospisil¹³¹, P. Postolache^{27c}, K. Potamianos¹²⁵, I.N. Potrap³⁸, C.J. Potter³², H. Potti¹, T. Poulsen⁴⁸, J. Poveda¹⁶¹, G. Pownall⁴⁸, M.E. Pozo Astigarraga³⁶, A. Prades Ibanez¹⁶¹, M.M. Prapa⁴⁶, D. Price¹⁰⁰, M. Primavera^{69a}, M.A. Principe Martin⁹⁸, M.L. Proffitt¹³⁷, N. Proklova³⁷, K. Prokofiev^{64c}, G. Proto^{75a,75b}, S. Protopopescu²⁹, J. Proudfoot⁶, M. Przybycien^{84a}, J.E. Puddefoot¹³⁸, D. Pudzha³⁷, P. Puzo⁶⁶, D. Pyatiiybyantseva³⁷, J. Qian¹⁰⁵, Y. Qin¹⁰⁰, T. Qiu⁹³, A. Quadt⁵⁵,

M. Queitsch-Maitland²⁴, G. Rabanal Bolanos⁶¹, D. Rafanoharana⁵⁴, F. Ragusa^{70a,70b}, J.L. Rainbolt³⁹,
J.A. Raine⁵⁶, S. Rajagopalan²⁹, E. Ramakoti³⁷, K. Ran^{14a,14d}, V. Raskina¹²⁶, D.F. Rassloff^{63a}, S. Rave⁹⁹,
B. Ravina⁵⁹, I. Ravinovich¹⁶⁷, M. Raymond³⁶, A.L. Read¹²⁴, N.P. Readioff¹³⁸, D.M. Rebuzzi^{72a,72b},
G. Redlinger²⁹, K. Reeves⁴⁵, J.A. Reidelsturz¹⁶⁹, D. Reikher¹⁵⁰, A. Reiss⁹⁹, A. Rej¹⁴⁰, C. Rembser³⁶,
A. Renardi⁴⁸, M. Renda^{27b}, M.B. Rendel¹⁰⁹, A.G. Rennie⁵⁹, S. Resconi^{70a}, M. Ressegotti^{57b,57a},
E.D. Resseguie^{17a}, S. Rettie⁹⁵, B. Reynolds¹¹⁸, E. Reynolds^{17a}, M. Rezaei Estabragh¹⁶⁹, O.L. Rezanova³⁷,
P. Reznicek¹³², E. Ricci^{77a,77b}, R. Richter¹⁰⁹, S. Richter^{47a,47b}, E. Richter-Was^{84b}, M. Ridel¹²⁶, P. Rieck¹¹⁶,
P. Riedler³⁶, M. Rijssenbeek¹⁴⁴, A. Rimoldi^{72a,72b}, M. Rimoldi⁴⁸, L. Rinaldi^{23b,23a}, T.T. Rinn²⁹,
M.P. Rinnagel¹⁰⁸, G. Ripellino¹⁴³, I. Riu¹³, P. Rivadeneira⁴⁸, J.C. Rivera Vergara¹⁶³, F. Rizatdinova¹²⁰,
E. Rizvi⁹³, C. Rizzi⁵⁶, B.A. Roberts¹⁶⁵, B.R. Roberts^{17a}, S.H. Robertson^{103,v}, M. Robin⁴⁸, D. Robinson³²,
C.M. Robles Gajardo^{136f}, M. Robles Manzano⁹⁹, A. Robson⁵⁹, A. Rocchi^{75a,75b}, C. Roda^{73a,73b},
S. Rodriguez Bosca^{63a}, Y. Rodriguez Garcia^{22a}, A. Rodriguez Rodriguez⁵⁴, A.M. Rodríguez Vera^{155b},
S. Roe³⁶, J.T. Roemer¹⁵⁸, A.R. Roepke-Gier¹¹⁹, J. Roggel¹⁶⁹, O. Røhne¹²⁴, R.A. Rojas¹⁶³, B. Roland⁵⁴,
C.P.A. Roland⁶⁷, J. Roloff²⁹, A. Romaniouk³⁷, E. Romano^{72a,72b}, M. Romano^{23b},
A.C. Romero Hernandez¹⁶⁰, N. Rompotis⁹¹, L. Roos¹²⁶, S. Rosati^{74a}, B.J. Rosser³⁹, E. Rossi⁴,
E. Rossi^{71a,71b}, L.P. Rossi^{57b}, L. Rossini⁴⁸, R. Rosten¹¹⁸, M. Rotaru^{27b}, B. Rottler⁵⁴, D. Rousseau⁶⁶,
D. Rousso³², G. Rovelli^{72a,72b}, A. Roy¹⁶⁰, A. Rozanov¹⁰¹, Y. Rozen¹⁴⁹, X. Ruan^{33g}, A. Rubio Jimenez¹⁶¹,
A.J. Ruby⁹¹, T.A. Ruggeri¹, F. Rühr⁵⁴, A. Ruiz-Martinez¹⁶¹, A. Rummeler³⁶, Z. Rurikova⁵⁴,
N.A. Rusakovich³⁸, H.L. Russell¹⁶³, J.P. Rutherford⁷, E.M. Rüttinger¹³⁸, K. Rybacki⁹⁰, M. Rybar¹³²,
E.B. Rye¹²⁴, A. Ryzhov³⁷, J.A. Sabater Iglesias⁵⁶, P. Sabatini¹⁶¹, L. Sabetta^{74a,74b}, H.F.W. Sadrozinski¹³⁵,
F. Safai Tehrani^{74a}, B. Safarzadeh Samani¹⁴⁵, M. Safdari¹⁴², S. Saha¹⁰³, M. Sahinsoy¹⁰⁹, M. Saimpert¹³⁴,
M. Saito¹⁵², T. Saito¹⁵², D. Salamani³⁶, G. Salamanna^{76a,76b}, A. Salnikov¹⁴², J. Salt¹⁶¹,
A. Salvador Salas¹³, D. Salvatore^{43b,43a}, F. Salvatore¹⁴⁵, A. Salzburger³⁶, D. Sammel⁵⁴, D. Sampsonidis¹⁵¹,
D. Sampsonidou^{62d,62c}, J. Sánchez¹⁶¹, A. Sanchez Pineda⁴, V. Sanchez Sebastian¹⁶¹, H. Sandaker¹²⁴,
C.O. Sander⁴⁸, J.A. Sandesara¹⁰², M. Sandhoff¹⁶⁹, C. Sandoval^{22b}, D.P.C. Sankey¹³³, A. Sansoni⁵³,
L. Santi^{74a,74b}, C. Santoni⁴⁰, H. Santos^{129a,129b}, S.N. Santpur^{17a}, A. Santra¹⁶⁷, K.A. Saoucha¹³⁸,
J.G. Saraiva^{129a,129d}, J. Sardain¹⁰¹, O. Sasaki⁸², K. Sato¹⁵⁶, C. Sauer^{63b}, F. Sauerburger⁵⁴, E. Sauvan⁴,
P. Savard^{154,ac}, R. Sawada¹⁵², C. Sawyer¹³³, L. Sawyer⁹⁶, I. Sayago Galvan¹⁶¹, C. Sbarra^{23b},
A. Sbrizzi^{23b,23a}, T. Scanlon⁹⁵, J. Schaarschmidt¹³⁷, P. Schacht¹⁰⁹, D. Schaefer³⁹, U. Schäfer⁹⁹,
A.C. Schaffer⁶⁶, D. Schaile¹⁰⁸, R.D. Schamberger¹⁴⁴, E. Schanet¹⁰⁸, C. Scharf¹⁸, V.A. Schegelsky³⁷,
D. Scheirich¹³², F. Schenck¹⁸, M. Schernau¹⁵⁸, C. Scheulen⁵⁵, C. Schiavi^{57b,57a}, Z.M. Schillaci²⁶,
E.J. Schioppa^{69a,69b}, M. Schioppa^{43b,43a}, B. Schlag⁹⁹, K.E. Schleicher⁵⁴, S. Schlenker³⁶, K. Schmieden⁹⁹,
C. Schmitt⁹⁹, S. Schmitt⁴⁸, L. Schoeffel¹³⁴, A. Schoening^{63b}, P.G. Scholer⁵⁴, E. Schopf¹²⁵, M. Schott⁹⁹,
J. Schovancova³⁶, S. Schramm⁵⁶, F. Schroeder¹⁶⁹, H-C. Schultz-Coulon^{63a}, M. Schumacher⁵⁴,
B.A. Schumm¹³⁵, Ph. Schune¹³⁴, A. Schwartzman¹⁴², T.A. Schwarz¹⁰⁵, Ph. Schwemling¹³⁴,
R. Schwienhorst¹⁰⁶, A. Sciandra¹³⁵, G. Sciolla²⁶, F. Scuri^{73a}, F. Scutti¹⁰⁴, C.D. Sebastiani⁹¹,
K. Sedlaczek⁴⁹, P. Seema¹⁸, S.C. Seidel¹¹¹, A. Seiden¹³⁵, B.D. Seidlitz⁴¹, T. Seiss³⁹, C. Seitz⁴⁸,
J.M. Seixas^{81b}, G. Sekhniaidze^{71a}, S.J. Sekula⁴⁴, L. Selem⁴, N. Semprini-Cesari^{23b,23a}, S. Sen⁵¹,
D. Sengupta⁵⁶, V. Senthilkumar¹⁶¹, L. Serin⁶⁶, L. Serkin^{68a,68b}, M. Sessa^{76a,76b}, H. Severini¹¹⁹,
S. Sevova¹⁴², F. Sforza^{57b,57a}, A. Sfyrila⁵⁶, E. Shabalina⁵⁵, R. Shaheen¹⁴³, J.D. Shahinian¹²⁷,
N.W. Shaikh^{47a,47b}, D. Shaked Renous¹⁶⁷, L.Y. Shan^{14a}, M. Shapiro^{17a}, A. Sharma³⁶, A.S. Sharma¹⁶²,
P. Sharma⁷⁹, S. Sharma⁴⁸, P.B. Shatalov³⁷, K. Shaw¹⁴⁵, S.M. Shaw¹⁰⁰, Q. Shen^{62c}, P. Sherwood⁹⁵,
L. Shi⁹⁵, C.O. Shimmin¹⁷⁰, Y. Shimogama¹⁶⁶, J.D. Shinner⁹⁴, I.P.J. Shipsey¹²⁵, S. Shirabe⁶⁰,
M. Shiyakova³⁸, J. Shlomi¹⁶⁷, M.J. Shochet³⁹, J. Shojaii¹⁰⁴, D.R. Shope¹⁴³, S. Shrestha¹¹⁸, E.M. Shrif^{33g},
M.J. Shroff¹⁶³, P. Sicho¹³⁰, A.M. Sickles¹⁶⁰, E. Sideras Haddad^{33g}, O. Sidiropoulou³⁶, A. Sidoti^{23b},
F. Siegert⁵⁰, Dj. Sijacki¹⁵, R. Sikora^{84a}, F. Sili⁸⁹, J.M. Silva²⁰, M.V. Silva Oliveira³⁶, S.B. Silverstein^{47a},
S. Simion⁶⁶, R. Simoniello³⁶, E.L. Simpson⁵⁹, N.D. Simpson⁹⁷, S. Simsek^{21d}, S. Sindhu⁵⁵, P. Sinervo¹⁵⁴,

V. Sinetckii³⁷, S. Singh¹⁴¹, S. Singh¹⁵⁴, S. Sinha⁴⁸, S. Sinha^{33g}, M. Sioli^{23b,23a}, I. Siral¹²², S.Yu. Sivoklov^{37,*}, J. Sjölin^{47a,47b}, A. Skaf⁵⁵, E. Skorda⁹⁷, P. Skubic¹¹⁹, M. Slawinska⁸⁵, V. Smakhtin¹⁶⁷, B.H. Smart¹³³, J. Smiesko¹³², S.Yu. Smirnov³⁷, Y. Smirnov³⁷, L.N. Smirnova^{37,a}, O. Smirnova⁹⁷, E.A. Smith³⁹, H.A. Smith¹²⁵, J.L. Smith⁹¹, R. Smith¹⁴², M. Smizanska⁹⁰, K. Smolek¹³¹, A. Smykiewicz⁸⁵, A.A. Snesarev³⁷, H.L. Snoek¹¹³, S. Snyder²⁹, R. Sobie^{163,v}, A. Soffer¹⁵⁰, C.A. Solans Sanchez³⁶, E.Yu. Soldatov³⁷, U. Soldevila¹⁶¹, A.A. Solodkov³⁷, S. Solomon⁵⁴, A. Soloshenko³⁸, K. Solovieva⁵⁴, O.V. Solovyanov³⁷, V. Solovyev³⁷, P. Sommer³⁶, A. Sonay¹³, W.Y. Song^{155b}, A. Sopczak¹³¹, A.L. Sopio⁹⁵, F. Sopkova^{28b}, V. Sothilingam^{63a}, S. Sottocornola^{72a,72b}, R. Soualah^{115c}, Z. Soumami^{35e}, D. South⁴⁸, S. Spagnolo^{69a,69b}, M. Spalla¹⁰⁹, F. Spanò⁹⁴, D. Sperlich⁵⁴, G. Spigo³⁶, M. Spina¹⁴⁵, S. Spinali⁹⁰, D.P. Spiteri⁵⁹, M. Spousta¹³², E.J. Staats³⁴, A. Stabile^{70a,70b}, R. Stamen^{63a}, M. Stamenkovic¹¹³, A. Stampekis²⁰, M. Standke²⁴, E. Stanecka⁸⁵, B. Stanislaus^{17a}, M.M. Stanitzki⁴⁸, M. Stankaityte¹²⁵, B. Stapf⁶⁴⁸, E.A. Starchenko³⁷, G.H. Stark¹³⁵, J. Stark¹⁰¹, D.M. Starke^{155b}, P. Staroba¹³⁰, P. Starovoitov^{63a}, S. Stärz¹⁰³, R. Staszewski⁸⁵, G. Stavropoulos⁴⁶, J. Steentoft¹⁵⁹, P. Steinberg²⁹, A.L. Steinhebel¹²², B. Stelzer^{141,155a}, H.J. Stelzer¹²⁸, O. Stelzer-Chilton^{155a}, H. Stenzel⁵⁸, T.J. Stevenson¹⁴⁵, G.A. Stewart³⁶, M.C. Stockton³⁶, G. Stoicea^{27b}, M. Stolarski^{129a}, S. Stonjek¹⁰⁹, A. Straessner⁵⁰, J. Strandberg¹⁴³, S. Strandberg^{47a,47b}, M. Strauss¹¹⁹, T. Strebler¹⁰¹, P. Strizenc^{28b}, R. Ströhmer¹⁶⁴, D.M. Strom¹²², L.R. Strom⁴⁸, R. Stroynowski⁴⁴, A. Strubig^{47a,47b}, S.A. Stucci²⁹, B. Stugu¹⁶, J. Stupak¹¹⁹, N.A. Styles⁴⁸, D. Su¹⁴², S. Su^{62a}, W. Su^{62d,137,62c}, X. Su^{62a,66}, K. Sugizaki¹⁵², V.V. Sulin³⁷, M.J. Sullivan⁹¹, D.M.S. Sultan^{77a,77b}, L. Sultanaliyeva³⁷, S. Sultansoy^{3b}, T. Sumida⁸⁶, S. Sun¹⁰⁵, S. Sun¹⁶⁸, O. Sunneborn Gudnadottir¹⁵⁹, M.R. Sutton¹⁴⁵, M. Svatos¹³⁰, M. Swiatlowski^{155a}, T. Swirski¹⁶⁴, I. Sykora^{28a}, M. Sykora¹³², T. Sykora¹³², D. Ta⁹⁹, K. Tackmann^{48,u}, A. Taffard¹⁵⁸, R. Tafirout^{155a}, J.S. Tafoya Vargas⁶⁶, R.H.M. Taibah¹²⁶, R. Takashima⁸⁷, K. Takeda⁸³, E.P. Takeva⁵², Y. Takubo⁸², M. Talby¹⁰¹, A.A. Talyshev³⁷, K.C. Tam^{64b}, N.M. Tamir¹⁵⁰, A. Tanaka¹⁵², J. Tanaka¹⁵², R. Tanaka⁶⁶, M. Tanasini^{57b,57a}, J. Tang^{62c}, Z. Tao¹⁶², S. Tapia Araya⁸⁰, S. Tapprogge⁹⁹, A. Tarek Abouelfadl Mohamed¹⁰⁶, S. Tarem¹⁴⁹, K. Tariq^{62b}, G. Tarna^{27b}, G.F. Tartarelli^{70a}, P. Tas¹³², M. Tasevsky¹³⁰, E. Tassi^{43b,43a}, A.C. Tate¹⁶⁰, G. Tateno¹⁵², Y. Tayalati^{35e}, G.N. Taylor¹⁰⁴, W. Taylor^{155b}, H. Teagle⁹¹, A.S. Tee¹⁶⁸, R. Teixeira De Lima¹⁴², P. Teixeira-Dias⁹⁴, J.J. Teoh¹⁵⁴, K. Terashi¹⁵², J. Terron⁹⁸, S. Terzo¹³, M. Testa⁵³, R.J. Teuscher^{154,v}, N. Themistokleous⁵², T. Theveneaux-Pelzer¹⁸, O. Thielmann¹⁶⁹, D.W. Thomas⁹⁴, J.P. Thomas²⁰, E.A. Thompson⁴⁸, P.D. Thompson²⁰, E. Thomson¹²⁷, E.J. Thorpe⁹³, Y. Tian⁵⁵, V. Tikhomirov^{37,a}, Yu.A. Tikhonov³⁷, S. Timoshenko³⁷, E.X.L. Ting¹, P. Tipton¹⁷⁰, S. Tisserant¹⁰¹, S.H. Tlou^{33g}, A. Tnourji⁴⁰, K. Todome^{23b,23a}, S. Todorova-Nova¹³², S. Todt⁵⁰, M. Togawa⁸², J. Tojo⁸⁸, S. Tokár^{28a}, K. Tokushuku⁸², R. Tombs³², M. Tomoto^{82,110}, L. Tompkins¹⁴², P. Tornambe¹⁰², E. Torrence¹²², H. Torres⁵⁰, E. Torró Pastor¹⁶¹, M. Toscani³⁰, C. Toscirri³⁹, D.R. Tovey¹³⁸, A. Traeet¹⁶, I.S. Trandafir^{27b}, T. Trefzger¹⁶⁴, A. Tricoli²⁹, I.M. Trigger^{155a}, S. Trincaz-Duvoid¹²⁶, D.A. Trischuk¹⁶², B. Trocme⁶⁰, A. Trofymov⁶⁶, C. Troncon^{70a}, L. Truong^{33c}, M. Trzebinski⁸⁵, A. Trzupek⁸⁵, F. Tsai¹⁴⁴, M. Tsai¹⁰⁵, A. Tsiamis¹⁵¹, P.V. Tsiarehka³⁷, S. Tsigaridas^{155a}, A. Tsirigotis^{151,s}, V. Tsiskaridze¹⁴⁴, E.G. Tskhadadze^{148a}, M. Tsopoulou¹⁵¹, Y. Tsujikawa⁸⁶, I.I. Tsukerman³⁷, V. Tsulaia^{17a}, S. Tsuno⁸², O. Tsur¹⁴⁹, D. Tsybychev¹⁴⁴, Y. Tu^{64b}, A. Tudorache^{27b}, V. Tudorache^{27b}, A.N. Tuna³⁶, S. Turchikhin³⁸, I. Turk Cakir^{3a}, R. Turra^{70a}, T. Turtuvshin³⁸, P.M. Tuts⁴¹, S. Tzamarias¹⁵¹, P. Tzani¹⁰, E. Tzovara⁹⁹, K. Uchida¹⁵², F. Ukegawa¹⁵⁶, P.A. Ulloa Poblete^{136c}, G. Unal³⁶, M. Unal¹¹, A. Undrus²⁹, G. Unel¹⁵⁸, K. Uno¹⁵², J. Urban^{28b}, P. Urquijo¹⁰⁴, G. Usai⁸, R. Ushioda¹⁵³, M. Usman¹⁰⁷, Z. Uysal^{21b}, V. Vacek¹³¹, B. Vachon¹⁰³, K.O.H. Vadla¹²⁴, T. Vafeiadis³⁶, C. Valderanis¹⁰⁸, E. Valdes Santurio^{47a,47b}, M. Valente^{155a}, S. Valentinetti^{23b,23a}, A. Valero¹⁶¹, A. Vallier¹⁰¹, J.A. Valls Ferrer¹⁶¹, T.R. Van Daalen¹³⁷, P. Van Gemmeren⁶, S. Van Stroud⁹⁵, I. Van Vulpen¹¹³, M. Vanadia^{75a,75b}, W. Vandelli³⁶, M. Vandenbroucke¹³⁴, E.R. Vandewall¹²⁰, D. Vannicola¹⁵⁰, L. Vannoli^{57b,57a}, R. Vari^{74a}, E.W. Varnes⁷, C. Varni^{17a}, T. Varol¹⁴⁷, D. Varouchas⁶⁶, L. Varriale¹⁶¹, K.E. Varvell¹⁴⁶, M.E. Vasile^{27b}, L. Vaslin⁴⁰, G.A. Vasquez¹⁶³, F. Vazeille⁴⁰, T. Vazquez Schroeder³⁶, J. Veatch³¹, V. Vecchio¹⁰⁰, M.J. Veen¹¹³,

I. Veliscek¹²⁵, L.M. Veloce¹⁵⁴, F. Veloso^{129a,129c}, S. Veneziano^{74a}, A. Ventura^{69a,69b}, A. Verbitskiy¹⁰⁹, M. Verducci^{73a,73b}, C. Vergis²⁴, M. Verissimo De Araujo^{81b}, W. Verkerke¹¹³, J.C. Vermeulen¹¹³, C. Vernieri¹⁴², P.J. Verschuuren⁹⁴, M. Vessella¹⁰², M.L. Vesterbacka¹¹⁶, M.C. Vetterli^{141.ac}, A. Vgenopoulos¹⁵¹, N. Viaux Maira^{136f}, T. Vickey¹³⁸, O.E. Vickey Boeriu¹³⁸, G.H.A. Viehhauser¹²⁵, L. Vigani^{63b}, M. Villa^{23b,23a}, M. Villaplana Perez¹⁶¹, E.M. Villhauer⁵², E. Vilucchi⁵³, M.G. Vinciter³⁴, G.S. Virdee²⁰, A. Vishwakarma⁵², C. Vittori^{23b,23a}, I. Vivarelli¹⁴⁵, V. Vladimirov¹⁶⁵, E. Voevodina¹⁰⁹, F. Vogel¹⁰⁸, P. Vokac¹³¹, J. Von Ahnen⁴⁸, E. Von Toerne²⁴, B. Vormwald³⁶, V. Vorobel¹³², K. Vorobev³⁷, M. Vos¹⁶¹, J.H. Vosseveld⁹¹, M. Vozak¹¹³, L. Vozdecky⁹³, N. Vranjes¹⁵, M. Vranjes Milosavljevic¹⁵, M. Vreeswijk¹¹³, R. Vuillermet³⁶, O. Vujanovic⁹⁹, I. Vukotic³⁹, S. Wada¹⁵⁶, C. Wagner¹⁰², W. Wagner¹⁶⁹, S. Wahdan¹⁶⁹, H. Wahlberg⁸⁹, R. Wakasa¹⁵⁶, M. Wakida¹¹⁰, V.M. Walbrecht¹⁰⁹, J. Walder¹³³, R. Walker¹⁰⁸, W. Walkowiak¹⁴⁰, A.M. Wang⁶¹, A.Z. Wang¹⁶⁸, C. Wang^{62a}, C. Wang^{62c}, H. Wang^{17a}, J. Wang^{64a}, P. Wang⁴⁴, R.-J. Wang⁹⁹, R. Wang⁶¹, R. Wang⁶, S.M. Wang¹⁴⁷, S. Wang^{62b}, T. Wang^{62a}, W.T. Wang⁷⁹, W.X. Wang^{62a}, X. Wang^{14c}, X. Wang¹⁶⁰, X. Wang^{62c}, Y. Wang^{62d}, Y. Wang^{14c}, Z. Wang¹⁰⁵, Z. Wang^{62d,51,62c}, Z. Wang¹⁰⁵, A. Warburton¹⁰³, R.J. Ward²⁰, N. Warrack⁵⁹, A.T. Watson²⁰, M.F. Watson²⁰, G. Watts¹³⁷, B.M. Waugh⁹⁵, A.F. Webb¹¹, C. Weber²⁹, M.S. Weber¹⁹, S.A. Weber³⁴, S.M. Weber^{63a}, C. Wei^{62a}, Y. Wei¹²⁵, A.R. Weidberg¹²⁵, J. Weingarten⁴⁹, M. Weirich⁹⁹, C. Weiser⁵⁴, C.J. Wells⁴⁸, T. Wenaus²⁹, B. Wendland⁴⁹, T. Wengler³⁶, N.S. Wenke¹⁰⁹, N. Wermes²⁴, M. Wessels^{63a}, K. Whalen¹²², A.M. Wharton⁹⁰, A.S. White⁶¹, A. White⁸, M.J. White¹, D. Whiteson¹⁵⁸, L. Wickremasinghe¹²³, W. Wiedenmann¹⁶⁸, C. Wiel⁵⁰, M. Wielers¹³³, N. Wieseotte⁹⁹, C. Wiglesworth⁴², L.A.M. Wiik-Fuchs⁵⁴, D.J. Wilbern¹¹⁹, H.G. Wilkens³⁶, D.M. Williams⁴¹, H.H. Williams¹²⁷, S. Williams³², S. Willocq¹⁰², P.J. Windischhofer¹²⁵, F. Winklmeier¹²², B.T. Winter⁵⁴, M. Wittgen¹⁴², M. Wobisch⁹⁶, A. Wolf⁹⁹, R. Wölker¹²⁵, J. Wollrath¹⁵⁸, M.W. Wolter⁸⁵, H. Wolters^{129a,129c}, V.W.S. Wong¹⁶², A.F. Wongel⁴⁸, S.D. Worm⁴⁸, B.K. Wosiek⁸⁵, K.W. Woźniak⁸⁵, K. Wraight⁵⁹, J. Wu^{14a,14d}, M. Wu^{64a}, S.L. Wu¹⁶⁸, X. Wu⁵⁶, Y. Wu^{62a}, Z. Wu^{134,62a}, J. Wuerzinger¹²⁵, T.R. Wyatt¹⁰⁰, B.M. Wynne⁵², S. Xella⁴², L. Xia^{14c}, M. Xia^{14b}, J. Xiang^{64c}, X. Xiao¹⁰⁵, M. Xie^{62a}, X. Xie^{62a}, J. Xiong^{17a}, I. Xiotidis¹⁴⁵, D. Xu^{14a}, H. Xu^{62a}, H. Xu^{62a}, L. Xu^{62a}, R. Xu¹²⁷, T. Xu¹⁰⁵, W. Xu¹⁰⁵, Y. Xu^{14b}, Z. Xu^{62b}, Z. Xu¹⁴², B. Yabsley¹⁴⁶, S. Yacoob^{33a}, N. Yamaguchi⁸⁸, Y. Yamaguchi¹⁵³, H. Yamauchi¹⁵⁶, T. Yamazaki^{17a}, Y. Yamazaki⁸³, J. Yan^{62c}, S. Yan¹²⁵, Z. Yan²⁵, H.J. Yang^{62c,62d}, H.T. Yang^{17a}, S. Yang^{62a}, T. Yang^{64c}, X. Yang^{62a}, X. Yang^{14a}, Y. Yang⁴⁴, Z. Yang^{62a,105}, W.-M. Yao^{17a}, Y.C. Yap⁴⁸, H. Ye^{14c}, J. Ye⁴⁴, S. Ye²⁹, X. Ye^{62a}, I. Yeletsikh³⁸, M.R. Yexley⁹⁰, P. Yin⁴¹, K. Yorita¹⁶⁶, C.J.S. Young⁵⁴, C. Young¹⁴², M. Yuan¹⁰⁵, R. Yuan^{62b,j}, L. Yue⁹⁵, X. Yue^{63a}, M. Zaazoua^{35e}, B. Zabinski⁸⁵, E. Zaid⁵², T. Zakareishvili^{148b}, N. Zakharchuk³⁴, S. Zambito⁵⁶, J. Zang¹⁵², D. Zanzi⁵⁴, O. Zaplatilek¹³¹, S.V. Zeiβner⁴⁹, C. Zeitnitz¹⁶⁹, J.C. Zeng¹⁶⁰, D.T. Zenger Jr²⁶, O. Zenin³⁷, T. Ženiš^{28a}, S. Zenz⁹³, S. Zerradi^{35a}, D. Zerwas⁶⁶, B. Zhang^{14c}, D.F. Zhang¹³⁸, G. Zhang^{14b}, J. Zhang⁶, K. Zhang^{14a,14d}, L. Zhang^{14c}, R. Zhang¹⁶⁸, S. Zhang¹⁰⁵, T. Zhang¹⁵², X. Zhang^{62c}, X. Zhang^{62b}, Z. Zhang^{17a}, Z. Zhang⁶⁶, H. Zhao¹³⁷, P. Zhao⁵¹, T. Zhao^{62b}, Y. Zhao¹³⁵, Z. Zhao^{62a}, A. Zhemchugov³⁸, Z. Zheng¹⁴², D. Zhong¹⁶⁰, B. Zhou¹⁰⁵, C. Zhou¹⁶⁸, H. Zhou⁷, N. Zhou^{62c}, Y. Zhou⁷, C.G. Zhu^{62b}, C. Zhu^{14a,14d}, H.L. Zhu^{62a}, H. Zhu^{14a}, J. Zhu¹⁰⁵, Y. Zhu^{62a}, X. Zhuang^{14a}, K. Zhukov³⁷, V. Zhulanov³⁷, N.I. Zimine³⁸, J. Zinsser^{63b}, M. Ziolkowski¹⁴⁰, L. Živković¹⁵, A. Zoccoli^{23b,23a}, K. Zoch⁵⁶, T.G. Zorbas¹³⁸, O. Zormpa⁴⁶, W. Zou⁴¹, L. Zwalinski³⁶.

¹Department of Physics, University of Adelaide, Adelaide; Australia.

²Department of Physics, University of Alberta, Edmonton AB; Canada.

³(^a)Department of Physics, Ankara University, Ankara; (^b)Division of Physics, TOBB University of Economics and Technology, Ankara; Türkiye.

⁴LAPP, Univ. Savoie Mont Blanc, CNRS/IN2P3, Annecy; France.

⁵APC, Université Paris Cité, CNRS/IN2P3, Paris; France.

⁶High Energy Physics Division, Argonne National Laboratory, Argonne IL; United States of America.

- ⁷Department of Physics, University of Arizona, Tucson AZ; United States of America.
- ⁸Department of Physics, University of Texas at Arlington, Arlington TX; United States of America.
- ⁹Physics Department, National and Kapodistrian University of Athens, Athens; Greece.
- ¹⁰Physics Department, National Technical University of Athens, Zografou; Greece.
- ¹¹Department of Physics, University of Texas at Austin, Austin TX; United States of America.
- ¹²Institute of Physics, Azerbaijan Academy of Sciences, Baku; Azerbaijan.
- ¹³Institut de Física d'Altes Energies (IFAE), Barcelona Institute of Science and Technology, Barcelona; Spain.
- ¹⁴(^a)Institute of High Energy Physics, Chinese Academy of Sciences, Beijing; (^b)Physics Department, Tsinghua University, Beijing; (^c)Department of Physics, Nanjing University, Nanjing; (^d)University of Chinese Academy of Science (UCAS), Beijing; China.
- ¹⁵Institute of Physics, University of Belgrade, Belgrade; Serbia.
- ¹⁶Department for Physics and Technology, University of Bergen, Bergen; Norway.
- ¹⁷(^a)Physics Division, Lawrence Berkeley National Laboratory, Berkeley CA; (^b)University of California, Berkeley CA; United States of America.
- ¹⁸Institut für Physik, Humboldt Universität zu Berlin, Berlin; Germany.
- ¹⁹Albert Einstein Center for Fundamental Physics and Laboratory for High Energy Physics, University of Bern, Bern; Switzerland.
- ²⁰School of Physics and Astronomy, University of Birmingham, Birmingham; United Kingdom.
- ²¹(^a)Department of Physics, Bogazici University, Istanbul; (^b)Department of Physics Engineering, Gaziantep University, Gaziantep; (^c)Department of Physics, Istanbul University, Istanbul; (^d)Istinye University, Sariyer, Istanbul; Türkiye.
- ²²(^a)Facultad de Ciencias y Centro de Investigaciones, Universidad Antonio Nariño, Bogotá; (^b)Departamento de Física, Universidad Nacional de Colombia, Bogotá; Colombia.
- ²³(^a)Dipartimento di Fisica e Astronomia A. Righi, Università di Bologna, Bologna; (^b)INFN Sezione di Bologna; Italy.
- ²⁴Physikalisches Institut, Universität Bonn, Bonn; Germany.
- ²⁵Department of Physics, Boston University, Boston MA; United States of America.
- ²⁶Department of Physics, Brandeis University, Waltham MA; United States of America.
- ²⁷(^a)Transilvania University of Brasov, Brasov; (^b)Horia Hulubei National Institute of Physics and Nuclear Engineering, Bucharest; (^c)Department of Physics, Alexandru Ioan Cuza University of Iasi, Iasi; (^d)National Institute for Research and Development of Isotopic and Molecular Technologies, Physics Department, Cluj-Napoca; (^e)University Politehnica Bucharest, Bucharest; (^f)West University in Timisoara, Timisoara; Romania.
- ²⁸(^a)Faculty of Mathematics, Physics and Informatics, Comenius University, Bratislava; (^b)Department of Subnuclear Physics, Institute of Experimental Physics of the Slovak Academy of Sciences, Kosice; Slovak Republic.
- ²⁹Physics Department, Brookhaven National Laboratory, Upton NY; United States of America.
- ³⁰Universidad de Buenos Aires, Facultad de Ciencias Exactas y Naturales, Departamento de Física, y CONICET, Instituto de Física de Buenos Aires (IFIBA), Buenos Aires; Argentina.
- ³¹California State University, CA; United States of America.
- ³²Cavendish Laboratory, University of Cambridge, Cambridge; United Kingdom.
- ³³(^a)Department of Physics, University of Cape Town, Cape Town; (^b)iThemba Labs, Western Cape; (^c)Department of Mechanical Engineering Science, University of Johannesburg, Johannesburg; (^d)National Institute of Physics, University of the Philippines Diliman (Philippines); (^e)University of South Africa, Department of Physics, Pretoria; (^f)University of Zululand, KwaDlangezwa; (^g)School of Physics, University of the Witwatersrand, Johannesburg; South Africa.

- ³⁴Department of Physics, Carleton University, Ottawa ON; Canada.
- ³⁵(^a)Faculté des Sciences Ain Chock, Réseau Universitaire de Physique des Hautes Energies - Université Hassan II, Casablanca;(^b)Faculté des Sciences, Université Ibn-Tofail, Kénitra;(^c)Faculté des Sciences Semlalia, Université Cadi Ayyad, LPHEA-Marrakech;(^d)LPMR, Faculté des Sciences, Université Mohamed Premier, Oujda;(^e)Faculté des sciences, Université Mohammed V, Rabat;(^f)Institute of Applied Physics, Mohammed VI Polytechnic University, Ben Guerir; Morocco.
- ³⁶CERN, Geneva; Switzerland.
- ³⁷Affiliated with an institute covered by a cooperation agreement with CERN.
- ³⁸Affiliated with an international laboratory covered by a cooperation agreement with CERN.
- ³⁹Enrico Fermi Institute, University of Chicago, Chicago IL; United States of America.
- ⁴⁰LPC, Université Clermont Auvergne, CNRS/IN2P3, Clermont-Ferrand; France.
- ⁴¹Nevis Laboratory, Columbia University, Irvington NY; United States of America.
- ⁴²Niels Bohr Institute, University of Copenhagen, Copenhagen; Denmark.
- ⁴³(^a)Dipartimento di Fisica, Università della Calabria, Rende;(^b)INFN Gruppo Collegato di Cosenza, Laboratori Nazionali di Frascati; Italy.
- ⁴⁴Physics Department, Southern Methodist University, Dallas TX; United States of America.
- ⁴⁵Physics Department, University of Texas at Dallas, Richardson TX; United States of America.
- ⁴⁶National Centre for Scientific Research "Demokritos", Agia Paraskevi; Greece.
- ⁴⁷(^a)Department of Physics, Stockholm University;(^b)Oskar Klein Centre, Stockholm; Sweden.
- ⁴⁸Deutsches Elektronen-Synchrotron DESY, Hamburg and Zeuthen; Germany.
- ⁴⁹Fakultät Physik , Technische Universität Dortmund, Dortmund; Germany.
- ⁵⁰Institut für Kern- und Teilchenphysik, Technische Universität Dresden, Dresden; Germany.
- ⁵¹Department of Physics, Duke University, Durham NC; United States of America.
- ⁵²SUPA - School of Physics and Astronomy, University of Edinburgh, Edinburgh; United Kingdom.
- ⁵³INFN e Laboratori Nazionali di Frascati, Frascati; Italy.
- ⁵⁴Physikalisches Institut, Albert-Ludwigs-Universität Freiburg, Freiburg; Germany.
- ⁵⁵II. Physikalisches Institut, Georg-August-Universität Göttingen, Göttingen; Germany.
- ⁵⁶Département de Physique Nucléaire et Corpusculaire, Université de Genève, Genève; Switzerland.
- ⁵⁷(^a)Dipartimento di Fisica, Università di Genova, Genova;(^b)INFN Sezione di Genova; Italy.
- ⁵⁸II. Physikalisches Institut, Justus-Liebig-Universität Giessen, Giessen; Germany.
- ⁵⁹SUPA - School of Physics and Astronomy, University of Glasgow, Glasgow; United Kingdom.
- ⁶⁰LPSC, Université Grenoble Alpes, CNRS/IN2P3, Grenoble INP, Grenoble; France.
- ⁶¹Laboratory for Particle Physics and Cosmology, Harvard University, Cambridge MA; United States of America.
- ⁶²(^a)Department of Modern Physics and State Key Laboratory of Particle Detection and Electronics, University of Science and Technology of China, Hefei;(^b)Institute of Frontier and Interdisciplinary Science and Key Laboratory of Particle Physics and Particle Irradiation (MOE), Shandong University, Qingdao;(^c)School of Physics and Astronomy, Shanghai Jiao Tong University, Key Laboratory for Particle Astrophysics and Cosmology (MOE), SKLPPC, Shanghai;(^d)Tsung-Dao Lee Institute, Shanghai; China.
- ⁶³(^a)Kirchhoff-Institut für Physik, Ruprecht-Karls-Universität Heidelberg, Heidelberg;(^b)Physikalisches Institut, Ruprecht-Karls-Universität Heidelberg, Heidelberg; Germany.
- ⁶⁴(^a)Department of Physics, Chinese University of Hong Kong, Shatin, N.T., Hong Kong;(^b)Department of Physics, University of Hong Kong, Hong Kong;(^c)Department of Physics and Institute for Advanced Study, Hong Kong University of Science and Technology, Clear Water Bay, Kowloon, Hong Kong; China.
- ⁶⁵Department of Physics, National Tsing Hua University, Hsinchu; Taiwan.
- ⁶⁶IJCLab, Université Paris-Saclay, CNRS/IN2P3, 91405, Orsay; France.
- ⁶⁷Department of Physics, Indiana University, Bloomington IN; United States of America.

- 68^(a) INFN Gruppo Collegato di Udine, Sezione di Trieste, Udine;^(b) ICTP, Trieste;^(c) Dipartimento Politecnico di Ingegneria e Architettura, Università di Udine, Udine; Italy.
- 69^(a) INFN Sezione di Lecce;^(b) Dipartimento di Matematica e Fisica, Università del Salento, Lecce; Italy.
- 70^(a) INFN Sezione di Milano;^(b) Dipartimento di Fisica, Università di Milano, Milano; Italy.
- 71^(a) INFN Sezione di Napoli;^(b) Dipartimento di Fisica, Università di Napoli, Napoli; Italy.
- 72^(a) INFN Sezione di Pavia;^(b) Dipartimento di Fisica, Università di Pavia, Pavia; Italy.
- 73^(a) INFN Sezione di Pisa;^(b) Dipartimento di Fisica E. Fermi, Università di Pisa, Pisa; Italy.
- 74^(a) INFN Sezione di Roma;^(b) Dipartimento di Fisica, Sapienza Università di Roma, Roma; Italy.
- 75^(a) INFN Sezione di Roma Tor Vergata;^(b) Dipartimento di Fisica, Università di Roma Tor Vergata, Roma; Italy.
- 76^(a) INFN Sezione di Roma Tre;^(b) Dipartimento di Matematica e Fisica, Università Roma Tre, Roma; Italy.
- 77^(a) INFN-TIFPA;^(b) Università degli Studi di Trento, Trento; Italy.
- 78 Universität Innsbruck, Department of Astro and Particle Physics, Innsbruck; Austria.
- 79 University of Iowa, Iowa City IA; United States of America.
- 80 Department of Physics and Astronomy, Iowa State University, Ames IA; United States of America.
- 81^(a) Departamento de Engenharia Elétrica, Universidade Federal de Juiz de Fora (UFJF), Juiz de Fora;^(b) Universidade Federal do Rio De Janeiro COPPE/EE/IF, Rio de Janeiro;^(c) Instituto de Física, Universidade de São Paulo, São Paulo;^(d) Rio de Janeiro State University, Rio de Janeiro; Brazil.
- 82 KEK, High Energy Accelerator Research Organization, Tsukuba; Japan.
- 83 Graduate School of Science, Kobe University, Kobe; Japan.
- 84^(a) AGH University of Science and Technology, Faculty of Physics and Applied Computer Science, Krakow;^(b) Marian Smoluchowski Institute of Physics, Jagiellonian University, Krakow; Poland.
- 85 Institute of Nuclear Physics Polish Academy of Sciences, Krakow; Poland.
- 86 Faculty of Science, Kyoto University, Kyoto; Japan.
- 87 Kyoto University of Education, Kyoto; Japan.
- 88 Research Center for Advanced Particle Physics and Department of Physics, Kyushu University, Fukuoka ; Japan.
- 89 Instituto de Física La Plata, Universidad Nacional de La Plata and CONICET, La Plata; Argentina.
- 90 Physics Department, Lancaster University, Lancaster; United Kingdom.
- 91 Oliver Lodge Laboratory, University of Liverpool, Liverpool; United Kingdom.
- 92 Department of Experimental Particle Physics, Jožef Stefan Institute and Department of Physics, University of Ljubljana, Ljubljana; Slovenia.
- 93 School of Physics and Astronomy, Queen Mary University of London, London; United Kingdom.
- 94 Department of Physics, Royal Holloway University of London, Egham; United Kingdom.
- 95 Department of Physics and Astronomy, University College London, London; United Kingdom.
- 96 Louisiana Tech University, Ruston LA; United States of America.
- 97 Fysiska institutionen, Lunds universitet, Lund; Sweden.
- 98 Departamento de Física Teórica C-15 and CIAFF, Universidad Autónoma de Madrid, Madrid; Spain.
- 99 Institut für Physik, Universität Mainz, Mainz; Germany.
- 100 School of Physics and Astronomy, University of Manchester, Manchester; United Kingdom.
- 101 CPPM, Aix-Marseille Université, CNRS/IN2P3, Marseille; France.
- 102 Department of Physics, University of Massachusetts, Amherst MA; United States of America.
- 103 Department of Physics, McGill University, Montreal QC; Canada.
- 104 School of Physics, University of Melbourne, Victoria; Australia.
- 105 Department of Physics, University of Michigan, Ann Arbor MI; United States of America.
- 106 Department of Physics and Astronomy, Michigan State University, East Lansing MI; United States of

America.

¹⁰⁷Group of Particle Physics, University of Montreal, Montreal QC; Canada.

¹⁰⁸Fakultät für Physik, Ludwig-Maximilians-Universität München, München; Germany.

¹⁰⁹Max-Planck-Institut für Physik (Werner-Heisenberg-Institut), München; Germany.

¹¹⁰Graduate School of Science and Kobayashi-Maskawa Institute, Nagoya University, Nagoya; Japan.

¹¹¹Department of Physics and Astronomy, University of New Mexico, Albuquerque NM; United States of America.

¹¹²Institute for Mathematics, Astrophysics and Particle Physics, Radboud University/Nikhef, Nijmegen; Netherlands.

¹¹³Nikhef National Institute for Subatomic Physics and University of Amsterdam, Amsterdam; Netherlands.

¹¹⁴Department of Physics, Northern Illinois University, DeKalb IL; United States of America.

¹¹⁵(^a)New York University Abu Dhabi, Abu Dhabi; (^b)United Arab Emirates University, Al Ain; (^c)University of Sharjah, Sharjah; United Arab Emirates.

¹¹⁶Department of Physics, New York University, New York NY; United States of America.

¹¹⁷Ochanomizu University, Otsuka, Bunkyo-ku, Tokyo; Japan.

¹¹⁸Ohio State University, Columbus OH; United States of America.

¹¹⁹Homer L. Dodge Department of Physics and Astronomy, University of Oklahoma, Norman OK; United States of America.

¹²⁰Department of Physics, Oklahoma State University, Stillwater OK; United States of America.

¹²¹Palacký University, Joint Laboratory of Optics, Olomouc; Czech Republic.

¹²²Institute for Fundamental Science, University of Oregon, Eugene, OR; United States of America.

¹²³Graduate School of Science, Osaka University, Osaka; Japan.

¹²⁴Department of Physics, University of Oslo, Oslo; Norway.

¹²⁵Department of Physics, Oxford University, Oxford; United Kingdom.

¹²⁶LPNHE, Sorbonne Université, Université Paris Cité, CNRS/IN2P3, Paris; France.

¹²⁷Department of Physics, University of Pennsylvania, Philadelphia PA; United States of America.

¹²⁸Department of Physics and Astronomy, University of Pittsburgh, Pittsburgh PA; United States of America.

¹²⁹(^a)Laboratório de Instrumentação e Física Experimental de Partículas - LIP, Lisboa; (^b)Departamento de Física, Faculdade de Ciências, Universidade de Lisboa, Lisboa; (^c)Departamento de Física, Universidade de Coimbra, Coimbra; (^d)Centro de Física Nuclear da Universidade de Lisboa, Lisboa; (^e)Departamento de Física, Universidade do Minho, Braga; (^f)Departamento de Física Teórica y del Cosmos, Universidad de Granada, Granada (Spain); (^g)Departamento de Física, Instituto Superior Técnico, Universidade de Lisboa, Lisboa; Portugal.

¹³⁰Institute of Physics of the Czech Academy of Sciences, Prague; Czech Republic.

¹³¹Czech Technical University in Prague, Prague; Czech Republic.

¹³²Charles University, Faculty of Mathematics and Physics, Prague; Czech Republic.

¹³³Particle Physics Department, Rutherford Appleton Laboratory, Didcot; United Kingdom.

¹³⁴IRFU, CEA, Université Paris-Saclay, Gif-sur-Yvette; France.

¹³⁵Santa Cruz Institute for Particle Physics, University of California Santa Cruz, Santa Cruz CA; United States of America.

¹³⁶(^a)Departamento de Física, Pontificia Universidad Católica de Chile, Santiago; (^b)Millennium Institute for Subatomic physics at high energy frontier (SAPHIR), Santiago; (^c)Instituto de Investigación Multidisciplinario en Ciencia y Tecnología, y Departamento de Física, Universidad de La Serena; (^d)Universidad Andres Bello, Department of Physics, Santiago; (^e)Instituto de Alta Investigación, Universidad de Tarapacá, Arica; (^f)Departamento de Física, Universidad Técnica Federico Santa María,

Valparaíso; Chile.

¹³⁷Department of Physics, University of Washington, Seattle WA; United States of America.

¹³⁸Department of Physics and Astronomy, University of Sheffield, Sheffield; United Kingdom.

¹³⁹Department of Physics, Shinshu University, Nagano; Japan.

¹⁴⁰Department Physik, Universität Siegen, Siegen; Germany.

¹⁴¹Department of Physics, Simon Fraser University, Burnaby BC; Canada.

¹⁴²SLAC National Accelerator Laboratory, Stanford CA; United States of America.

¹⁴³Department of Physics, Royal Institute of Technology, Stockholm; Sweden.

¹⁴⁴Departments of Physics and Astronomy, Stony Brook University, Stony Brook NY; United States of America.

¹⁴⁵Department of Physics and Astronomy, University of Sussex, Brighton; United Kingdom.

¹⁴⁶School of Physics, University of Sydney, Sydney; Australia.

¹⁴⁷Institute of Physics, Academia Sinica, Taipei; Taiwan.

¹⁴⁸^(a)E. Andronikashvili Institute of Physics, Iv. Javakhishvili Tbilisi State University, Tbilisi; ^(b)High Energy Physics Institute, Tbilisi State University, Tbilisi; ^(c)University of Georgia, Tbilisi; Georgia.

¹⁴⁹Department of Physics, Technion, Israel Institute of Technology, Haifa; Israel.

¹⁵⁰Raymond and Beverly Sackler School of Physics and Astronomy, Tel Aviv University, Tel Aviv; Israel.

¹⁵¹Department of Physics, Aristotle University of Thessaloniki, Thessaloniki; Greece.

¹⁵²International Center for Elementary Particle Physics and Department of Physics, University of Tokyo, Tokyo; Japan.

¹⁵³Department of Physics, Tokyo Institute of Technology, Tokyo; Japan.

¹⁵⁴Department of Physics, University of Toronto, Toronto ON; Canada.

¹⁵⁵^(a)TRIUMF, Vancouver BC; ^(b)Department of Physics and Astronomy, York University, Toronto ON; Canada.

¹⁵⁶Division of Physics and Tomonaga Center for the History of the Universe, Faculty of Pure and Applied Sciences, University of Tsukuba, Tsukuba; Japan.

¹⁵⁷Department of Physics and Astronomy, Tufts University, Medford MA; United States of America.

¹⁵⁸Department of Physics and Astronomy, University of California Irvine, Irvine CA; United States of America.

¹⁵⁹Department of Physics and Astronomy, University of Uppsala, Uppsala; Sweden.

¹⁶⁰Department of Physics, University of Illinois, Urbana IL; United States of America.

¹⁶¹Instituto de Física Corpuscular (IFIC), Centro Mixto Universidad de Valencia - CSIC, Valencia; Spain.

¹⁶²Department of Physics, University of British Columbia, Vancouver BC; Canada.

¹⁶³Department of Physics and Astronomy, University of Victoria, Victoria BC; Canada.

¹⁶⁴Fakultät für Physik und Astronomie, Julius-Maximilians-Universität Würzburg, Würzburg; Germany.

¹⁶⁵Department of Physics, University of Warwick, Coventry; United Kingdom.

¹⁶⁶Waseda University, Tokyo; Japan.

¹⁶⁷Department of Particle Physics and Astrophysics, Weizmann Institute of Science, Rehovot; Israel.

¹⁶⁸Department of Physics, University of Wisconsin, Madison WI; United States of America.

¹⁶⁹Fakultät für Mathematik und Naturwissenschaften, Fachgruppe Physik, Bergische Universität Wuppertal, Wuppertal; Germany.

¹⁷⁰Department of Physics, Yale University, New Haven CT; United States of America.

^a Also Affiliated with an institute covered by a cooperation agreement with CERN.

^b Also at Borough of Manhattan Community College, City University of New York, New York NY; United States of America.

^c Also at Bruno Kessler Foundation, Trento; Italy.

^d Also at Center for High Energy Physics, Peking University; China.

- e* Also at Centro Studi e Ricerche Enrico Fermi; Italy.
- f* Also at CERN, Geneva; Switzerland.
- g* Also at Département de Physique Nucléaire et Corpusculaire, Université de Genève, Genève; Switzerland.
- h* Also at Departament de Física de la Universitat Autònoma de Barcelona, Barcelona; Spain.
- i* Also at Department of Financial and Management Engineering, University of the Aegean, Chios; Greece.
- j* Also at Department of Physics and Astronomy, Michigan State University, East Lansing MI; United States of America.
- k* Also at Department of Physics and Astronomy, University of Louisville, Louisville, KY; United States of America.
- l* Also at Department of Physics, Ben Gurion University of the Negev, Beer Sheva; Israel.
- m* Also at Department of Physics, California State University, East Bay; United States of America.
- n* Also at Department of Physics, California State University, Sacramento; United States of America.
- o* Also at Department of Physics, King's College London, London; United Kingdom.
- p* Also at Department of Physics, University of Fribourg, Fribourg; Switzerland.
- q* Also at Department of Physics, University of Thessaly; Greece.
- r* Also at Department of Physics, Westmont College, Santa Barbara; United States of America.
- s* Also at Hellenic Open University, Patras; Greece.
- t* Also at Institutio Catalana de Recerca i Estudis Avancats, ICREA, Barcelona; Spain.
- u* Also at Institut für Experimentalphysik, Universität Hamburg, Hamburg; Germany.
- v* Also at Institute of Particle Physics (IPP); Canada.
- w* Also at Institute of Physics, Azerbaijan Academy of Sciences, Baku; Azerbaijan.
- x* Also at Institute of Theoretical Physics, Ilia State University, Tbilisi; Georgia.
- y* Also at Lawrence Livermore National Laboratory, Livermore; United States of America.
- z* Also at Physics Department, An-Najah National University, Nablus; Palestine.
- aa* Also at The City College of New York, New York NY; United States of America.
- ab* Also at The Collaborative Innovation Center of Quantum Matter (CICQM), Beijing; China.
- ac* Also at TRIUMF, Vancouver BC; Canada.
- ad* Also at Università di Napoli Parthenope, Napoli; Italy.
- ae* Also at University of Chinese Academy of Sciences (UCAS), Beijing; China.
- af* Also at University of Colorado Boulder, Department of Physics, Colorado; United States of America.
- ag* Also at Yeditepe University, Physics Department, Istanbul; Türkiye.
- * Deceased